

CIAMTIS

U.S. DOT Region 3 University Transportation Center

Strategic Prioritization and Planning of Multi-Asset Transportation Infrastructure Maintenance, Rehabilitation, and Improvements: Phase 1 – Prioritization through Optimization

December 2, 2021

Prepared by:

**E. Miller Hooks, S. McNeil, D. Lattanzi, K. Papakonstantinou, S. Stoffels,
W. Zhou, P. Kamranfar, M. Saifullah, C. Andriotis and A. Withers
Department of Civil and Environmental Engineering
The Pennsylvania State University**

r3utc.psu.edu



PennState
College of Engineering

**LARSON
TRANSPORTATION
INSTITUTE**

DISCLAIMER

The contents of this report reflect the views of the authors, who are responsible for the facts and the accuracy of the information presented herein. This document is disseminated in the interest of information exchange. The report is funded, partially or entirely, by a grant from the U.S. Department of Transportation's University Transportation Centers Program. However, the U.S. Government assumes no liability for the contents or use thereof.

1. Report No. CIAM-UTC-REG5	2. Government Accession No.	3. Recipient's Catalog No.	
4. Title and Subtitle Strategic Prioritization and Planning of Multi-Asset Transportation Infrastructure Maintenance, Rehabilitation, and Improvements: Phase 1 – Prioritization through Optimization		5. Report Date December 2, 2021	
7. Author(s) Elise Miller Hooks, https://orcid.org/0000-0002-6849-2916 Sue McNeil, https://orcid.org/0000-0001-5983-8623 David Lattanzi, https://orcid.org/0000-0001-9247-0680 Kostas Papakonstantinou, https://orcid.org/0000-0002-5254-1066 Shelley Stoffels, https://orcid.org/0000-0002-2072-1521 Weiwen Zhou, Parastoo Kamranfar, Mohammad Saifullah, Charalampos Andriotis and Alexis Withers		8. Performing Organization Report No. LTI 2022-02	
9. Performing Organization Name and Address George Mason University 4400 University Drive Fairfax, VA 22030		10. Work Unit No. (TRAIS)	
12. Sponsoring Agency Name and Address U.S. Department of Transportation Research and Innovative Technology Administration 3rd Fl, East Bldg E33-461 1200 New Jersey Ave, SE Washington, DC 20590		11. Contract or Grant No. 69A3551847103	
15. Supplementary Notes Work funded through The Pennsylvania State University through the University Transportation Center Grant Agreement, Grant No. 69A3551847103.		13. Type of Report and Period Covered Final Report 03/01/2019 – 05/17/2021	
12. Sponsoring Agency Name and Address U.S. Department of Transportation Research and Innovative Technology Administration 3rd Fl, East Bldg E33-461 1200 New Jersey Ave, SE Washington, DC 20590		14. Sponsoring Agency Code	
16. Abstract This project advances technologies to support strategic planning of maintenance, repair, and rehabilitation options (improvement actions) and their implementation prioritization for our nation's roadway systems. The work takes a multi-asset approach with emphasis on pavements and bridges. It accounts for system-wide traffic impacts of postponed treatments, downtime impacts of construction work zones on traffic performance, and post-action benefits in terms of capacity and speed. It further incorporates uncertainty in system state due to stochasticity in the evolution of deterioration and its underlying physical processes. The technologies enable a deeper understanding of the nature of sensed data and its utility specific to the perception of roadway condition and the ability to detect deteriorated conditions and ascertain relationships between sensed condition and serviceability levels across assets. Performance indices, deterioration rates, and collected data are often significantly different between asset classes. Consequently, maintenance planning tools and managing practices often focus on only one distinct asset class, without integrating other asset types into their analysis, resulting in different asset classes competing for limited funds and suboptimal performance of the larger roadway network. Compatible serviceability assessments of individual asset types, as well as overall system serviceability, are directly supported. This effort provides important tools needed to enhance decision making. Opportunities to integrate these tools into existing software are identified. Phase 2 of the project will extend the work to provide case studies that demonstrate the benefits to enhanced safety, reliability, and durability of these more sophisticated decision-making tools.			
17. Key Words Pavement, bridge, maintenance, repair, rehabilitation, construction, roadway system, work zone		18. Distribution Statement No restrictions. This document is available from the National Technical Information Service, Springfield, VA 22161	
19. Security Classif. (of this report) Unclassified	20. Security Classif. (of this page) Unclassified	21. No. of Pages 136	22. Price

Table of Contents

<i>SUMMARY</i>	<i>X</i>
<i>INTRODUCTION</i>	<i>1</i>
Background.....	1
Objectives.....	1
Overview of the Methodology and Report.....	2
Report Outline.....	3
<i>PRIORITIZATION AND DECISION SUPPORT</i>	<i>5</i>
<i>INTRODUCTION</i>	<i>5</i>
State of the Practice versus State of the Art.....	7
Application.....	14
Anticipated Opportunities and Barriers to Implementation.....	15
<i>STOCHASTIC MODELING OF PAVEMENTS AND BRIDGES FOR CROSS-ASSET MANAGEMENT</i>	<i>16</i>
Introduction & Overview.....	16
Pavements.....	16
Bridges.....	27
Conclusion.....	32
<i>A REINFORCEMENT LEARNING METHOD FOR MULTI-ASSET ROADWAY IMPROVEMENT SCHEDULING CONSIDERING TRAFFIC IMPACTS</i>	<i>33</i>
Introduction.....	33
Literature Review.....	35
Mathematical Model.....	38
Solution Methods.....	42
Evaluating the Proposed Multi-Asset Roadway Improvement Scheduling Model and Solution Method on an Illustrative Network.....	49
Conclusions.....	57
<i>VALUE OF INFORMATION IN INFRASTRUCTURE ASSET MANAGEMENT POLICIES</i>	<i>59</i>
Introduction & Overview.....	59
Markov Decision Process.....	60
Partially Observable Markov Decision Process.....	62
Value-Based Information Gains.....	63
Numerical Application with Three-Component System.....	67
Conclusions.....	71

<i>PAVEMENT DISTRESS RECOGNITION VIA WAVELET-BASED CLUSTERING OF SMARTPHONE SENSOR DATA</i>	72
Introduction	72
Methodology	74
Experimental Evaluation	80
Conclusions	86
<i>SUMMARY, CONCLUSIONS AND FUTURE WORK</i>	87
Summary	87
Conclusions	87
Future Work	88
<i>REFERENCES</i> ⁹⁰	
<i>APPENDIX A: LIST OF ACRONYMS</i>	102
<i>APPENDIX B: TAMP THRESHOLDS AND TARGETS FOR BRIDGES AND PAVEMENTS</i>	104
<i>APPENDIX C: DECISION TREES</i>	114
Delaware	114
Maryland	116
Pennsylvania	117
Virginia	118
<i>APPENDIX D: MAINTENANCE ACTIVITIES AND GAMMA PROCESS PARAMETERS</i>	120
<i>APPENDIX E: STATE TRANSITION PROBABILITIES FOR ILLUSTRATIVE EXAMPLE</i>	122
<i>APPENDIX F: COST AND DURATION FOR IMPROVEMENT ACTIONS FOR ILLUSTRATIVE EXAMPLE</i>	124
<i>APPENDIX G: SARSA-LFA AND DCMAC PARAMETERS</i>	126
SARSA-LFA parameters	126
DCMAC parameters	127

List of Figures

Figure 2-1. Asset management elements.	6
Figure 3-1. Modeled mean CCI for different levels of traffic.	18
Figure 3-2. (a) Fitted gamma model, (b) s	19
Figure 3-3. Transition probabilities for Traffic level A, with (a) starting state = 6, (b) starting state = 5, smoothed over time with a 5-point window.....	19
Figure 3-4. Example of observation probability calculation for actual CCI = 55.	20
Figure 3-5. Transition probabilities in time, moving from states 9 (left) and 8 (right) to lower states.	28
Figure 4-1. Deep centralized multi-agent actor critic neural network (generated with NN-SVG (LeNail, 2019)).....	49
Figure 4-2. Roadway network.....	50
Figure 4-3. Expected total cost during SARSA learning for bilevel model (with traffic).....	52
Figure 4-4. Expected total cost evolution during learning by the DCMAC method applied on the bilevel model (with traffic).	53
Figure 4-5. Pavement states and decisions for pavement segment 3.	53
Figure 4-6. States and decisions for all pavements and bridges.	54
Figure 4-7. Costs under different values of ρ	54
Figure 4-8. Influence of including stochasticity in deterioration on realized cost of the optimal improvement action schedule (with $\rho = 0.05$).....	56
Figure 5-1. Probabilistic graphical model of a POMDP in time (shaded nodes denote hidden states).	63
Figure 5-2. Probabilistic graphical model of a POMDP as a belief-MDP in time (observations depend on states which are hidden).	63
Figure 5-3. Performance of different point-based POMDP algorithms in the three-component system problem, with $p=0.90$, for Setting 1 (optional monitoring setting).	69
Figure 5-4. Performance of different point-based POMDP algorithms in the three-component system problem, with $p=0.90$, for Setting 2 (permanent monitoring setting).	69
Figure 5-5. Policy realization of three-component system Setting 1 (optional inspection setting), with $p=0.90$, for all components.....	70
Figure 5-6. Policy realization of three-component system Setting 2 (permanent monitoring setting), with $p=0.90$, for all components.	70
Figure 5-7. Optimal value functions of three-component system for Settings 1 and 2 and respective VoSHM and VoI, for different observability levels.....	70
Figure 6-1. Schematic overview of the proposed framework.....	75
Figure 6-2. Common mother wavelet functions suitable for vibration signal (a) DB6 (b) Morlet.....	76
Figure 6-3. Good- versus poor-quality road condition from a user’s perspective: (a) z-acceleration signal, (b) spectrogram, and (c) scalogram from Morlet wavelet. All three diagrams detect two different behaviors in the signal, with the second starting after the first 30 seconds (first 6,000 samples).....	82
Figure 6-4. Distribution of known conditions over nine clusters recognized by hierarchical clustering.	84
Figure 6-5. Two roads with patching labels.....	85
Figure 6-6. (a) Earth Mover Distance matrix per class label among CWT feature distributions for 54 labeled data, (b) Earth Mover Distance matrix among CWT feature distributions of Pareto-optimal configuration.	86

Figure C-1. Delaware flexible pavement decision tree for structural distress. 115
Figure C-2. Delaware flexible pavement decision tree for non-structural distress..... 115
Figure C-3. Delaware flexible and composite pavement decision tree for IRI. 116
Figure C-4. Delaware flexible pavement decision tree for rutting. 116
Figure C-5. VDOT decision tree for preventive maintenance on bituminous interstate
highways (de León Izeppi, Morrison, Flintsch, & McGhee, 2015). 119

List of Tables

Table 2-1. Software systems used by selected states.	9
Table 2-2. Illustrative commercial asset management tools.	10
Table 3-1. State discretization based on CCI values.	19
Table 3-2. Observation probability $p(\mathbf{ot} \mathbf{st})$ given actual state \mathbf{st} , with $\sigma_{error}^2 = 72$	21
Table 3-3. Observation probability $p(\mathbf{ot} \mathbf{st})$ given actual state \mathbf{st} , with $\sigma_{error}^2 = 18$	21
Table 3-4. Inspection action costs (in USD/lane-mile or USD/m ²) for CCI using three different techniques.	22
Table 3-5. Minor Repair transition probabilities for 6 CCI states.	23
Table 3-6. Major Repair transition probabilities for 6 CCI states.	23
Table 3-7. Reconstruction transition probabilities for 6 CCI states.	23
Table 3-8. Maintenance action costs for asphalt pavements, reported in USD/m ²	24
Table 3-9. Maintenance actions duration in days per lane-mile.	24
Table 3-10. State classification based on IRI (m/km) values.	25
Table 3-11. Do Nothing transition probabilities for 5 IRI states.	25
Table 3-12. Minor Repair transition probabilities for 5 IRI states.	25
Table 3-13. Major Repair transition probabilities for 5 IRI states.	26
Table 3-14. Reconstruction transition probabilities for 5 IRI states.	26
Table 3-15. Observation probability $p(o_i s_i)$ for IRI given state s_i	27
Table 3-16. Pavement inspection cost (i.e., combined cost of IRI and CCI).	27
Table 3-17. Bridge failure probability given bridge condition state.	28
Table 3-18. Minor Repair transition probabilities for deck states.	29
Table 3-19. Major Repair transition probabilities for deck states.	29
Table 3-20. Reconstruction transition probabilities for deck states.	30
Table 3-21. Cost of maintenance actions in USD/m ²	30
Table 3-22. Maintenance action durations in days.	31
Table 3-23. Inspection action costs for three different techniques.	31
Table 3-24. Observation probability $p(\mathbf{ot} \mathbf{st})$ given state \mathbf{st} , for low-fidelity inspection techniques.	31
Table 3-25. Observation probability $p(\mathbf{ot} \mathbf{st})$ given state \mathbf{st} , for high fidelity inspection techniques.	32
Table 4-1. Contribution of most relevant works.	37
Table 4-2. Pseudo code for threshold-based method {N set to number of iterations}.	43
Table 4-3. Pseudo code for SARSA-LFA.	46
Table 4-4. Pseudo code for DCMAC.	48
Table 4-5. Roadway information.	50
Table 4-6. Road improvement cost and traffic delay cost (with $\rho = 0.05$).	52
Table 4-7. Multi-asset class versus single-asset class management (with $\rho = 0.05$).	57
Table 5-1. Individual component costs (negative rewards) of maintenance and observation actions for three-component deteriorating system.	69
Table 6-1. Pareto-optimal winners selected by internal evaluation metrics.	83
Table 6-2. Pareto-optimal winners selected by internal and external evaluation metrics.	83
Table 6-3. Distribution of samples with known conditions over nine clusters detected by Pareto-optimal winner.	85
Table B-1. Pavement targets and thresholds from TAMPs.	105
Table B-2. Bridge targets and thresholds from TAMPs.	109
Table B-3. FHWA Pavement condition rating system (Source: (Pennsylvania Department of Transportation, 2018))	113
Table B-4. FHWA Bridge condition rating system (Source: (Pennsylvania Department of Transportation, 2018))	113

Table C-1. PennDOT treatment strategies.	117
Table C-2. PennDOT treatments for bituminous pavements distress types.....	118
Table C-3. PennDOT treatment matrix for bituminous pavements for fatigue cracking.....	118
Table D-1. Maintenance activities for interstate and primary pavements under different categories (Virginia Department of Transportation, 2016).....	120
Table D-2. Gamma process scale and shape parameters, $f(t)$ and $g(t)$	121
Table E-1. State transition probabilities for pavements: Do Nothing.....	122
Table E-2. State transition probabilities for pavements: Minor Repair.	122
Table E-3. State transition probabilities for pavements: Major Repair.....	122
Table E-4. State transition probabilities for bridge decks: Do Nothing.....	123
Table E-5. State transition probabilities for bridge decks: Minor Repair.	123
Table E-6. State transition probabilities for bridge decks: Major Repair.	123
Table F-2. Duration of pavement improvement actions.....	124
Table F-3. Cost of improvement actions for bridges.....	124
Table F-4. Duration of bridge improvement actions.....	124
Table F-5. User cost for pavements.	125
Table F-6. User cost for bridges.....	125
Table G-1. Feature function	126

Summary

This project advances technologies to support strategic planning of maintenance, repair, and rehabilitation options (improvement actions) and their implementation prioritization for our nation's roadway systems. The work takes a multi-asset approach with emphasis on pavements and bridges. It accounts for system-wide traffic impacts of postponed treatments, downtime impacts of construction work zones on traffic performance, and post-action benefits in terms of capacity and speed. It further incorporates uncertainty in system state due to stochasticity in the evolution of deterioration and its underlying physical processes. The technologies enable a deeper understanding of the nature of sensed data and its utility specific to the perception of roadway condition and the ability to detect deteriorated conditions and ascertain relationships between sensed condition and serviceability levels across assets. Performance indices, deterioration rates, and collected data are often significantly different between asset classes. Consequently, maintenance planning tools and managing practices often focus on only one distinct asset class, without integrating other asset types into their analysis, resulting in different asset classes competing for limited funds and suboptimal performance of the larger roadway network. Compatible serviceability assessments of individual asset types, as well as overall system serviceability, are directly supported.

Outputs include artificial intelligence methods for extracting roadway quality metrics from crowdsourced smartphone data, which provide the ability to track roadway performance metrics over time for predictive purposes. Also developed are predictive models for multi-asset (pavement and bridge deck) condition metrics and network performance considering maintenance and rehabilitation actions, as well as monitoring data and inspection intervals and their precision. Multi-asset infrastructure system management is enabled through dynamic programming approaches and deep reinforcement learning. The project creates descriptive and normative implementations, with algorithms, of the multi-asset planning and prioritization problem as bilevel, stochastic mathematical programs with embedded Markov decision process concept and traffic system representation that enables assessment of state-based (threshold) maintenance strategies and development of a priori prioritization and scheduling.

This effort provides important tools needed to enhance decision making. Opportunities to integrate these tools into existing software are identified. Phase 2 of the project will extend the work to provide case studies that demonstrate the benefits to enhanced safety, reliability, and durability of these more sophisticated decision-making tools.

CHAPTER 1

Introduction

BACKGROUND

Advances in ubiquitous sensing enable enhanced predictive analytics and state-dependent decision making on the timing of maintenance, repair, rehabilitation, and improvement. The state of the assets can be provided in the form of measured serviceability levels, for example. Continuously sensed measurements from new data sources, such as pervasive imaging systems and connected vehicle sensor arrays, can be employed to supplement traditional data in identifying long-term system performance and usage trends and predicting the timing of categorical (level) changes.

Mathematical and algorithmic techniques are needed to exploit these information-rich, high-frequency sources in strategic prioritization of projects and allocation of resources. These techniques ideally explicitly consider uncertainty in measurements and future deterioration rates. They enable the quantification of risk and system-wide consequences of postponed action. The benefits of timing treatments in response to current and updated predicted state changes as sensed, that is, state-based action, can be assessed off-line and demonstrated on a chosen application.

Performance indices, deterioration rates and collected data are often significantly different between asset classes. Consequently, maintenance planning tools and managing practices often focus on only one distinct asset class, without integrating other asset types into their analysis, resulting in different asset classes competing for limited funds and suboptimal performance of the larger roadway network. Furthermore, the actions for any one class of assets result in service disruptions that are manifested across asset classes and influenced by network topology.

In this project, the strategies utilized to support strategic planning with the support of continuously sensed data are explored considering compatible serviceability assessments of individual asset types, with emphasis on pavements and bridges, as well as overall system serviceability. The project consists of two phases. The first phase assembles the data, models, tools, and methods to support the project and includes an exploration of data from mobile phones. The second phase extends this work to other types of data, specifically exploiting continuously sensed data for condition assessment and integrating partial information on condition in the prioritization tool, and exploring other networks. This report presents the results for Phase 1.

OBJECTIVES

The objectives of the first phase of this project are to explore and develop:

- Condition monitoring and forecasting capabilities that exploit continuously sensed data technologies;
- Algorithms that incorporate continuously sensed asset condition states and updated forecasts in strategic planning of maintenance, repair, and rehabilitation options and their implementation prioritizations;

- Methods that explicitly account for uncertainty in state predictions; and
- Tools that can be deployed in practice for large, complex roadway networks.

Outcomes of the first phase are:

- A deeper understanding of the nature of crowdsourced vehicle response data and its utility;
- Quantification of the value of information regarding asset condition;
- Assessment of existing practices in asset management decision making;
- Development of probabilistic predictive models of roadway systems;
- Conceptualization of the multi-asset, strategic planning of maintenance, repair, and rehabilitation options (improvement actions) and their prioritization for implementation as a bilevel, stochastic mathematical program;
- Solution algorithms based on concepts of machine learning;
- Comparison to existing mathematical modeling approaches;
- Comparison of optimally derived prioritized schedules; and
- Connection to current practices.

OVERVIEW OF THE METHODOLOGY AND REPORT

This work supports strategic long-term planning for maintaining and repairing our roadway systems. Phase 1 of the project is structured around five tasks leading to the development of this report. The task descriptions outline the methodology used and are summarized as follows:

- **Task 1. Predictive analytics:** Machine-learning techniques are adapted for interpreting new forms of continuously collected data. The emphasis is on dynamic response measurements from on-board accelerometers and on-board imaging systems, data increasingly available on a continuous basis from connected vehicle communications technology. Originally, it was anticipated that such data were readily available in open databases. This proved to not be the case and data had to be collected. Algorithms were designed to autonomously identify long-term system performance trends in support of asset management and decision making. This was achieved through high-dimensional feature-space analysis of the signal data, adapting recent advances in speech recognition and language processing. Ultimately, the results of this task will support the decision making and prioritization aspects of subsequent tasks.
- **Task 2. Estimating and controlling serviceability of assets in multi-asset systems:** Models are based on a comprehensive literature review including state DOT practices to predict the effects of inaction on asset serviceability, as well as controlling effects of available maintenance, repair, and rehabilitation actions, at component and system levels. This information is employed to update anticipated timing of categorical (level) serviceability changes. Particular emphasis is on measures of serviceability that will reflect the information obtained from continuously sensed data. The relevant Value of Information (VoI) framework is theoretically derived. Pavements and bridges are the focus, but the models can be extended to other asset classes. Serviceability objectives and metrics considered include measurements of travel time, ride quality, and remaining life, among others.
- **Task 3. Prioritization techniques:** Models and algorithms for state-dependent decision making on the timing of maintenance, repair and rehabilitation actions

are created. The developed techniques exploit discrete information and serviceability forecasts in prioritizing and scheduling preventative and restorative actions, along with needed resources, while explicitly accounting for uncertainty in condition assessments and future deterioration rates. The techniques can be extended for assessing risk of deferred action due to other priorities or lack of funding.

- **Task 4. Decision tools:** Opportunities to integrate and embed predictive analytics, serviceability estimation, prioritization, and resource allocation techniques in decision support tools for strategic planning are identified. The barriers and opportunities for using these tools in practice and on large-scale, complex roadway networks are considered.
- **Task 5. Evaluation and demonstration:** The benefits of timing treatments in response to updated sensed or predicted state changes, that is, state-based action, are assessed off-line and demonstrated on a modest network, including the value of cross-asset optimization methods in place of single asset-class methods currently used in practice. Techniques from all earlier tasks are revisited based on evaluation findings.

The techniques developed through this effort enhance condition-state monitoring and prediction, as well as current time- and threshold-based approaches to strategic planning of maintenance, repair, and rehabilitation scheduling of roadways and bridges (and can be extended to other assets such as light poles, pavement markings, and tunnels). By explicitly recognizing the uncertainty in deterioration rates and impacts of service actions, as well as impacts on traffic flows of reduced serviceability, the techniques can then be used to quantify the risk and system-wide consequences of postponed or reduced action. Additionally, through enhancing prediction capabilities, this effort projects future maintenance, repair, and rehabilitation needs.

REPORT OUTLINE

In addition to this introductory chapter, the report is organized in five chapters:

- Chapter 2: Prioritization and Decision Support. This chapter connects the research to asset management requirements and practices, and documents the current practices in state DOTs.
- Chapter 3: Stochastic Modeling of Pavements and Bridges for Cross-asset Management. This chapter reviews the processes, performance measures for serviceability, and costs and durations of various actions to preserve, maintain, and enhance pavements and bridges.
- Chapter 4: A Bilevel Reinforcement Learning Method for Multi-Asset Roadway Improvement Scheduling Considering Traffic Impacts. This chapter develops optimal strategies for prioritizing actions. This chapter has been prepared as a paper that has been submitted to *Journal of Infrastructure Systems* for review.
- Chapter 5: Value of Information in Infrastructure Asset Management Policies. This chapter presents an analysis of value-based information metrics and their computation for no information, optional inspection visits, and continuously available condition information. This chapter is largely based on the published paper: “Value of structural health information in partially observable stochastic environments” (Andriotis, Papakonstantinou, & Chatzi, 2021).
- Chapter 6: Pavement Distress Recognition via Wavelet-Based Clustering of Smartphone Sensor Data. This chapter presents a framework for processing

crowdsourced data for pavement distress. An earlier version of this chapter was submitted to the *Journal of Computing in Civil Engineering* for review.

- Chapter 7: Summary, Conclusions, and Future Work. This chapter presents a summary of and conclusions from the Phase 1 project and an outline of the Phase 2 project.

In addition, appendices provide supporting data developed as part of the project. Appendix A is a list of acronyms. Appendix B presents the pavement and bridge thresholds and targets used for each. Appendix C documents the decision trees used for pavement decisions in the Mid-Atlantic states. Appendix D provides details of the maintenance actions and deterioration models developed in Chapter 3. Appendices E through G provide the supporting details for the illustrative example in Chapter 4.

CHAPTER 2

Prioritization and Decision Support

INTRODUCTION

Asset management processes have been adopted by state departments of transportation in response to legislative requirements to use these processes to support decision making related to pavements and bridges on the National Highway System. These roadway assets function to provide a service to the users but these assets also degrade with time and age and require frequent maintenance and upgrading. Scheduling such upgrades must account for the impacts on the users, but there is a significant gap between the methods in the literature and current decision support tools that are embedded in asset management practices. This chapter provides the context and background for the tools developed in this research. The challenges in developing the necessary inputs, solving a real-world network, and interpreting the results are presented in the context of the asset management processes used by most state departments of transportation.

Background and Context

Aging transportation infrastructure, traffic growth, higher expectations for improved mobility, accessibility and safety, and a declining funding base for infrastructure renewal and improvement place pressure on decision-makers. The need to do more with less underscores the role transportation asset management plays in the maintenance and renewal of these assets.

Moving Ahead for Progress in the 21st Century Act (MAP-21) (112th Congress, 2012), the surface transportation legislation from 2012, required performance-based management and the development of risk-based asset management plans. The subsequent 2015 legislation Fix America's Surface Transport (FAST) Act (114th Congress, 2015) reinforced this. The final rule "Asset Management Plans and Periodic Evaluations of Facilities Repeatedly Requiring Repair and Reconstruction Due to Emergency Events" requiring each state to develop and maintain a risk-based asset management plan for pavements and bridges on the National Highway System (NHS) to improve or preserve the condition of the assets and the performance of the system became effective in October 2017 (FHWA, 2016).

Asset management is a strategic and systematic process of operating, maintaining, and improving physical assets, with a focus on engineering and economic analysis based upon quality information, to identify a structured sequence of maintenance, preservation, repair, rehabilitation, and replacement actions that will achieve and sustain a desired state of good repair over the lifecycle of the assets at minimum practicable cost. (23 U.S.C. 101(a)(2), MAP-21 § 1103) (112th Congress, 2012)

The fundamental elements of asset management are shown in the generic asset management process in Figure 2-1. A key element is "Alternative Evaluation and Program Optimization" and takes as input the asset inventory, condition, and performance modeling. This element addresses the challenges in managing these assets. This element is implemented using many different strategies, constraints, scopes, scales, and timeframes. For example, the optimization may occur within a program (such as a pavement or bridge program) or across

programs (scope). The evaluation of alternatives may simply be based on the cost of the action to the agency, the lifecycle costs, user costs including delays and disruptions, or a lifecycle assessment. The decisions can include uncertainty. Different districts, jurisdictions, or regions (scale) can be recognized. The decisions can be optimized for a year, a program (e.g., 5 or 10 years), or over the life of a project or network (timeframe).

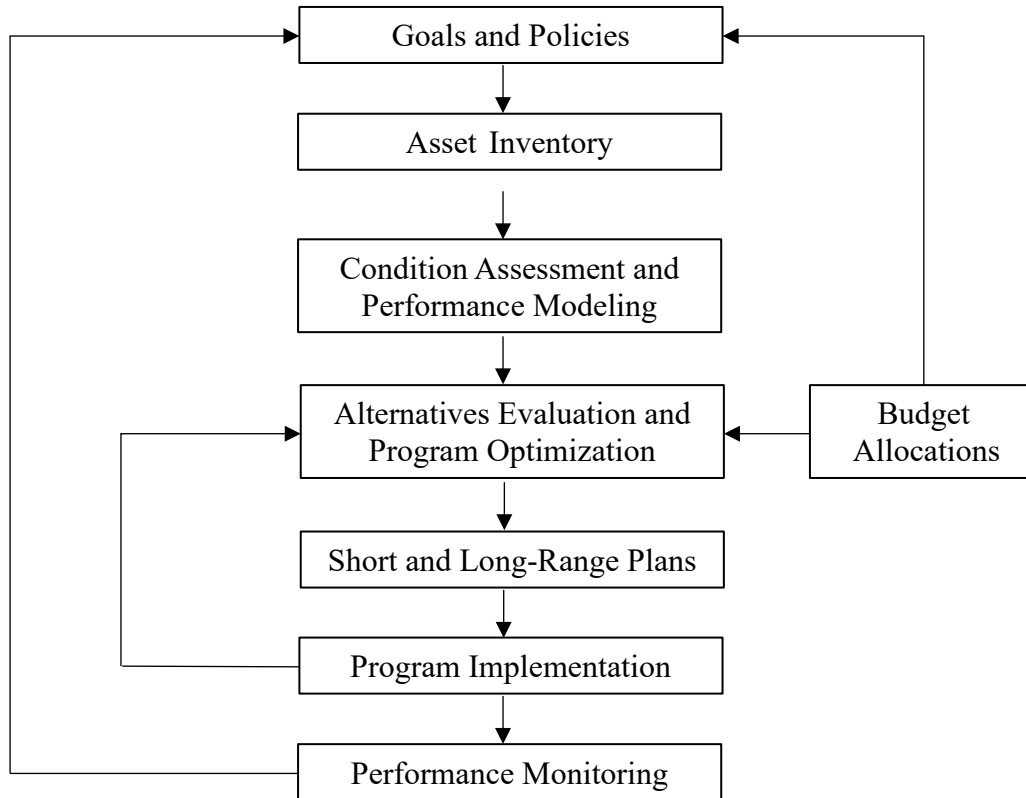


Figure 2-1. Asset management elements.

The simplest evaluations are rank and prioritize activities (Haas, Hudson, & Cowe Falls, 2015). The more sophisticated and complex asset management tools use optimization to make decisions that select and prioritize activities. Formulations, which define the decision variables, objective function, and constraints, are classified as project or network level, single objective, or multi-objective, and deterministic, heuristic, or other (Chen & Bai, 2019). Another classification also considers whether the decision variables are discrete or continuous and whether uncertainty is considered. Optimization problems can also be classed as activity selection, scheduling, or both selection and scheduling. Invariably optimization problems focus on a discrete set of locations and activities, a finite time period (planning horizon), the condition of the asset, and the agency cost. To simplify the solution process or reduce the size of the solution space, assumptions are usually made. The assumptions limit the scale (for example, a class of roads, or a particular jurisdiction), the type of activities (for example, maintenance or rehabilitation), the type of assets (for example, pavements or bridges, although they are part of the same network), and the time frame (for example, 1 year, 5 years, or 10 years) considered.

Recognizing the importance of condition and its evolution as a performance measure, this research accounts for new types of condition data and the influence of facility downtime on users’ travel decisions. A bilevel program prioritizes and schedules roadway improvement activities recognizing users’ costs and disruption (Zhou, Miller-Hooks, Papakonstantinou, Stoffels, & McNeil, 2021). The upper level involves a Markov decision process (MDP) to

identify and prioritize potential roadway improvement actions. The MDP approach accounts for uncertainty in system component states reflecting roadway degradation over time while also capturing the benefits of improvement actions that are taken. The upper level takes as input estimates of traffic flows (obtained from the lower level), which affects roadway serviceability. The lower level seeks to determine traffic flows based on a network user equilibrium solution across paths that is affected by capacities determined through actions determined at the upper level. The optimal solution is obtained at a Stackelberg equilibrium between upper and lower-level programs. Karush–Kuhn–Tucker (KKT) conditions are applied to reduce the bilevel model to an equivalent, single-level program. The KKT conditions include nonlinear complementarity constraints that can be linearized through the inclusion of binary variables. As solution of the resulting stochastic mixed-integer linear program is formidable, a reinforcement learning method is applied.

In addition to the challenges involved in solving these problems, acquiring realistic data and relevant deterioration models is another challenge. There is also a fear of “black box” solutions. Given this context, this paper addresses the following research questions:

- How do optimization tools compare with common approaches used in practice in terms of data of needs and benefits?
- What does it take for state departments of transportation to implement sophisticated decision support algorithms?

The following section reviews the state of the art versus the state of the practice regarding decision making and optimization in asset management practice. The subsequent section structures an application based on the bilevel program tool. This section reviews the data and models required for its implementation, describes a proposed case study based on a realistic network, and presents the scenarios implemented including evaluation and validation. The final section presents anticipated opportunities and barriers to implementation.

STATE OF THE PRACTICE VERSUS STATE OF THE ART

Different tools are used to make decisions related to improvements to pavements and bridges for different purposes and at different levels of government. Consider the following three examples for pavements. The first example is the Highway Economic Requirements System (HERS). HERS is used to advise Congress on setting budgets (Government Accountability Office, 2000; Bryce, Elkins, & Thompson, 2020). In HERS, decisions about pavement improvements are made on the basis of an incremental benefit-cost analysis. A second example are the thresholds and targets that are used to make strategic decisions as part of the state Transportation Asset Management Plans (TAMPs). A third example are the decision trees that are commonly part of the pavement management systems used by state DOTs. In this section, the federal asset management requirements for state Departments of Transportation (DOTs) are reviewed, together with the existing software tools used to support these requirements and asset management more generally. The role optimization plays is also reviewed. The section concludes with an analysis of the gaps between practice and the state of the art.

Likewise, there are tools to support asset management for bridges for different purposes. For example, similar to HERS, the National Bridge Investment Analysis System (NBIAS) analyzes bridge investment needs based on lifecycle scenarios and increment benefit-cost analysis (Robert, 2018). A second example for bridges is the AASHTOWare™ Bridge Management (BrM) tool (Johnson & Boyle, 2017). BrM assesses the utility of decisions.

Asset Management Requirements

The Moving Ahead for Progress in the 21st Century Act (MAP-21) (112th Congress, 2012), the surface transportation legislation from 2012, required performance-based management and the development of risk-based asset management plans. The subsequent 2015 legislation, Fix America’s Surface Transport (FAST) Act (114th Congress, 2015), reinforced this requirement. The final rule, “Asset Management Plans and Periodic Evaluations of Facilities Repeatedly Requiring Repair and Reconstruction Due to Emergency Events,” requiring each state to develop and maintain a risk-based asset management plan for the National Highway System (NHS) to improve or preserve the condition of the assets and the performance of the system, became effective October 2017 (FHWA, 2016). Although focused on pavements and bridges on the National Highway System, the rules require state DOTs to develop investment strategies to achieve and sustain a state of good repair over the lifecycle of the asset, to improve or preserve condition, and to achieve targets for asset condition and performance.

Software Tools

State DOTs use a variety of homegrown and commercial off-the-shelf tools (COTS), often with some degree of customization, to perform asset management. Some of these tools are specific to a class of assets, others are purpose built to address specific issues. Table 2-1 summarizes the tools used by eight states participating in an FHWA-sponsored asset management peer exchange in 2020 (FHWA, 2021), as well as the tools identified in the Transportation Asset Management Plans of states in the mid-Atlantic region (excluding Maryland, as the plan is not publicly available) and some selected other states. The table distinguishes among Enterprise Systems, Bridge Management, Pavement Management and Routine Maintenance to reflect how states are organized. Clearly there are common functions and data.

The table illustrates the variety of software. Commercial products are italicized. AASHTO or FHWA products are shown in bold. The remaining systems are developed in-house. For these selected states, no state has a single platform or tool to support asset management but uses a variety of tools and platforms to provide access to data, models, and decision support tools. Several vendors offer integrated platforms that are continuously evolving. Table 2-2 provides a snapshot of some of these resources and the attributes based on information on websites, presentations, and marketing material to provide a sense of the resources available. While most vendors claim to optimize decisions and consider cross-asset tradeoffs, the methods used are not described or accessible.

Table 2-1. Software systems used by selected states.

State	Enterprise Systems of Record (SoR)	Bridge Management	Pavement Management	Routine Maintenance
Connecticut (1)	Transportation Enterprise Database (TED)	<i>dTIMS</i> <i>InspecTech</i>	<i>dTIMS</i>	Maintenance Management System (MMS)
Delaware (2)	Transportation System Data Management (TSDM)	AASHTOWare™ Bridge Management (BrM)	<i>AgileAssets</i> <i>Pavement Analyst</i>	Maximo
District of Columbia (3)		BrM	Paver	SABER (Tunnel Management), CityWorks
Hawaii (4)		BrM	BrM (customized for pavements)	
Indiana (5)	<i>Arc GIS Roads and Highways</i>	National Bridge Investment Analysis System (NBIAS)	<i>dTIMS</i>	<i>Agile Assets</i>
Michigan (5)	<i>Arc GIS</i>	BrM	Project Identification Tool (PIT)	<i>VueWorks</i>
Minnesota (5)		BrM, Bridge Information Modeling (BrIM), InspecTech	Highway Pavement Management Application (HPMA)	<i>AgileAssets</i>
New York (5)	Systems of Engagement (SoE); <i>AgileAssets – Enterprise Asset Management Project (EAMP)</i> <i>Arc GIS Roads and Highways (LRS)</i>	Bridge Data Information System (BDIS), Structure Management System (SMS)	Pavement Management System (PMS)	Maintenance Management System (MMS)
North Dakota (5)	<i>Arc GIS, Arc GIS Roads and Highways</i>	BrM	<i>dTIMS</i>	
Ohio (5)	Transportation Information Mapping System (TIMS), <i>Arc GIS Collector, Arc GIS Roads and Highways</i> , Ellis (capital projects)	BrM	<i>dTIMS</i>	<i>Enterprise Information Management System (EIMS)</i>
Pennsylvania (5)	Bridge Management System 2 (BMS2), Roadway Management System (RMS), Engineering and Construction Management System (ECMS)	BridgeCare	<i>dTIMS</i> RoadCare	
Rhode Island (6)	<i>Arc GIS Roads and Highways, VueWorks</i>	BrM	<i>dTIMS</i>	
South Carolina (7)		Highway Maintenance	Pavement	Highway Maintenance

State	Enterprise Systems of Record (SoR)	Bridge Management	Pavement Management	Routine Maintenance
		Management System (HMMS) Bridge Deficiency Module BrM	Management System (PMS)	Management System (HMMS)
Virginia (8)		BrM	<i>AgileAssets</i> <i>Pavement Analyst</i>	Pavement Maintenance Scheduling System (PMSS)
West Virginia (5)	<i>Arc GIS Roads and Highways</i>	<i>InspecTech</i> <i>BMS</i>	<i>dTIMS</i>	

Sources: (1) (Connecticut Department of Transportation, 2019); (2) (Delaware Department of Transportation, 2019); (3) (District Department of Transportation, 2019); (4) (Hawaii Department of Transportation, 2019); (5) (FHWA, 2021); (6) (Rhode Island Department of Transportation, 2019); (7) (South Carolina Department of Transportation, 2019); (8) (Virginia Department of Transportation, 2019).

Table 2-2. Illustrative commercial asset management tools.

Vendor	Software	Optimization	Cross Asset Tradeoffs	Website
AgileAssets	Transportation Asset Lifecycle Management Solution	✓	✓	https://www.agileassets.com/
AssetWorks	AssetWorks	✓		https://www.assetworks.com/
Deighton Associates	dTIMS	✓	✓	https://www.deighton.com/
Bentley	Assetwise InspecTech			https://www.bentley.com/en/products/brands/assetwise
ESRI	ArcGIS Roads and Highways	✓		https://www.esri.com/en-us/arcgis/products/arcgis-roads-highways/overview
DTS	VueWorks	✓		https://www.vueworks.com/

AASHTO also supports the Multi-Objective Decision Analysis Tool (MODAT) that supports cross-asset tradeoffs (Maggiore & Ford, 2015; National Academies of Sciences, Engineering, and Medicine, 2019). The tool requires the input of potential projects details, including the measures, costs, and objectives. The scale of measures can be either linear or logistic with defined parameters. Measures may be weighted in terms of the contribution to the objectives. Two different methods can be used to prioritize projects based on the overall budget specified:

- Weighted score, a linear combination of the weighted measures and the weighted objectives, and
- Data envelopment analysis, which does not use the subjective weights but chooses weights to optimize the efficiency of each project.

MODAT includes visualization tools and documents that analysis. Either method depends on expert judgement to determine the weights of the measures.

In addition, some states use generic decision support software such as Decision Lens, which is based on the analytical hierarchical process.

Decision Support Tools: State of the Art

There is a large body of literature of decision support tools for asset management. Building from work in pavement management, the seminal work of Golabi, Kulkarni and Way (Golabi, Kulkarni, & Way, 1982) served as a foundation for advanced and more sophisticated optimization of maintenance and resurfacing decisions for pavements that recognized deterioration and uncertainty and then extended the work to bridges.

A comprehensive review of the state of the art is beyond the scope of this project. Some recent review papers provide an overview and context. Chen and Bai (Chen & Bai, 2019) review over 300 papers on optimization in asset management. Chen et al. (Chen, Liang, Wu, & Sun, 2019) provide a review of optimization in transportation asset management for roads and bridges. Chen et al. (Chen, Henning, Raith, & Shamseldin, 2015) focus on multi-objective optimization for maintenance decisions. These papers provide a clear picture of the variety of approaches to the problem formulation and solution methods, both of which are tailored to a particular application.

Optimization in Practice

A review of the selected state DOTs' Transportation Asset Management Plans revealed¹ that most states aim to optimize their investments but do not optimize in the mathematical sense of the word. The selected states included all Region 3 DOTs except Maryland (Delaware, District of Columbia, Pennsylvania, Virginia, and West Virginia) and a range of other states (Alaska, California, Connecticut, Hawaii, Minnesota, New Hampshire, North Carolina, Rhode Island, South Carolina, Virginia, Washington, and West Virginia), reflecting different geography, size, and types of assets.

At best, the states optimized investment in their bridge program or pavement program. Most conduct scenario analysis and explore alternative strategies. However, the TAMPs do recognize the value of optimization, the potential gains, and the importance of good models and reliable data. The following quotes illustrate the range of sentiments expressed in the TAMPs:

¹ The plans were downloaded from the FHWA website that serves as a repository for TAMPs (http://www.tamptemplate.org/existing-tamp/?fwp_sections=11-risk) or from the AASHTO TAMP Library (<https://www.tamptemplate.org/existing-tamp/>).

- Alaska DOT (Alaska Department of Transportation & Public Facilities, 2019): In the message from the Commission, “We must become as skilled at optimizing the life-cycle planning and overall performance of transportation assets as we are traditionally at engineering and building them.”
- California DOT (Caltrans, 2018): From the section on risk, “If we do not have reliable asset performance models (including reliable decay rates and reasonable goals), then investment decisions will not be optimal.”
- Connecticut DOT (Connecticut Department of Transportation, 2019): A TAM objective is to “Deliver an efficient and effective program to optimize the life of our infrastructure.” An incremental benefit-cost analysis is used to optimize investments in pavements and bridges independently. The need to optimize cross-asset decisions is also recognized.
- Delaware DOT (Delaware Department of Transportation, 2019): The TAMP aligns with the first principle of the Long-Range Transportation Plan: “system preservation and optimization.” For pavements, the optimization uses benefit as the objective function and costs as the constraint. For bridges, scenario analysis is based on maximizing utility or minimizing costs, both subject to performance constraints.
- District DOT (District Department of Transportation, 2019): District DOT’s TAMP, in the section on pavement performance targets, states “the application of good practice asset management can enable DDOT to optimize available resources and performance.”
- Hawaii DOT (Hawaii Department of Transportation, 2019): Hawaii DOT uses a weighted benefit-cost ratio to select work actions for bridges based on a score. The results are used to develop an “optimal” long-term network-level strategy.
- Minnesota DOT (Minnesota Department of Transportation, 2018): From the section on investment priorities, “The infrastructure preservation investments documented in this TAMP are targeted to optimize investments in asset management (considering fiscal constraints) while making progress toward established goals and objectives.”
- New Hampshire (New Hampshire Department of Transportation, 2019): The New Hampshire DOT plan seeks to “optimize employee health and safety” and states that operations and maintenance activities “optimize performance and existing capacity.”
- North Carolina (North Carolina Department of Transportation, 2019): Pavement and bridge treatments are optimized based on lifecycle cost analysis.
- Pennsylvania DOT (Pennsylvania Department of Transportation, 2018): Discusses optimal decisions in the context of lowest lifecycle costs (LLCC), “The combination of forecasts with professional judgment representing various viewpoints and in-depth data allows the optimal choices to be made in order to maintain the system to LLCC.”
- Rhode Island Department of Transportation (Rhode Island Department of Transportation, 2019): The network-level LCCA for pavements uses an optimization procedure that considers the objective and the resource constraints. The investment strategies are based on three optimization options: (1) maximizing benefits based on incremental benefit-cost ratios, (2) maximizing benefits using other criteria, and (3) minimizing cost. The performance gap analysis presents three targets: (1) optimal performance, (2) planned performance, and (3)

deteriorating performance. The optimal performance achieves and maintains a state of good repair for all bridge assets and NHS pavement assets.

- South Carolina DOT (South Carolina Department of Transportation, 2019): A guiding principle is “to optimize investments” and the 10-year performance outcome is “to optimize system performance.” The target-setting process is intended to “provide optimal preservation/rehabilitation choices.” In action items, SCDOT plans to “Investigate alternative methods for cross-asset resource allocation, tradeoff analysis, and optimization to achieve system objectives.”
- Virginia DOT (Virginia Department of Transportation, 2019): The lifecycle decisions are “intended to optimize available funding to meet network performance goals.” Optimized pavement and bridge needs and investments are identified using existing tools.
- Washington DOT (Washington State Department of Transportation, 2018): Identifies the following system improvements to optimize asset management: (1) add other asset information into the web-based project management system; (2) create GIS Asset Management Web Application; (3) address bridge recommendations from a 2014 Study; (4) implement AASHTO Bridge Management Software (BrM); (5) strengthen the relation between assets and transportation projects; (6) increase management system functionality; and (7) implement use of priority and resource optimization software (Decision Lens).
- West Virginia (West Virginia Division of Highways, 2019): Uses scenario analysis to perform lifecycle optimization analysis using various objectives (utility or cost) and constraints (budgets or performance targets).

Overall, the states are aiming to develop optimal plans that deliver the best serviceability given the budget constraints. Invariably, the implementations focus on independently reached optimization decisions for pavements and bridges based on a predefined set of scenarios. Essentially, the objective function is computed for each scenario that meets the constraints and the “optimal” solution chosen. Given the fact that there are many tradeoffs in terms of actions, timing, and location, it is possible for an optimal solution to be overlooked. However, given that scenarios are developed based on experience and data, the optimal solution selected is likely to be very desirable, and for the given problem and objective, either optimal or near optimal.

Gaps

Thresholds for determining when to undertake a maintenance or improvement activity, decision trees, simulation, and scenario analysis are widely used in practice. While the strategies have proven to be effective for pavements and bridges independently, the need to consider cross-asset tradeoff and integrate more complex objectives, such as users’ costs, disruption, and sustainability, adds to the complexity. On the other hand, the “black box syndrome” means that agencies are skeptical of the outputs from elaborate mathematical models. Wang and Pyle (Wang & Pyle, 2019) recommend engaging the users, verification of results, and continued validation.

Another important gap in developing and implementing optimal decisions is the difficulty in assembling the required data. These problems require current and predicted condition, the cost of implementing an action, the impact of the action in terms of the changes to the condition and the future condition, and the impacts for the users, including changes in travel time and disruption. Ideally, the decisions should capture the changes in users’

behavior, any safety or security concerns, any damage to vehicles, and the relationship among the projects. Interdependencies can be physical or functional.

This is important because data collection is costly, and resources for maintaining and improving roads are scarce. Taking advantage of innovative data collection methods, more accurate and more timely data, and making better use of resources is important. Although agencies may not implement an “optimal” solution, exploring alternative solution methods provides insight into the factors that influence these decisions and will ultimately help agencies to deliver better transportation services.

APPLICATION

The application of the results of this research requires data and models to support the appropriate decisions. While subsequent chapters elaborate on these data and models, this section outlines the potential sources and case studies, as well as the parameters that need to be explored in a sensitivity analysis of their application. These applications will be pursued in Phase 2 of this project.

Data and Models Needed and Availability

The basic data and models needed to identify appropriate actions are of three types:

- Network inventory and condition: Typically, a network is depicted as a series of connected links. The network information includes link connectivity and link attributes, such as length and capacity. Usage is in the form of an origin-destination (O-D) matrix and may be differentiated by vehicle class and time of day. Condition data for each link is also critical. Potential forms are discussed in Chapter 3 and potential sources are discussed in Chapter 7.
- Potential maintenance and improvement actions: These actions are the decision variables (the decision is commonly represented as a binary variable indicating whether the action is taken or not). Actions can be differentiated by location and time of occurrence. Decisions require knowledge of costs, duration of activity, impact on capacity during and after the activity, and impact on condition after completion. These data are described in more detail in Chapter 3.
- Deterioration models: These models, in this case Markov transition probabilities, are needed to understand how condition changes over time. These models are discussed in Chapter 3.

In Phase 1 of the research, data collected from Northern Virginia are used to illustrate new data sources but are not integrated into the decision-making process. The decision-making process uses a simple network modified from (Medury & Madanat, 2013) to demonstrate the concepts.

Phase 2 will explore more elaborate network models. While a variety of networks have been considered, the Hampton Road network (see <https://www.hrpdcva.gov/page/maps/> and <https://www.hrtpotip.org/>) will be utilized, as the network is well-documented and has adequate complexity to illustrate the application and explore the relevant scenarios, compare the results to thresholds and decision trees, and complete a sensitivity analysis.

Analysis, Evaluation and Validation

To analyze our findings, multiple scenarios will be considered to explore the sensitivity of the results to changes in inputs, to explore, qualitatively and quantitatively, whether the models and the results are logical and consistent. The scenarios include changes to the following variables and models:

- Discount rate,
- Costs including treatment cost and value of time,
- Traffic predictions including growth rates,
- Deterioration prediction including different parameters and models,
- Observed condition including the quality of the data and the frequency at which data are updated,
- Relationship between traffic and condition, for example, accounting for lower speeds on roads with very poor conditions, and
- Role of downtime as captured by the weight parameter.

The analysis in Phase 1 includes some limited exploration of the impacts of the changes in these variables and models. Phase 2 will include a more systematic analysis.

Phase 2 will also involve a comparison of the results to existing methods commonly applied. In preparation for this comparison, materials are assembled for targets, thresholds, and decision trees. Appendix B summarizes threshold-based decision methods and targets for pavements on the National Highway System for all states as reported in the Transportation Asset Management Plan (TAMP). Appendix C documents the decision trees used in the six Mid-Atlantic states for pavement-related decisions.

The case study is also intended to provide insights into the decision making that can be used to determine appropriate policies and budgets and to enhance asset-specific tools.

ANTICIPATED OPPORTUNITIES AND BARRIERS TO IMPLEMENTATION

Asset management, the strategic prioritization and planning of transportation infrastructure maintenance, rehabilitation, and improvements, is a data-driven process aimed at delivering the best levels of services given the available resources. Practices vary in sophistication and purposes and range from establishing policies and budgets, to demonstrating the connections between outcomes and investments, to selecting and scheduling specific actions. This project supports the selection and scheduling of actions, which in turn supports the other strategic initiatives.

Opportunities for improving strategic prioritization and planning of transportation infrastructure maintenance, rehabilitation, and improvements abound. This project focuses on new data sources, accounting for uncertainty in deterioration, integrated user impacts, specifically the cost of disruption and understanding cross-asset tradeoffs. This involves exploring new data sources, enhancing existing deterioration models, and formulating and solving an alternative optimization model. The objective is to enhance condition and minimize user disruption by coordinating actions. Most importantly, the network impact and the impacts of downtime are recognized and accounted for.

While there are many opportunities to enhance these decision-making processes, there are also many barriers. These barriers include:

- The prevalence of commercial software to support state DOT asset management activities that use widely accepted methods, but the details are not accessible, nor are the codes open source;
- Concern among agencies that the outputs from “black boxes” or complex mathematical relationships are not transparent;
- A perception that the data needed to support new models and decision support tools are not available; and
- “Siloing” of decision support functions, which makes cross-asset tradeoffs difficult.

These barriers can be addressed through demonstrations and dissemination of new methods and research results.

CHAPTER 3

Stochastic Modeling of Pavements and Bridges for Cross-Asset Management

INTRODUCTION & OVERVIEW

Cross-asset management is essential nowadays with all the challenges facing the U.S. Department of Transportation (U.S. DOT), particularly the deteriorating infrastructure and the scarcity of resources. According to the 2021 ASCE infrastructure report card (ASCE, 2021), the nation's infrastructure is in fair to poor condition with a cumulative rating of C-, with elements approaching the end of their service life and having a high risk of failure. Pavements and bridges are part of this poor infrastructure: 1 out of every 5 miles of pavement in the United States is in poor condition, while 7.5% of the nation's bridges are structurally deficient. However, DOTs have been changing their decision-making strategies to meet the serviceability demand. Thus, comprehensive modeling, which can incorporate multiple aspects of infrastructure assets over their lifecycle, such as structural degradation, age-related deterioration rates, different maintenance actions, and lifecycle costs, is needed now more than ever, so that it can be readily utilized for solving optimal planning and control problems for large transportation networks.

In this work, we approach the modeling of infrastructure degradation and management using Markov decision processes and partially observable MDPs (POMDPs), as reported in the literature (Madanat & Ben-Akiva, 1994; Papakonstantinou & Shinozuka, 2014; Papakonstantinou, Andriotis, & Shinozuka, 2018; Madanat S. , 1993). Many attempts have been made to solve optimal infrastructure management problems using stochastic models, some of which utilize stationary Markovian transition probabilities for bridges (Saydam & Frangopol, 2014; Frangopol, Lin, & Estes, 1997) and pavements (Madanat S. , 1993; Madanat & Ben-Akiva, 1994; Faddoul, Raphael, Soubra, & Chateauneuf, 2013). However, many studies have only considered hypothetical scenarios and have assumed stationarity for the transition probability models.

In this chapter, a holistic modeling environment of both pavements and bridges is developed based on their corresponding damage state indices, which characterize their condition states. The stationary and nonstationary Markovian transition probabilities are obtained. Four broader categories of maintenance actions are also considered—namely, Do Nothing, Minor Repair, Major Repair, and Reconstruction—for both pavements and bridges. Observation actions are also defined as no inspection, low-fidelity inspection, and high-fidelity inspection for both asset types. The costs for the maintenance and inspection actions are obtained from actual data and up-to-date literature, wherever possible.

PAVEMENTS

There are various indicators that can characterize the condition state of pavements, some that are used internationally and others that are state agency specific, such as Pavement Condition

Index (PCI), Pavement Quality Index (PQI), Critical Condition Index (CCI), and International Roughness Index (IRI), among many others. CCI and IRI are used in this work.

Critical Condition Index

The CCI model in this report is a modified version of the modeling described in (Katicha, Ercisli, Flintsch, Bryce, & Diefenderfer, 2016), where a regression model is presented that estimates mean CCI using collected data from years 2007-12, 2014, and 2015, from the Virginia Department of Transportation (VDOT) Pavement Management System (PMS). The age of the pavement is calculated as the difference between the year of condition reporting and the last year of recorded maintenance. The total dataset in (Katicha, Ercisli, Flintsch, Bryce, & Diefenderfer, 2016) consists of 3,473 observations from the years 2007 to 2012, and 1,560 observations from the years 2014 and 2015. The mean regression model in (Katicha, Ercisli, Flintsch, Bryce, & Diefenderfer, 2016) directly incorporates the effect of age of the pavement section and indirectly considers the impact of the traffic load and other pavement structural parameters. Figure 3-1 shows the mean CCI as a function of pavement age for different traffic levels (A to E), where levels A through E indicate heavy to light traffic conditions, assuming other structural parameters constant. In the following section, a nonstationary gamma process is fitted to estimate the relevant nonstationary transition probabilities.

Fitting a nonstationary gamma process

A gamma process is utilized in this section, with its mean in time equal to the modified mean CCI predictions in Figure 3-1 and a relevant model variance $\sigma_s^2(t)$, primarily determined based on (Katicha, Ercisli, Flintsch, Bryce, & Diefenderfer, 2016) and the observed data trends there. The marginal probability of CCI at every step t can be obtained by estimating the damage index DI , where $DI = 100 - CCI$, using the gamma distribution with probability density function:

$$Ga(DI|f(t), g(t)) = \frac{g(t)^{f(t)}}{\Gamma(f(t))} DI^{f(t)-1} e^{-g(t)DI} \quad (3.1)$$

The gamma process is parametrized here by a non-negative time-varying scale parameter function $g(t)$ and a non-negative time-varying shape parameter function $f(t)$, and $\Gamma(u) = \int_0^\infty v^{u-1} e^{-v} dv$. The relevant parameters are estimated in time based on the mean DI prediction model and the model variance $\sigma_s^2(t)$. The relationship between the gamma process parameter functions and μ_{DI}, σ_s is given as:

$$\mu_{DI}(t) = \frac{f(t)}{g(t)}, \sigma_s(t) = \frac{\sqrt{f(t)}}{g(t)} \quad (3.2)$$

Due to their monotonicity, gamma processes are readily used as a suitable modeling choice in stochastic deterioration engineering applications and can describe continuous Markovian transitions. For time instant $t_1 < t_2$, the increment of DI follows a gamma distribution:

$$DI(t_2) - DI(t_1) \sim Ga(\cdot | f(t_2) - f(t_1), g(t_2)), \quad (3.3)$$

with $g(t)$ assumed constant in (t_1, t_2)

In Figure 3-2, relevant simulation results are indicatively shown for traffic level A with 300 different realizations. All corresponding $f(t)$ and $g(t)$ values are shown in Table D-1 in Appendix D, for different traffic levels.

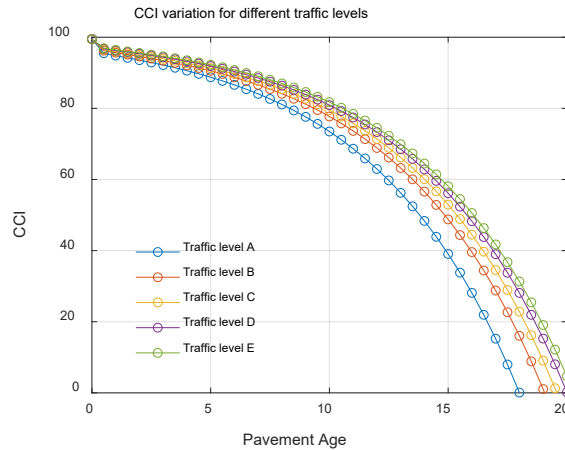


Figure 3-2. Modeled mean CCI for different levels of traffic.

Determining transition probabilities

To determine the transition probabilities, the discrete condition states are first defined, as shown in Table 3-1. These discretized condition states in the table are herein largely adapted by the prescribed VDOT maintenance guidelines in (Virginia Department of Transportation, 2016), which for interstate highways are:

- For CCI values above 89 the treatment category is always Do Nothing (DN).
- For CCI values above 84 the treatment category is always DN or Routine (Preventive) Maintenance (PM).
- For CCI values below 60 the treatment category is at least Corrective Maintenance (CM), Restorative Maintenance (RM), or Rehabilitation/Reconstruction (RC).
- For CCI values below 49 the treatment category is at least RM or RC.
- For CCI values below 37 the treatment category is always RC.

Sampling is then performed by generating CCI and pavement age pairs, which are further propagated in time following the described gamma process in the previous section. In total, 106 sequences are generated to obtain the transition probabilities for a given traffic level. Figure 3-3 indicatively shows computed transition probabilities for traffic level A.

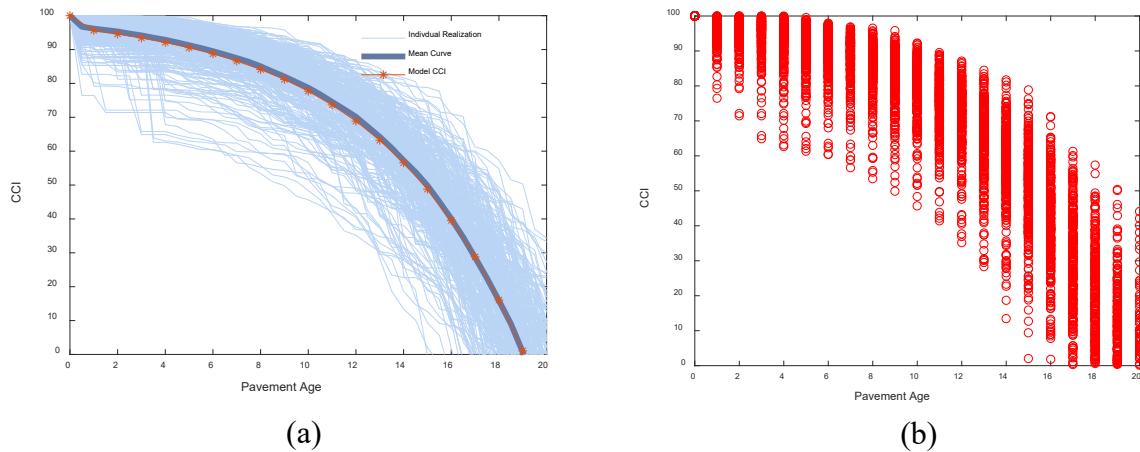


Figure 3-3. (a) Fitted gamma model, (b) scatter plot for CCI for traffic level A.

Table 3-3. State discretization based on CCI values.

States of the pavement section	CCI value
$s = 6$	100-90
$s = 5$	89-80
$s = 4$	79-61
$s = 3$	60-50
$s = 2$	49-37
$s = 1$	<37

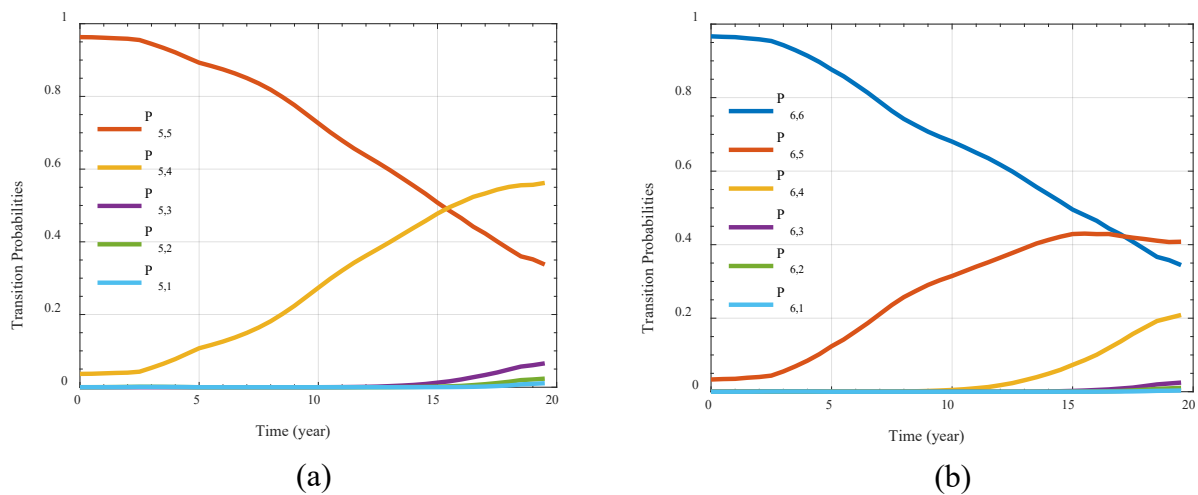


Figure 3-4. Transition probabilities for Traffic level A, with (a) starting state = 6, (b) starting state = 5, smoothed over time with a 5-point window.

Observation probabilities for CCI inspection action

Observation uncertainty can be appropriately modeled by the likelihood functions $p(o_t|s_t)$ which quantify the probability of observing an observation o_t at time t given a state s_t at that

instant. To calculate the observation probability $p(o_t | s_t)$ a normal distribution is considered with mean equal to the actual CCI value and an error variance $\sigma_{error}^2 = 72$, based on (Katicha, Ercisli, Flintsch, Bryce, & Diefenderfer, 2016), and is considered as a low fidelity inspection due to the large error. The error variance is linked to the variability in the measurement of CCI and the error in the reported pavement condition by an inspector. These conditional observation probabilities $p(o_t | s_t)$ are generated by calculating the area under the curve of the normal distribution, as shown in Figure 3-4.

It has been observed that the observation probabilities are largely independent of different traffic levels (in reference to Figure 3-1) due to the constant σ_{error}^2 value, so the average values have been reported in CCI = 55.

Table 3-2 can be used for all traffic levels. High-fidelity inspections can also be considered, which rely on higher precision, expensive devices, and multi-modality. These techniques may also require significant post-processing, which increases the overall inspection cost. Hence, a much smaller error variance, $\sigma_{error}^2 = 18$, is used to compute the observation probabilities, as compared to the previous case. Using these inspection techniques, we derive the observation probabilities as shown in Table 3-3. For the no-inspection case, one has equal probability of observing each state, i.e., $p(o_t | s_t) = 1/6 \forall o_t, s_t \in \{1, 2 \dots, 6\}$. In Table 3-2, we notice observation probabilities less than 50% for observing the actual states, which are attributed to the non-uniform CCI partitioning.

As discussed earlier, the cost of inspections depends on the techniques used for observing the pavement condition along with the postprocessing time/complexity. The inspection techniques have been categorized into three precision categories of no-inspection, low-fidelity inspection, and high-fidelity inspection, as previously mentioned, and the associated costs informed from MDOT survey (MDOT, 2014) for monitoring highway assets. These costs are summarized in Table 3-4.

Maintenance, rehabilitation, and reconstruction actions in relation to CCI

For ease of notation and to simplify expressions, the word maintenance is used here forth as a general term encompassing all actions in relation to preventive treatments, repairs, restorations, and reconstructions. There are various guidelines for pavement maintenance for different agencies/states. According to VDOT (Virginia Department of Transportation, 2016), four different maintenance actions are recommended (*Do Nothing*, *Minor Repair*, *Major Repair*, and *Reconstruction*). Further details of maintenance actions are provided in Appendix D, Table D-2.

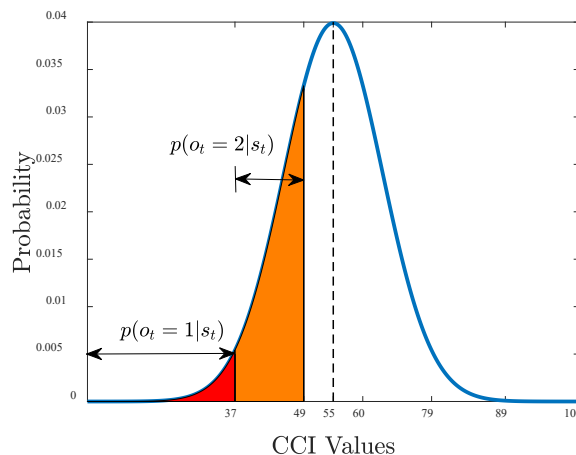


Figure 3-5. Example of observation probability calculation for actual CCI = 55.

Table 3-4. Observation probability $p(o_t|s_t)$ given actual state s_t , with $\sigma_{error}^2 = 72$.

Actual State	$p(o_t = 6 s_t)$	$p(o_t = 5 s_t)$	$p(o_t = 4 s_t)$	$p(o_t = 3 s_t)$	$p(o_t = 2 s_t)$	$p(o_t = 1 s_t)$
$s_t = 6$	0.687	0.259	0.054	0.000	0.000	0.000
$s_t = 5$	0.276	0.422	0.297	0.005	0.000	0.000
$s_t = 4$	0.023	0.139	0.648	0.167	0.022	0.001
$s_t = 3$	0.000	0.003	0.266	0.455	0.248	0.028
$s_t = 2$	0.000	0.000	0.031	0.224	0.486	0.259
$s_t = 1$	0.000	0.000	0.000	0.005	0.059	0.936

Table 3-5. Observation probability $p(o_t|s_t)$ given actual state s_t , with $\sigma_{error}^2 = 18$.

Actual State	$p(o_t = 6 s_t)$	$p(o_t = 5 s_t)$	$p(o_t = 4 s_t)$	$p(o_t = 3 s_t)$	$p(o_t = 2 s_t)$	$p(o_t = 1 s_t)$
$s_t = 6$	0.801	0.197	0.002	0.000	0.000	0.000
$s_t = 5$	0.153	0.664	0.183	0.000	0.000	0.000
$s_t = 4$	0.001	0.078	0.822	0.099	0.000	0.000
$s_t = 3$	0.000	0.000	0.149	0.693	0.158	0.000
$s_t = 2$	0.000	0.000	0.001	0.137	0.718	0.144
$s_t = 1$	0.000	0.000	0.000	0.000	0.042	0.958

Table 3-6. Inspection action costs (in USD/lane-mile or USD/m²) for CCI using three different techniques.

Inspection Technique	Description	Observation Error (σ_{error}^2)	Cost (USD/Lane-mile)	Cost (USD/m ²)
i_2	High fidelity	18	0.57	0.16
i_1	Low fidelity	72	0.27	0.08
i_0	No Inspection	∞	0.00	0.00

The maintenance action transition probabilities for CCI are shown in Table 3-5 through Table 3-7, similar to the line of work presented in (Madanat & Ben-Akiva, 1994). It is assumed that the Minor Repair (crack filling, moderate patching, etc.) cannot change the rate of deterioration but the state of the component. The change in condition states is considered based on Table 3-5.

For a Major Repair maintenance action, deterioration rate is reduced to that of an asset younger by 5 years or to that of a newly built pavement component, i.e., $(T_{age})_{updated} = \max(0, T_{age} - 5)$ years. Major Repairs also alter the CCI conditions, with the transition probabilities shown in Table 3-6.

The Reconstruction maintenance action brings the CCI condition back to the intact state (i.e., $s_t = 6$) with certainty, as shown in Table 3-7, and its deterioration rate to the initial intact value. Transitions in these tables do not include the transition because of the environment. Decoupled environmental transitions can essentially allow us to include action duration effects, among others. In Table 3-5 and Table 3-6, we can observe that after applying maintenance actions the system can go to a worse state with a non-zero probability. This happens because we are accounting for the inherent uncertainty present in the outcome of the applied actions, which also includes the possibility of failed actions.

Maintenance action costs

The cost of different maintenance actions is considered from (Virginia Department of Transportation, 2016; FDOT, 2020; PennDOT, 2017; Russell, 2021) and provided for interstate, primary, and secondary roads in Table 3-8. It is reported in USD/m² and the total cost can be calculated using the components' length and width (which is considered as ~3.7 m (12 ft) per lane). Here, it is important to mention that the action descriptions provided in Table 3-8 for *Minor Repair*, *Major Repair* are indicative actions of the corresponding category and these actions are a subset of actions used in (Virginia Department of Transportation, 2016) as presented in Appendix D, Table D-1.

Table 3-7. Minor Repair transition probabilities for 6 CCI states.

Condition State	$s_{t+1} = 6$	$s_{t+1} = 5$	$s_{t+1} = 4$	$s_{t+1} = 3$	$s_{t+1} = 2$	$s_{t+1} = 1$
$s_t = 6$	0.97	0.03	0.00			
$s_t = 5$	0.87	0.10	0.03			
$s_t = 4$	0.40	0.47	0.10	0.03		
$s_t = 3$		0.40	0.47	0.10	0.03	
$s_t = 2$			0.40	0.47	0.10	0.03
$s_t = 1$				0.40	0.47	0.13
Deterioration rate	Does not change					

Table 3-8. Major Repair transition probabilities for 6 CCI states.

Condition State	$s_{t+1} = 6$	$s_{t+1} = 5$	$s_{t+1} = 4$	$s_{t+1} = 3$	$s_{t+1} = 2$	$s_{t+1} = 1$
$s_t = 6$	1.00	0.00	0.00			
$s_t = 5$	0.96	0.04	0.00			
$s_t = 4$	0.80	0.20	0.00			
$s_t = 3$	0.65	0.25	0.10			
$s_t = 2$	0.50	0.30	0.20			
$s_t = 1$	0.40	0.30	0.30			
Deterioration rate	Reset by 5 years					

Table 3-9. Reconstruction transition probabilities for 6 CCI states.

Condition State	$s_{t+1} = 6$	$s_{t+1} = 5$	$s_{t+1} = 4$	$s_{t+1} = 3$	$s_{t+1} = 2$	$s_{t+1} = 1$
$s_t = 6$	1.00	0.00	0.00			
$s_t = 5$	1.00	0.00	0.00			
$s_t = 4$	1.00	0.00	0.00			
$s_t = 3$	1.00	0.00	0.00			
$s_t = 2$	1.00	0.00	0.00			
$s_t = 1$	1.00	0.00	0.00			
Deterioration rate	Reset to new pavement section					

Table 3-10. Maintenance action costs for asphalt pavements, reported in USD/m².

Actions	Description	Cost (USD/m ²) Interstate	Cost (USD/m ²) Primary	Cost (USD/m ²) Secondary
Do Nothing	NA	0.00	0.00	0.00
Minor Repair	Moderate patching (<10%), surface treatment, partial depth patching, thin overlay	20	16	10
Major Repair	Heavy patching (<20% of the pavement area), full depth patching, structural overlay	75	68	52
Reconstruction	Replacing the entire pavement section	350	330	250

Maintenance action durations

The duration of different maintenance actions is inferred from (ADOT, 2018; PennDOT, 2019). It is further assumed that no action takes more than 2 years, and no Major action takes more than a year to complete for a component. This can be justified by assuming multiple maintenance activities at a time for longer and multi-lane components. These durations are provided in Table 3-9.

International Roughness Index

IRI (m/km) is another metric that quantifies the functional pavement condition in terms of the roughness experienced by vehicle passengers. IRI is calculated from measured longitudinal road profiles using the simulated vertical displacement response of a quarter-car (Sayer, Gillespie, & Paterson, 1986). IRI (m/km) in this work is discretized into 5 states, as in (Faddoul, Raphael, Soubra, & Chateaufneuf, 2013; FHWA, 1999) presented in Table 3-10. The transition probabilities for IRI for the Do Nothing action are given in Table 3-11.

Table 3-11. Maintenance actions duration in days per lane-mile.

Actions	Days per Lane-mile	Additional Days per Mile for Shoulder, etc.
Do Nothing	0	0
Minor Repair	3.5	1
Major Repair	6.5	2
Reconstruction	32	10

Table 3-12. State classification based on IRI (m/km) values.

Condition State (s)	IRI (m/km)	Pavement Condition
$s = 5$	<0.95	Very Good
$s = 4$	0.95-1.56	Good
$s = 3$	1.57-2.19	Fair
$s = 2$	2.20-3.14	Mediocre
$s = 1$	≥ 3.15	Poor

Table 3-13. Do Nothing transition probabilities for 5 IRI states.

Condition State	$s_{t+1} = 5$	$s_{t+1} = 4$	$s_{t+1} = 3$	$s_{t+1} = 2$	$s_{t+1} = 1$
$s_t = 5$	0.840	0.121	0.039		
$s_t = 4$		0.788	0.142	0.070	
$s_t = 3$			0.708	0.192	0.01
$s_t = 2$				0.578	0.422
$s_t = 1$					1.000

Maintenance actions in relation to IRI

The same four maintenance actions are considered for IRI: *Do Nothing*, *Minor Repair*, *Major Repair*, and *Reconstruction*. The IRI transitions for Minor Maintenance to Reconstruction actions are given in Table 3-12 through Table 3-14, respectively, similar to the CCI case.

Table 3-14. Minor Repair transition probabilities for 5 IRI states.

Condition State	$s_{t+1} = 5$	$s_{t+1} = 4$	$s_{t+1} = 3$	$s_{t+1} = 2$	$s_{t+1} = 1$
$s_t = 5$	0.97	0.03	0.00		
$s_t = 4$	0.85	0.12	0.03		
$s_t = 3$	0.45	0.40	0.12	0.03	
$s_t = 2$		0.45	0.40	0.12	0.03
$s_t = 1$			0.45	0.40	0.15

Table 3-15. Major Repair transition probabilities for 5 IRI states.

Condition State	$s_{t+1} = 5$	$s_{t+1} = 4$	$s_{t+1} = 3$	$s_{t+1} = 2$	$s_{t+1} = 1$
$s_t = 5$	1.00	0.00	0.00		
$s_t = 4$	0.95	0.05	0.00		
$s_t = 3$	0.80	0.20	0.00		
$s_t = 2$	0.70	0.25	0.05		
$s_t = 1$	0.45	0.35	0.20		

Table 3-16. Reconstruction transition probabilities for 5 IRI states.

Condition State	$s_{t+1} = 5$	$s_{t+1} = 4$	$s_{t+1} = 3$	$s_{t+1} = 2$	$s_{t+1} = 1$
$s_t = 5$	1.00	0.00	0.00		
$s_t = 4$	1.00	0.00	0.00		
$s_t = 3$	1.00	0.00	0.00		
$s_t = 2$	1.00	0.00	0.00		
$s_t = 1$	1.00	0.00	0.00		

Maintenance action costs in relation to IRI

The cost of maintenance actions in relation to IRI is the same as the one reported in Table 3-8. Maintenance actions taken at any given time will improve both CCI and IRI indices simultaneously.

Observation probabilities for IRI inspection actions

Three assumed inspection actions of different fidelities are again considered in this case and the measurement errors related to the respective inspection technologies are assumed to be normally distributed with zero mean and standard deviations (SD) of 0.08, 0.32, and ∞ m/km, respectively, as reported in (Faddoul, Raphael, Soubra, & Chateauneuf, 2013). The observation probabilities are summarized in Table 3-15, where o_t is the observed state and s_t is the (hidden) actual state. The underlying assumption is that more costly inspections are high-fidelity inspections and provide more accurate information. For the last inspection technique, an infinite standard deviation is considered, thus this inspection is completely uninformative, equivalent to a no-inspection action.

Inspection costs are considered independent of the pavement state, as also considered in (Faddoul, Raphael, Soubra, & Chateauneuf, 2013), and depend on the fidelity of the inspection technology that is utilized. In Table 3-15 costs are equal to 0.10, 0.03, and 0 dollars per m^2 , respectively.

Table 3-17. Observation probability $p(o_t | s_t)$ for IRI given state s_t .

Inspection Technique	SD (m/km)	$P(o_t = j - 2 s_t = j)$	$P(o_t = j - 1 s_t = j)$	$P(o_t = j s_t = j)$	$P(o_t = j + 1 s_t = j)$	$P(o_t = j + 2 s_t = j)$	Cost (USD/m ²)
i_2	0.08	0	0.05	0.90	0.05	0	0.10
i_1	0.32	0	0.20	0.60	0.20	0	0.03
i_0	∞	0.20	0.20	0.20	0.20	0.20	0

Combined Inspection Costs for IRI and CCI

Table 3-4 and Table 3-15 provide the costs of individual inspection actions for CCI and IRI, respectively, while in Table 3-16 the joint cost of pavement inspection is considered, when both IRI and CCI are observed.

Table 3-18. Pavement inspection cost (i.e., combined cost of IRI and CCI).

Inspection Technique	Description	Cost (USD/m ²)
i_2	High fidelity	0.20
i_1	Low fidelity	0.10
i_0	No Inspection	0.00

BRIDGES

In the United States, 7.5% of the total 617,084 bridges were structurally deficient in 2020 (ASCE, 2021), and 42% were 50 years old or older. On average, 178 million trips are occurring each day on structurally deficient bridges. Each bridge consists of various structural subsystems, yet only decks are considered in this report, due to their expensive and frequent maintenance needs, in relation to other subsystems. Decks often have the most rapid rate of deterioration among bridge components, and in the United States factors like corrosion-induced degradation, freezing and thawing cycles, and direct exposure to traffic loads contribute toward their degradation.

Bridge Decks

For bridge deck serviceability, nine total states are generally considered, with state 9 being the undamaged state, as per the convention adopted by (PennDOT, 2009) and other DOTs. For this report, state 4 characterizes all subsequent states, as also considered in (Manafpour, Guler, Radlinska, Rajabipour, & Warn, 2018). Thus, in this study, six bridge deck states along with a failure state are used. The transition probabilities of those six states are based on approximately 30 years of in-service performance data for over 22,000 bridges in Pennsylvania, as analyzed in (Manafpour, Guler, Radlinska, Rajabipour, & Warn, 2018) for different exogenous parameters, i.e., deck length, location, protective coating, span type, etc. Figure 3-5 shows an indicative case based on the following exogenous parameters: deck length = 90 ft; location type = 4; reinforcement bar protection = 1 (no protective coating); type of span interaction for main unit = 1 (simple, non-composite); primary load carrying members = 1 (reinforced concrete); deck surface type = 1 (concrete); total number of spans in

main unit = 2 (multi-span); NHS = 1 (interstate route); maintenance type = type 1 (no maintenance). Apart from these six nonstationary transitions, stationary failure probabilities are also considered, as shown in Table 3-17.

Table 3-19. Bridge failure probability given bridge condition state.

Condition State	$s_t = 9$	$s_t = 8$	$s_t = 7$	$s_t = 6$	$s_t = 5$	$s_t = 4, \dots$	$s_t = \text{failed}$
Failure prob. ($s_{t+1} = \text{failed}$)	0.001	0.001	0.005	0.005	0.005	0.01	1.0

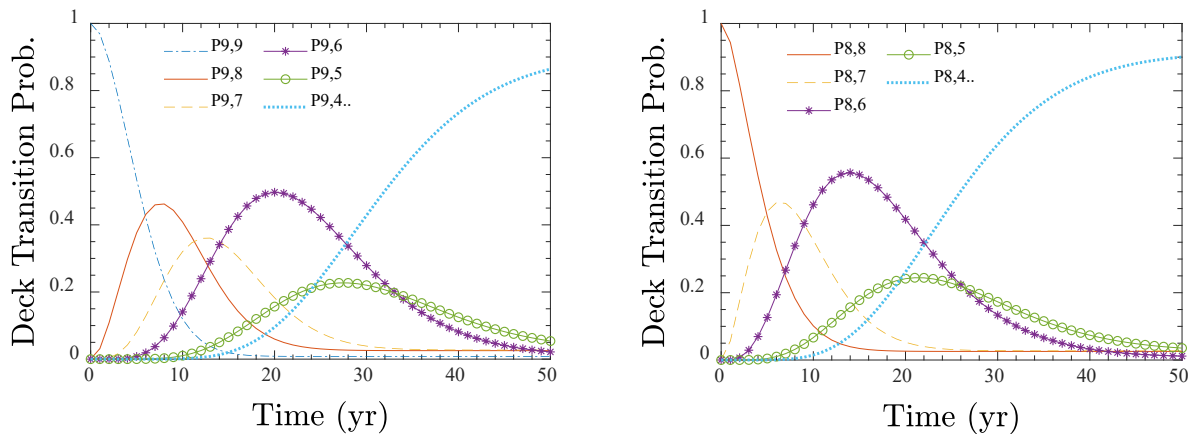


Figure 3-6. Transition probabilities in time, moving from states 9 (left) and 8 (right) to lower states.

Maintenance actions for bridge decks

Similar to pavements, four maintenance actions are considered for maintaining the bridge decks: *Do Nothing*, *Minor Repair*, *Major Repair*, and *Reconstruction*. It is again assumed here that the *Minor Repair* action does not change the rate of deterioration of the deck, but it can change the condition state of the structure, as per the transition probabilities given in Table 3-18. However, a *Major Repair* action can improve the deterioration rate to that of a deck younger by 5 years or a reset to a newly made deck, i.e., $(T_{age})_{updated} = \max(0, T_{age} - 5)$ years, and the change in condition state is now considered as reported in Table 3-19. The transition probabilities for the *Reconstruction* action are shown in Table 3-20 and reset the state and deterioration rate of the deck to a newly built one.

Table 3-20. Minor Repair transition probabilities for deck states.

Condition State	$s_t = 9$	$s_t = 8$	$s_t = 7$	$s_t = 6$	$s_t = 5$	$s_t = 4, \dots$	$s_t = \text{failed}$
$s_t = 9$	0.97	0.03	0.00				
$s_t = 8$	0.85	0.12	0.03				
$s_t = 7$	0.40	0.45	0.12	0.03			
$s_t = 6$		0.40	0.45	0.12	0.03		
$s_t = 5$			0.40	0.45	0.12	0.03	
$s_t = 4, \dots$				0.40	0.45	0.15	
$s_t = \text{failed}$							1.0
Deterioration rate	Does not change	Does not change	Does not change	Does not	Does not change	Does not change	

Table 3-21. Major Repair transition probabilities for deck states.

Condition State	$s_t = 9$	$s_t = 8$	$s_t = 7$	$s_t = 6$	$s_t = 5$	$s_t = 4, \dots$	$s_t = \text{failed}$
$s_t = 9$	1.00	0.00	0.00				
$s_t = 8$	0.95	0.05	0.00				
$s_t = 7$	0.80	0.20	0.00				
$s_t = 6$	0.60	0.30	0.10				
$s_t = 5$	0.40	0.40	0.20				
$s_t = 4, \dots$	0.30	0.40	0.30				
$s_t = \text{failed}$							1.0
Deterioration rate	Reset by 5 years						

Table 3-22. Reconstruction transition probabilities for deck states

Condition State	$s_t = 9$	$s_t = 8$	$s_t = 7$	$s_t = 6$	$s_t = 5$	$s_t = 4, \dots$	$s_t = \text{failed}$
$s_t = 9$	1.00	0.00	0.00				
$s_t = 8$	1.00	0.00	0.00				
$s_t = 7$	1.00	0.00	0.00				
$s_t = 6$	1.00	0.00	0.00				
$s_t = 5$	1.00	0.00	0.00				
$s_t = 4, \dots$	1.00	0.00	0.00				
$s_t = \text{failed}$	1.00	0.00	0.00				
Deterioration rate	Reset to newly built deck						

Maintenance action costs for bridge decks

The cost of maintenance actions has small dependence upon the current state of the bridge deck. As a result, maintenance costs are considered independent of the state of the deck here. The cost for a reconstruction action is obtained from (FHWA, 2019) and the costs for minor and major maintenance actions are considered as 15% and 45% of that, inferred from (Wells, 1995). Table 3-21 shows the costs of performing individual actions in USD/m². It can be observed that the unit costs of actions for bridges are higher than the unit costs of pavement actions.

Maintenance action durations for bridge decks

The duration of different maintenance actions is mainly inferred from (ADOT, 2018; Oakgrove, 2013; Goodspeed & Brown, 2017). For large bridges it is assumed that maintenance activity is performed at multiple locations simultaneously to increase efficiency. The action durations are provided in Table 3-22 for three different types of bridges, types I-III, categorized based on their sizes, where type I bridges are the largest size (length > 2.0 km), type II are intermediate (length ~ 1 km - 2.0 km), and type III are the smallest (length < 1 km).

Table 3-23. Cost of maintenance actions in USD/m².

Actions	Description	Cost (USD/m ²)
Do Nothing	NA	0.00
Minor Repair	Moderate cracks filling and patching area < 10% of the deck area, minor replacement of reinforcement	400.00
Major Repair	Fixing spalls/delamination with deck area < 25%, major replacement of reinforcement	1,200.00
Reconstruction	Replacing the entire deck	2,650.00

Table 3-24. Maintenance action durations in days.

Actions	Type I Bridges	Type II Bridges	Type III Bridges
Do Nothing	0	0	0
Minor Repair	25	12	6
Major Repair	70	30	15
Reconstruction	300	150	70

Inspection actions and observation probabilities

There are a variety of destructive and nondestructive inspection techniques that are used for bridge decks, like visual inspection, acoustic sensing, infrared (IR)/thermal imaging, ground penetrating radar (GPR), coring and chipping, and half-cell potential test, among many others. Based on their accuracy, inspection techniques can be characterized as i_0 , i_1 , and i_2 , corresponding to uninformative, low-fidelity, and high-fidelity inspection techniques, respectively, and the relevant inspection costs are related to their accuracy. As assumed for the pavements, we here again relate the inspection costs to the reconstruction cost of the bridge and we consider 0.1% and 0.5% of the rebuild cost for less and more accurate inspection techniques, respectively. The resulting costs are shown in Table 3-23.

Table 3-25. Inspection action costs for three different techniques.

Inspection Technique	Example techniques	Cost (USD/m ²)
i_2	High fidelity	1.20
i_1	Low fidelity	0.50
i_0	No Inspection	0.00

Table 3-26. Observation probability $p(o_t|s_t)$ given state s_t , for low-fidelity inspection techniques.

Actual State (s_t)	$p(o_t = 9 s_t)$	$p(o_t = 8 s_t)$	$p(o_t = 7 s_t)$	$p(o_t = 6 s_t)$	$p(o_t = 5 s_t)$	$p(o_t = 4, \dots s_t)$	$p(o_t = failed s_t)$
$s_t = 9$	0.80	0.15	0.05				
$s_t = 8$	0.15	0.65	0.15	0.05			
$s_t = 7$	0.05	0.15	0.60	0.15	0.05	0.0	
$s_t = 6$		0.05	0.15	0.60	0.15	0.05	
$s_t = 5$			0.05	0.15	0.65	0.15	
$s_t = 4, \dots$				0.05	0.15	0.80	
$s_t = failed$							1.0

The observation probabilities for the bridge decks are considered similarly to (Madanat & Ben-Akiva, 1994; Faddoul, Raphael, Soubra, & Chateaufneuf, 2013; Madanat S. , 1993) and for the no-inspection case $p(o_t|s_t) = 1/6 \forall o_t, s_t \in \{1,2 \dots ,6\}$ is used. Table 3-24 and Table 3-25 describe observation probabilities for low- and high-fidelity inspection techniques, respectively.

Table 3-27. Observation probability $p(o_t|s_t)$ given state s_t , for high fidelity inspection techniques.

Actual State (s_t)	$p(o_t = 9 s_t)$	$p(o_t = 8 s_t)$	$p(o_t = 7 s_t)$	$p(o_t = 6 s_t)$	$p(o_t = 5 s_t)$	$p(o_t = 4, \dots s_t)$	$p(o_t = failed s_t)$
$s_t = 9$	0.90	0.10					
$s_t = 8$	0.10	0.80	0.10				
$s_t = 7$		0.10	0.80	0.10			
$s_t = 6$			0.10	0.80	0.10		
$s_t = 5$				0.10	0.80	0.10	
$s_t = 4, \dots$					0.10	0.90	
$s_t = failed$							1.0

CONCLUSION

This chapter has developed a detailed, realistic modeling framework, following principles of Markov decision processes and partially observable MDPs, for both pavements and bridges. For pavements, two indices are considered, the Critical Condition Index and the International Roughness Index, as the structural condition and serviceability indicators, and the corresponding transition probabilities are obtained for both indices. For bridges, the deck performance is used due to its faster rate of deterioration and its high cost of maintenance. Four maintenance action categories are considered for both pavements and bridges: Do Nothing, Minor Repair, Major Repair, and Reconstruction. The actual actions within these categories may be different for the different asset classes. The state transitions and the costs associated with each maintenance action are appropriately quantified. Similarly, three inspection action types are considered: no-inspection, low-fidelity, and high-fidelity inspections, and their corresponding inspection accuracies and costs are reported. Overall, the developed framework can be used in modeling and management decisions support of a wide variety of transportation networks with different types of pavements and bridges.

CHAPTER 4

A Reinforcement Learning Method for Multi-asset Roadway Improvement Scheduling Considering Traffic Impacts

INTRODUCTION

Roadway improvements through maintenance, repair, and rehabilitation actions on pavements and bridge decks are essential to overall traffic network performance and travel reliability. The implementation of these actions requires system downtime, which is primarily in the form of reduced roadway capacity and occasional roadway or bridge closures. These improvements are typically scheduled by asset class, yet downtime scheduling for either asset type will impact network-wide performance. Thus, coordinating actions across assets to minimize the impact on roadway users is important. The impact of downtime due to improvement actions on one or more network components, from one or more asset classes, on the performance of the entire traffic network over a time horizon can be assessed, and this information can be used to provide decision support for optimal, multi-asset class improvement action scheduling. This work proposes and develops mathematical tools to support such multi-asset (pavements and bridge decks) roadway network improvement prioritization and scheduling for a designated planning horizon.

These prioritization and scheduling tools are developed using a bilevel, stochastic, dynamic programming formulation with an embedded Markov decision process (Puterman, 1994) model at the upper level. The MDP conceptualization enables state-dependent decision-making under stochastic condition state deterioration. The model accounts for the effects of reduced roadway capacity on traffic congestion resulting from the downtime needed to execute chosen improvement actions. The approach facilitates the inclusion of multiple asset classes, each with unique deterioration processes and multiple improvement action options.

Decisions in the upper level of the bilevel program on which actions to take and the order in which to take them account for the experience of roadway users as assessed in the lower level through a user equilibrium (UE) formulation. By considering multiple asset classes simultaneously, prioritization and scheduling decisions of both asset classes can be coordinated to have reduced traffic impacts.

In addition to including delays due to reduced roadway capacity from execution of the chosen improvement actions, the model also accounts for other roadway user costs, including increased fuel costs and vehicle depreciation due to poor roadway conditions. User costs are mitigated by favorable actions, such as improved pavement serviceability resulting from the improved roadway condition they induce. Tradeoffs between these benefits and detriments of action and inaction are considered simultaneously.

Threshold-based methods are widely used in roadway maintenance prioritization (USDOT, 2017; Wei & Tighe, 2004; Wei & Tighe, 2004). The bilevel model can be reduced to a simpler threshold version wherein the upper level calculates now the expected total cost

of maintaining the system to prespecified thresholds. The model presumes that improvement actions are implemented when asset conditions fall below these preset levels. Solution is achievable by complete enumeration of potential threshold settings as it is applied on a small problem instance, but formidable for large, more realistic problem instances. Results from runs of this approach provide a baseline for comparison.

Threshold-based methods are widely used in roadway maintenance prioritization (Wei & Tighe, 2004; USDOT, 2017). The bilevel model can be reduced to a simpler threshold version wherein the upper level calculates now the expected total cost of maintaining the system based on optimally specified thresholds. The approach presumes that improvement actions are implemented when asset conditions reach or fall below these designated levels. Solution is achievable by complete enumeration of potential threshold settings in this case, but this is formidable, in general, for larger problem instances. Results from runs of this approach provide a baseline for comparison.

To solve the proposed bi-level formulation in this work, a cutting-edge Deep Centralized Multi-agent Actor Critic (DCMAC) method is proposed (Andriotis & Papakonstantinou, 2019; Andriotis & Papakonstantinou, 2021). Its performance is compared with that of the typical temporal difference (TD)-learning method, SARSA (State Action Reward State Action) (Sutton & Barto, 2018), which has also been previously used in the literature for related asset management problems (Medury & Madanat, 2013). The solution quality of SARSA depends on the choice of feature functions needed to approximate a Q-function. In this application, Q-functions provide an estimate of expected cumulative cost that is updated over the steps of the algorithm. The selection of these feature functions can be difficult (even combinatorial). The DCMAC method addresses the state and action dimensionality problem by: (1) using neural networks, and thus nonlinear, approximations for state values and (2) assuming conditional independence in generating policies. The use of the more efficient DCMAC enables inclusion of the various complicating factors of traffic impact, stochastic deterioration models in the form of transition matrices, and multiple assets.

To solve the proposed bilevel formulation in this work, a cutting-edge Deep Centralized Multi-agent Actor Critic (DCMAC) deep reinforcement learning method is proposed (Andriotis & Papakonstantinou, 2019; Andriotis & Papakonstantinou, 2021). Its performance is compared with that of the typical temporal difference (TD)-learning method, SARSA (State Action Reward State Action) (Sutton & Barto, Reinforcement Learning: An Introduction, 2018), which has also been previously used in the literature for related asset management problems (Medury & Madanat, 2013). The solution quality of SARSA depends on the choice of feature functions needed to approximate a Q-function. Q-functions are key to reinforcement learning techniques. Here, it provides an estimate of expected cumulative cost that is updated over the steps of the algorithm. The selection of these feature functions can be difficult (even combinatorial). DCMAC does not rely on such a Q-function. Moreover, it addresses the state and action dimensionality problem by using neural network approximations for state values and the mathematically derived policy.

In the next section, relevant literature is reviewed and this work's contributions in light of prior works are established. The Multi-asset Roadway Improvement Scheduling Considering Traffic Impacts problem is formulated as a stochastic, bilevel program in Section 3 and DCMAC, a deep reinforcement learning algorithm, is presented for its solution in Section 4. The model application is illustrated on a hypothetical network adapted from the literature (Medury & Madanat, 2013). Adaptations are related to advancements in deterioration and improvement activity effectiveness modeling from (Faddoul, Raphael, Soubra, & Chateaufneuf, 2013; Virginia Department of Transportation, 2016). Results of the numerical experiments show the importance of considering traffic delays, stochastic

deterioration, downtime from improvement actions, and multi-asset class management into the optimization framework.

LITERATURE REVIEW

This work contributes to this literature through the presentation of a multi-asset-class model that simultaneously accounts for deterioration stochasticity, downtime and improvement action impacts, and traffic network effects. Further, a cutting-edge, efficient deep reinforcement learning methodology is utilized for its solution.

Optimal resurfacing frequency and intensity in roadway maintenance, repair, and rehabilitation is a focus of numerous relevant works. Pavement deterioration is a continuous process unless rehabilitation or maintenance actions are taken to reduce or reverse its effects. Resurfacing decreases the roughness of roadway assets and the level of roughness improvement depends on the number of applications, material, and other factors, as described in numerous related works (e.g., (George, Rajagopal, & Lim, 1989; Labi & Sinha, 2003; Ouyang & Madanat, 2004; Ouyang & Madanat, 2006)). Li and Madanat (Li & Madanat, 2002) and Ouyang and Madanat (2004, 2006) aimed to minimize lifecycle costs consisting of cost for resurfacing pavement assets incurred by a transportation agency and user operating costs.

Extending on earlier advances, (Ouyang, 2007) and (Durango-Cohen & Sarutipand, 2009) incorporated traffic network effects by associating deterioration and maintenance actions with roadway conditions (e.g., pavement roughness) that affect driver experience and route choice. Ouyang (2007) modeled these traffic effects through a UE model that is embedded at the lower level of a bilevel modeling framework. The upper level in their work seeks an optimal resurfacing plan for the highway network. The lower level uses a UE formulation to model traffic flows and downtime effects were not considered. A policy iteration method was proposed for solution of their model on a network with two pavement segments. Such an exact methodology can only be employed on small problem instances. Durango-Cohen and Sarutipand (2009) measured the demand for use of a roadway segment as a function of its condition. Deterioration, as well as the results of maintenance actions taken to reverse deterioration effects, impact long-term roadway capacity and connectivity. Thus, in their paper they use capacity loss to account for the impacts of deterioration and implemented improvements on roadway facility condition within their model. Both works presume that deterioration processes are known deterministically.

Infrastructure deterioration also affects user operating costs and safety, but the actions that are taken to rehabilitate the deteriorated infrastructure and eliminate these effects create capacity losses during their implementations. The time for implementation can be extensive, affecting performance in a period as short as multiple hours to as long as multiple weeks or even months.

While most studies in the network-level, strategic prioritization literature account for the improved roadway segment performance resulting from maintenance actions that are completed, few consider the downtime effects of pavement improvement actions during the period of action implementation (e.g., while the roadway is being resurfaced) (Medury & Madanat, 2013; Ng, Lin, & Waller, 2009). Medury and Madanat (2013) incorporated these downtime effects in roadway asset management by accounting for differences in capacity due to various maintenance actions. Solution in their work was obtained through a TD-learning (SARSA) approach. However, they also employed a simplified traffic model that merely restricts maximum flows. Building on the bilevel formulation in (Ouyang, 2007), Ng et al. (2009) incorporated capacity loss during maintenance activities in optimal maintenance planning. They account for the downtime associated with the related activities in increments

of years. A heuristic genetic algorithm with arbitrary performance was used for problem solution.

Chu and Chen (Chu & Chen, 2012) also applied a bilevel optimization approach with UE at the lower level, capturing deterioration and downtime effects on traffic. However, at the upper level their approach uses a threshold-based maintenance plan. The model presumes a deterministic but continuous deterioration process. A tabu search algorithm is applied to choose from various threshold options. Chu and Huang (Chu & Huang, 2018) proposed mixed-integer programs (MIPs) for scheduling pavement maintenance actions under worst-first, best-first, threshold-based, optimization-based, and mixed strategies. A solution procedure is proposed for the optimization-based and mixed strategies that uses concepts from MIP, greedy algorithms and Lagrangian relaxation.

A synthesis of these most relevant works is given in Table 4-1. The table also highlights the contributions of this work: accepted traffic modeling, incorporation of downtime impacts from activity execution, stochastic deterioration, multi-asset class consideration, and a cutting-edge solution methodology that can scale for large problem instances.

The MDP-based approach is widely used in infrastructure management, as it relies on firm stochastic dynamic programming principles that can tackle the curse of history, provides closed-loop stochastic control optimum solutions, and can combine, in a unified mathematical framework, stochastic deterioration modeling with relevant observations collected in time (Papakonstantinou & Shinozuka, 2014; Puterman, 1994). Despite their unique qualities, MDP solutions for transportation systems can often suffer from the curse of dimensionality, as system state and action spaces scale exponentially with the number of components and Markovian transition matrices can become extremely large. Reinforcement Learning (RL) is theoretically able to alleviate the curse of dimensionality related to the state space, either under model-free approaches that do not utilize explicit information on transition dynamics in the solution process, or via model-based approaches (Sutton & Barto, 2018).

Table 4-28. Contribution of most relevant works.

Citation	Model Characteristics	Solution Methodology	Network Size	Traffic Network Modeling	Downtime from Improvement Actions	Stochasticity in Deterioration	Multi-asset Class
Ouyang & Madanat (2004)	Mixed-integer nonlinear program	Branch-and-bound and greedy heuristics	Single pavement segment			✓	
Ouyang (2007)	Dynamic programming model	Policy iteration	2 pavement segments	✓ Delays approximated			
Ng et al. (2009)	Mixed-integer bilevel model with UE at lower level	Genetic algorithm	24 two-lane pavement segments	✓ UE	✓ by year		
Medury & Madanat (2013)	Approximate dynamic programming model	TD learning – (i.e. SARSA)	11 pavement segments	✓ Max flow restrictions		✓	
Chu & Chen (2012)	Mixed-integer bilevel dynamic model, seeks optimal maintenance threshold	Tabu search	270 pavement segments	✓ UE			
Our work	Bilevel approximate dynamic programming model in upper level with UE at lower level	Deep reinforcement learning (DCMAC); SARSA	11 pavement segments + 2 bridges	✓ UE	✓ by day	✓	✓

Unfortunately, RL suffers from several limitations in practice when deployed in stochastic system domains, mainly manifesting algorithmic instabilities with solutions that can significantly diverge from optimal regions. However, with the aid of deep learning, RL has become a viable option with excellent performance (Mnih, et al., 2015).

Deep Reinforcement Learning (DRL) agents have proven capable of discovering meaningful parameterizations for problems with immense state spaces through appropriate deep neural network architectures and learning near-optimal control policies by interacting with the environment. Reinforcement learning was previously employed by Medury and Madanat (2013) and (Durango-Cohen P. L., 2004) for a related, simpler problem class. This work significantly extends their work by including a more realistic representation of traffic through a UE traffic representation, a leader-follower (bilevel) conceptualization, where the leader makes decisions that affect the roadway conditions and the followers respond by changing routes, and a significantly more advanced RL approach (a multi-agent DRL with actor-critic neural network structure and independent output layers) for efficiently solving this complicated, large-scale problem class. By more realistically capturing traffic, the impacts of improvement activity execution can be accounted for in prioritization and scheduling.

The Deep Centralized Multi-agent Actor Critic (DCMAC) RL algorithm is utilized in this work. DCMAC is a deep, off-policy, actor-critic algorithm with experience replay. DCMAC interacts directly with models of pavement deterioration and improvement action effects that determine condition states, and thus operates in the state space of the underlying MDP problem. It can provide efficient solutions in otherwise practically intractable problems of multi-component systems with high-dimensional state and action spaces. This is important here, as the state and action spaces are expanded by the inclusion of multiple assets and asset classes, stochastic deterioration represented by state transition matrices, and traffic modeling. Very generally, DCMAC may be viewed as a consistently formulated multi-agent version of the advantage actor-critic (A2C) method (Mnih, et al., 2016).

MATHEMATICAL MODEL

Model Construction

Before proceeding to the formulation of the Multi-asset Roadway Improvement Scheduling Considering Traffic Impacts problem, nomenclature used in its development is presented.

Sets

\mathbf{K}	set of roadway pavement $k = \{1, 2, 3, \dots, \mathbf{K} \}$
\mathbf{B}	set of bridge $b = \{1, 2, 3, \dots, \mathbf{B} \}$
B_k	set of bridge b on segment $k, k \in \mathbf{K}$
\mathbb{N}	set of nodes n connecting adjacent roadway segments
O	set of origin r
D	set of destination q
Ψ^{rq}	set of OD pairs $rq, r \in O, q \in D$
\mathcal{S}^k	state space of condition of roadway segment k
\mathcal{S}^b	state space of condition of bridge b
A_k	set of potential pavement improvement actions for pavements, $a^k \in A_k$

A_b	set of potential bridge improvement actions for bridges, $a^b \in A_b$
P	set of paths p through the roadway network
P_{rq}	set of paths between OD pair rq , $r \in O$, $q \in D$
T	set of years that together comprise the planning horizon, $T = \{1, 2, \dots, T\}$, for T the number of years in the planning horizon
\mathcal{T}	set of time increments on a planning year, $t \in \mathcal{T} = \{1, 2, \dots, 365\}$

Parameters

α, β, φ_k	parameters of roadway segment k performance function where φ_k is the free flow travel time along segment k , α is the scale parameter and β is the shape parameter of the function
γ	a discount factor for time-value of money
$c_{a^k}^k$	cost of implementing action $a^k \in A_k$ on segment $k \in \mathbf{K}$
$c_{a^b}^b$	cost of implementing action $a^b \in A_b$ on bridge $b \in \mathbf{B}$
f_{rq}^t	traffic demand for OD pair rq at year t , $r \in O$, $q \in D$
$\ell^k(a^k)$	downtime duration in days on segment $k \in \mathbf{K}$ under action $a^k \in A_k$
$\ell^b(a^b)$	downtime duration in days on bridge $b \in \mathbf{B}$ under action $a^b \in A_b$
$l^k(a^k)$	percentage of capacity loss of segment $k \in \mathbf{K}$ under action $a^k \in A_k$
\overline{cap}_k	initial capacity of pavement segment k while no road improvement actions are taken and segment is in perfect condition
c_{vot}	estimated value of time (VoT) of roadway users in one time increment
ρ	weight parameter for traffic delay, >0 (with a highest value of 1) to account for traffic delay costs or $=0$ if traffic delay costs are to be excluded

Upper-level variables

Decision variables

$x_{a^k,t}^k$	binary variable, equals 1 if action a^k is selected for application on pavement segment k at year t ; 0 otherwise
$y_{a^b,t}^b$	binary variable, equals 1 if action a^b is selected for application on bridge b at year t ; 0 otherwise

Dependent Variables

$z_{t,i}^k$	binary variable, equals 1 if any action is taken on pavement segment k in day i during year t ; 0 otherwise
$z_{t,i}^b$	binary variable, equals 1 if any action is taken on bridge deck b in day i during year t ; 0 otherwise
s_t^k	end state of pavement segment k reached at the beginning of month t , $s_t^k \in S^k$

s_t^b end state of bridge b reached at the beginning of month t , $s_t^b \in S^b$
 $u_k(s_t^k)$ user cost for pavement segment k in year $t \in \mathbf{T}$, a state-based cost that includes costs of damage, wear-and-tear, and fuel
 $u_b(s_t^b)$ user costs for bridge b in year $t \in \mathbf{T}$, a state-based cost that includes costs of damage, wear-and-tear, and fuel

Lower-level variables

Decision variables

$\psi_{t,t}^p$ traffic flow along path p of day $t \in \mathcal{T}$ at year $t \in \mathbf{T}$

Dependent Variables

$\psi_{k,t,t}$ total traffic flow on segment $k \in K$ during day $t \in \mathcal{T}$ of year $t \in \mathbf{T}$

$\tau_k(\psi_{k,t,t}, cap_{k,t}^t)$ travel time along pavement segment k at time increment $t \in \mathbf{T}$ under capacity of $cap_{k,t}^t$ and traffic flow of $\psi_{k,t,t}$

$\delta_{k,rq,t,t}^p$ binary variable, equals to 1 if path p between OD pair rq contains segment k at day $t \in \mathcal{T}$ of year $t \in \mathbf{T}$, 0 otherwise

Upper-level model

The problem of identifying an optimal multi-asset class roadway maintenance and improvement prioritization schedule under stochastic deterioration, accounting for traffic impacts from deteriorated pavements and bridge decks, reduced capacity during improvement implementation, and benefits from improved post-activity pavement and bridge deck serviceability is presented in this section. The goal of the model is to minimize the total improvement investment and the traffic delays resulting from capacity reduction due to the execution of the actions within the planning horizon.

$$\text{Min} \sum_{t=1}^T \gamma^{t-1} (c_1(\mathbf{a}_t) + c_2(\mathbf{s}_t) + \rho c_{\text{vot}} \mathcal{G}(\mathbf{a}_t)) \quad (4.4)$$

where $\mathbf{s}_t = \{s_t^k\}_{k=1}^{|\mathbf{K}|} \cup \{s_t^b\}_{b=1}^{|\mathbf{B}|}$ is a vector representing joint pavement and bridge condition states. The joint state space for pavements and bridges is, thus, $\mathbf{S} = S^1 \times S^2 \dots \times S^{|\mathbf{K}|} \times S^1 \times S^2 \times \dots \times S^{|\mathbf{B}|}$. $\mathbf{a}_t = (\mathbf{x}_t, \mathbf{y}_t)$ denotes the pair of pavement and bridge actions taken at time t , where $\mathbf{x}_t = \{x_t^1, x_t^2, \dots, x_t^{|\mathbf{K}|}\}$ is the set of action vectors over $|\mathbf{K}|$ pavement segments for $x_t^k = \{x_{1,t}^k, x_{2,t}^k, \dots, x_{|A_k|,t}^k\}$ and $\sum_{a^k \in A_k} x_{a^k,t}^k = 1$, and $\mathbf{y}_t = \{y_t^1, y_t^2, \dots, y_t^{|\mathbf{B}|}\}$ is the set of action vectors over $|\mathbf{B}|$ bridge deck for $y_t^b = \{y_{1,t}^b, y_{2,t}^b, \dots, y_{|A_b|,t}^b\}$ and $\sum_{a^b \in A_b} y_{a^b,t}^b = 1$. The joint action space is then $\mathbf{A} = A_k^{|\mathbf{K}|} \times A_b^{|\mathbf{B}|}$.

In Eqn. (4.1), term $c_1(\mathbf{a}_t)$ denotes the total costs for improvements at year t , the term $c_2(\mathbf{s}_t)$ (Eq. (3)) reflects the cost for roadway users and the term $\rho c_{\text{vot}} \mathcal{G}(\mathbf{a}_t)$ denotes the minimal traffic delay cost under improvement actions \mathbf{a}_t . $\rho c_{\text{vot}} \mathcal{G}(\mathbf{a}_t)$ is obtained via solution of a UE lower-level subproblem. For small problem instances, these values can be determined in a pre-processing stage. The term $c_1(\mathbf{x}_t, \mathbf{y}_t)$ can be expanded, as in Eqn. (4.2).

$$c_1(\mathbf{x}_t, \mathbf{y}_t) = \sum_{k \in K} \sum_{a^k \in A_k} c_{a^k}^k \cdot x_{a^k, t}^k + \sum_{b \in B} \sum_{a^b \in A_b} c_{a^b}^b \cdot y_{a^b, t}^b \quad (4.5)$$

The second term in Eqn. (4.1) enables the inclusion of user costs, specifically fuel and vehicle value depreciation, associated with the pavement segments and bridge decks. $\mathbf{s}_t = \{s_t^1, s_t^2, \dots, s_t^{|K|}\} \cup \{s_t^1, s_t^2, \dots, s_t^{|B|}\}$ is a set of state of bridges and pavement states.

$$c_2(\mathbf{s}_t) = \sum_{k \in K} u_k(s_t^k) + \sum_{b \in B} u_b(s_t^b) \quad (4.6)$$

Worse roadway conditions lead to higher fuel costs and faster depreciation in vehicle value. Thus, user costs are a function of condition state. Adapted from (Medury & Madanat, 2013) and (Faddoul, Raphael, Soubra, & Chateaufneuf, 2013), total user cost, $c_2(\mathbf{s}_t)$, is calculated in this work with a presumed traffic flow rate.

$\mathcal{G}(\mathbf{a}_t)$ denotes the traffic delay in hours during planning year t when applying joint improvement actions \mathbf{a}_t and is evaluated via Eqn. (4.4).

$$\mathcal{G}(\mathbf{a}_t) = \sum_{t=0}^{365} \sum_{k \in K} \left(\psi_{k,t,t} \cdot \tau_k(\psi_{k,t,t}, cap_{k,t}^t) - \psi_{k,t} \cdot \tau_k(\psi_{k,t}, \overline{cap}_k) \right) \quad (4.7)$$

where $cap_{k,i}^t = \overline{cap}_k * (1 - z_{t,t}^k \sum_{a_1 \in A_1} l^k(a_1) x_{a_1,t}^k) * (1 - z_{t,t}^b)$ for $b \in B_k$. $b \in B_k$ maps the bridges to the pavement segments. The capacity of a bridge affects the capacity of the relevant pavement segment. If a bridge is closed, the pavement segment will have zero capacity. $cap_{k,i}^t$ reflects how the capacity of segment k at day i of year t is influenced by the ongoing improvement action. It is presumed that improvement action $\mathbf{x}_t^k = \{x_{1,t}^k, x_{2,t}^k, \dots, x_{|A_k|,t}^k\}$ on pavement segment k in year t starts at the beginning of the year and lasts $\sum_{a \in A_k} \rho^k(a^k) x_{a^k,t}^k$ days. Likewise, improvement action $\mathbf{y}_t^b = \{y_{1,t}^b, y_{2,t}^b, \dots, y_{|A_b|,t}^b\}$ on bridge b in year t starts at the beginning of the year and lasts $\sum_{a \in A_b} \rho^b(a^b) y_{a^b,t}^b$ days. $z_{t,t}^k$ and $z_{t,t}^b$ equal 1 when pavement segment k or bridge deck b is under improvement action execution. These binary variables aid Eqn. (4.4) in ensuring that the appropriate partial or zero capacity of a pavement or pavement segment overlaying a bridge deck, respectively, is applied when the asset is being maintained and is at full capacity otherwise. Traffic flow then changes according to the lower-level UE model.

The deterioration of the roadway assets and condition improvements achieved through improvement actions follow a one-step transition probability. Thus, only the present state \mathbf{s}_t of an asset and action \mathbf{a}_t taken on it will affect the state of that asset in the next planning year \mathbf{s}_{t+1} (Eqn. (4.5)).

$$P(\mathbf{s}_{t+1} | \mathbf{s}_1, \mathbf{s}_2, \dots, \mathbf{s}_t, \mathbf{a}_1, \mathbf{a}_2, \dots, \mathbf{a}_t) = P(\mathbf{s}_{t+1} | \mathbf{s}_t, \mathbf{a}_t) \quad (4.8)$$

Lower-level model

$$\text{Min} \sum_{k \in K} \int_0^{\psi_{k,t,t}} \tau_k(\psi, \text{cap}_{k,t}^t) d\psi \quad (4.9)$$

s.t.

$$\sum_{\pi \in P_{rq}} \psi_{t,t}^p = f_{rq}^t \quad \forall rq \in OD, \forall t \in \mathbf{T}, t \in \mathcal{T} \quad (4.10)$$

$$\psi_{k,t,t} = \sum_{rq \in OD} \sum_{p \in P_{rq}} \delta_{k,rq,t,t}^{\pi} \psi_{t,t}^{\pi} \quad \forall rq \in OD, \forall k \in K, \forall t \in \mathbf{T}, t \in \mathcal{T} \quad (4.11)$$

$$\psi_{t,t}^p \geq 0 \quad \forall rq \in OD, \forall p \in P_{rq}, \forall t \in \mathbf{T}, t \in \mathcal{T} \quad (4.12)$$

$$\psi_{k,t,t} \geq 0 \quad \forall k \in K, \forall p \in P, \forall t \in \mathbf{T}, t \in \mathcal{T} \quad (4.13)$$

The lower level seeks a user equilibrium under improvement actions determined in the upper level, accounting for capacity reduction associated with the downtime required for action implementation. The UE formulation follows Beckmann's formulation (Beckmann et al., 1956) and objective function (Eqn. (4.6)) is known as the Beckmann function. A Bureau of Public Roads (BPR) function (United States Department of Commerce, 1964) is used as the link performance function as in Eqn. (4.11) (i.e., $\tau_k(\psi) = \tau_k(\psi_{k,t,t}, \text{cap}_{k,t}^t)$):

$$\tau_k(\psi_{k,t,t}, \text{cap}_{k,t}^t) = \varphi_k \left(1 + \alpha * \left(\frac{\psi_{k,t,t}}{\text{cap}_{k,t}^t} \right)^{\beta} \right) \quad \forall k \in K, \forall t \in \mathbf{T}, t \in \mathcal{T} \quad (4.14)$$

Constraints in Eqn. (4.7) ensure that, for all pairs r - q , flow on paths from origin r to destination q equal fixed OD pair demand for pair r - q . Constraints in Eqn. (4.8) connect link flows to path flows. Nonnegativity is ensured through constraints in Eqns. (4.9) and (4.10). Upper-level solutions, \mathbf{x}_t^k and \mathbf{y}_t^b , affect asset element capacities, and $\text{cap}_{k,t}^t$ of link performance function (Eqn. (4.11)) is employed in the lower-level objective in Eqn. (4.6). With the value of traffic flow $\psi_{k,t,t}$ and travel time of each link $\tau_k(\psi_{k,t,t}, \text{cap}_{k,t}^t)$, traffic delay can be calculated through Eqn. (4.4). Note that O-D demand is presumed to be fixed.

SOLUTION METHODS

A DCMAC method is adapted to solve the Multi-asset Roadway Improvement Scheduling Considering Traffic Impacts problem. Descriptions of the threshold-based and SARSA-LFA methods precede presentation of the DCMAC approach. They were implemented to provide appropriate baselines for comparison. Alternative baselines, such as worst-first, can be also used, as suggested in Chu and Huang (2018), for example.

Threshold-based Method

A threshold-based method is adapted as a basis for comparison. This method finds the optimal threshold settings $\{(\zeta_1, \zeta_2, \dots, \zeta_{|A_1|}), (\sigma_1, \sigma_2, \dots, \sigma_{|A_2|})\}$ for pavements and bridges as a function of

their condition state. $(\zeta_1, \zeta_2, \dots, \zeta_{|A_1|})$ is the set of thresholds settings for pavements with $\zeta_1 < \zeta_2 < \dots < \zeta_{|A_1|} \leq |S^k|$ and $(\sigma_1, \sigma_2, \dots, \sigma_{|A_2|})$ is the set of threshold settings for bridges with $\sigma_1 < \sigma_2 < \dots < \sigma_{|A_2|} \leq |S^b|$. In this work, the optimal thresholds are identified through an exhaustive testing of all thresholds options as in Eqn. (4.12).

$$\text{Min}_{\text{threshold} \sim TH} \mathbb{E}_{\mathbf{a}_t \sim \text{thr}} \left(\sum_{t=1}^T \gamma^{t-1} (c_1(\mathbf{a}_t) + c_2(\mathbf{s}_t) + \rho c_{\text{vot}} \mathcal{G}(\mathbf{a}_t)) \right) \quad (4.15)$$

where TH is a set of all threshold options. Pseudo code for the threshold-based method is shown in Table 4-2.

**Table 4-29. Pseudo code for threshold-based method
{N set to number of iterations}**

<p>List all the threshold settings $\{[(\zeta_1, \zeta_2, \dots, \zeta_{ A_1 }), (\sigma_1, \sigma_2, \dots, \sigma_{ A_2 })]_i\}$ and store the mean cost in order in $\mathbf{C} = \{C_1/N, C_2/N, \dots\}$.</p> <p>For each threshold setting $[(\zeta_1, \zeta_2, \dots, \zeta_{ A_1 }), (\sigma_1, \sigma_2, \dots, \sigma_{ A_2 })]_i$:</p> <p style="padding-left: 20px;">$C_i = 0$</p> <p style="padding-left: 20px;">For each iteration:</p> <p style="padding-left: 40px;">$C_n = 0$</p> <p style="padding-left: 40px;">Initialize \mathbf{s}_1 and take action \mathbf{a}_1 given the threshold setting.</p> <p style="padding-left: 40px;">Call lower-level UE and compute cost $C_n = C_n + C(\mathbf{s}_1, \mathbf{a}_1)$.</p> <p style="padding-left: 20px;">For $t = 2, 3, \dots, T$:</p> <p style="padding-left: 40px;">Observe state \mathbf{s}_t and take action \mathbf{a}_t given the threshold setting.</p> <p style="padding-left: 40px;">Call lower-level UE and compute cost $C_n = C_n + C(\mathbf{s}_t, \mathbf{a}_t)$.</p> <p style="padding-left: 20px;">$C_i = C_i + C_n$</p> <p style="padding-left: 20px;">$\mathbf{C} = \mathbf{C} \cup \frac{C_i}{N}$</p> <p>Pick optimal threshold index $i^* = \underset{C_i \in \mathbf{C}}{\text{argmin}} C_i$</p>

The MDP Formulation

MDPs take as input transition probability matrices that provide the probabilities, $Pr(\mathbf{s}_{t+1} | \mathbf{s}_t, \mathbf{a}_t)$, of each system element transitioning from a given state \mathbf{s}_t , to another \mathbf{s}_{t+1} in the next time increment $t + 1$ given any action \mathbf{a}_t that is taken in the current time increment t .

With the aim of maximizing total reward (or minimizing total cost), a mathematical policy $\pi = \{\pi_1^k\}_{k=1}^{|K|} \cup \{\pi_2^b\}_{b=1}^{|B|}$ is sought, which gives a mapping from system state to suitable actions. Action-value $Q_\pi(\mathbf{s}_t, \mathbf{a}_t)$ denotes the expected cost through the end of the planning horizon for taking action \mathbf{a}_t when in system state \mathbf{s}_t at time t from policy π :

$$Q_\pi(\mathbf{s}_t, \mathbf{a}_t) = \mathbb{E}_\pi \left(\sum_{k=0}^{T-t} \gamma^k c_{t+k} | \mathbf{s}_t, \mathbf{a}_t \right), \forall t \in T \quad (4.16)$$

with $c_t = c_1(\mathbf{x}_t, \mathbf{y}_t) + c_2(\mathbf{s}_t) + \rho c_{\text{vot}} \mathcal{G}(\mathbf{x}_t)$ denoting the current cost. The state value is equivalently calculated as the expected return from state \mathbf{s}_t to the end of the planning horizon following policy π . $\mathbf{a}_t \sim \pi$ in the value function V denotes that \mathbf{a}_t follows from policy π .

$$V_{\pi}(\mathbf{s}_t) = \mathbb{E}_{\mathbf{a}_t \sim \pi}(Q_{\pi}(\mathbf{s}_t, \mathbf{a}_t)), \quad \forall t \in \mathbf{T} \quad (4.17)$$

Value function $V_{\pi}(\mathbf{s}_t)$ can be equivalently expressed as the sum of the cost at time t plus the cost of the succeeding state-value at time $t + 1$, $V_{\pi}(\mathbf{s}_{t+1})$.

$$V_{\pi}(\mathbf{s}_t) = \mathbb{E}_{\mathbf{a}_t \sim \pi}(c_t + \gamma \cdot V_{\pi}(\mathbf{s}_{t+1})), \quad \forall t \in \mathbf{T} \quad (4.18)$$

Dynamic programming provides an approach for computing the optimal policy π^* based on Bellman equations (Eqn. (4.16)) (Puterman, 1994). Eqn. (4.15) can be then expanded, as in Eqn. (4.16).

$$V^*(\mathbf{s}_t) = \min_{\mathbf{a}_t} \mathbb{E}(c_t + \gamma \cdot Pr(\mathbf{s}_{t+1} | \mathbf{s}_t, \mathbf{a}_t) \cdot V^*(\mathbf{s}_{t+1})). \quad \forall t \in \mathbf{T} \quad (4.19)$$

The Multi-asset Roadway Improvement Scheduling Considering Traffic Impacts problem is a high-dimensional, stochastic, bilevel program with recursive objective function. The state space increases exponentially as the number of roadway assets increases, and therefore exact solutions are formidable due to the high dimensionality. In the next section, the DCMAC algorithm, introduced in (Andriotis & Papakonstantinou, 2019), a deep reinforcement learning method, is proposed for the MDP solution. It is particularly well suited for stochastic control problems with multiple components. DRL is well designed for problem instances with large dimensionality and complexity, enabling exceptional parameterization capabilities for huge state spaces. However, this is not the case, in general, for similarly large discrete action spaces, which are also present in multi-component transportation systems. The DCMAC approach was introduced in (Andriotis & Papakonstantinou, 2019) and is particularly well suited for stochastic control problems of systems with multiple components. DCMAC takes advantage of the parameterization capabilities of deep policy gradient methods in large state spaces, and further originally extends them to large action spaces that have numerous distinct action categories.

The SARSA-LFA algorithm and state-action value approximation

The SARSA algorithm is an on-policy TD learning method, a type of reinforcement learning methodology, that builds on concepts of both Monte Carlo control and dynamic programming (Sutton & Barto, Reinforcement Learning: An Introduction, 2018). In general, RL techniques seek a mapping from system state to suitable action vectors that seek to optimize defined objectives, such as total cost minimization or total reward maximization. In this work, a minimum total cost to both the system and its users is sought. As discussed in (Sutton & Barto, 2018), RL methods learn from experience over their iterations and are particularly useful when the problem's dimensionality is too large to obtain an exact solution, a modeling environment is only provided through black box solvers, or only actual data are available.

For problems with multiple states, the SARSA method does not scale up. To address this, a SARSA with linear function approximation (SARSA-LFA) method was proposed in (Sutton, et al., 2009), wherein manually chosen feature functions are used to approximate the action-value $Q(\mathbf{s}_t, \mathbf{a}_t)$. Thus, the SARSA-LFA method is highly dependent on the quality of the feature functions. As the number of roadway assets grows, state space \mathbf{S} and action space \mathbf{A} grow

exponentially, making these feature functions also difficult to construct for larger problem instances. Most SARSA methods use this approximate approach. Instead, DRL methods, such as deep Q-network (DQN) methods (Mnih, et al., 2015), embed a neural network structure to represent these feature functions that lead to more efficient parametrization of $Q(\mathbf{s}_t, \mathbf{a}_t)$. These approaches are also similarly problematic to scale up with respect to the action space.

The SARSA-LFA algorithm approximates the state-action value $Q(\mathbf{s}_t, \mathbf{a}_t)$ using a weighted sum of feature functions, $f_i(\mathbf{s}_t, \mathbf{a}_t, t)$ as in Eqn. (4.17).

$$Q(\mathbf{s}_t, \mathbf{a}_t) = \sum_{i \in \Omega} w_i * f_i(\mathbf{s}_t, \mathbf{a}_t, t) \quad (4.20)$$

where the total number of feature functions is given by $|\Omega|$, for Ω the set of feature functions, and feature function i is weighted by $w_i \in \mathbf{w}$. Given weight \mathbf{w} and state \mathbf{s}_t , the temporal error is calculated:

$$\Delta_t = \sum_{k=0}^{n-1} \gamma^k c_{t+k} + \gamma^n Q(\mathbf{s}_{t+n}, \mathbf{a}_{t+n}) - Q(\mathbf{s}_t, \mathbf{a}_t) \quad (4.21)$$

The first two terms of Eqn. (4.18) approximate the total cost within the planning horizon using the summation of sample cost from time step t to $t + n - 1$ and action-value $Q(\mathbf{s}_{t+n}, \mathbf{a}_{t+n})$. When $n=1$, the TD method is a one-step look ahead approach. At the other extreme, when $n=T$, the TD method is equivalent to a Monte Carlo control approach.

Weights are updated given updated Δ_t for increased accuracy following Eqn. (4.19).

$$w_i = w_i + lr * \Delta_t \quad (4.22)$$

The learning rate, lr , in Eqn. (4.19) affects algorithm convergence.

The SARSA method balances exploration of the search space against exploitation in a local neighborhood in determining actions to take under a given state. The action is chosen probabilistically either from a feasible action set with probability ϵ or, with probability $1 - \epsilon$, to be the action that leads to the minimal action-value $Q_\pi(\mathbf{s}_t, \mathbf{a}_t)$. A synthesis of the proposed SARSA-LFA method as specified for the Multi-asset Roadway Improvement Scheduling Considering Traffic Impacts problem is given in pseudo code for SARSA-LFA in Table 4-3.

Deep Centralized Multi-agent Actor Critic

The Multi-asset Roadway Improvement Scheduling Considering Traffic Impacts problem is a single-agent RL problem in which the agent schedules improvement actions on all pavement segments and bridges. The problem can be defined as a 6-tuple of pavements, bridge decks, states, actions, transition probabilities and costs: $\langle \mathbf{K}, \mathbf{B}, \mathbf{S}, \mathbf{A}, P, C \rangle$, where P represents the transition function: $\mathbf{S} \times \mathbf{A} \times \mathbf{S} \rightarrow [0,1]$. To reduce the solution size of the action space, the problem is reformulated as a multi-agent problem, where each agent makes decisions on improvement actions for only one pavement segment or bridge. The states of all roadway assets and the value of the objective function are shared to enable agents to work cooperatively. A joint policy for application across all roadway assets, $\pi: \mathbf{S} \rightarrow \mathbf{A}$, is finally, thus, identified. It minimizes the total cost incurred, C .

Table 4-30. Pseudo code for SARSA-LFA

<p>Initialize feature function weights \mathbf{w} and learning rate lr Repeat:</p> <p style="text-align: center;">$t=1$</p> <p>Randomly generate \mathbf{s}_1, take action \mathbf{a}_1 as identified by (\mathbf{u}_t the vector of feasible actions over all segments for time t, $\mathbf{u}_t \in \mathbf{U}$ for $t = 1, 2, \dots, T$):</p> $\mathbf{a}_t = \begin{cases} \mathbf{u}_t: \text{such that } Q(\mathbf{s}_t, \mathbf{u}_t) \text{ is minimum} & \text{chosen with probability } 1 - \varepsilon \\ \text{any feasible solution } \mathbf{u}_t & \text{chosen with probability } \varepsilon \end{cases}$ <p style="text-align: center;">Calculate C_1, calling lower-level UE as needed Store $\mathbf{s}_1, \mathbf{a}_1, C_1, Q(\mathbf{s}_1, \mathbf{a}_1)$ for training purposes</p> <p>For $t = 2, 3, \dots, T$:</p> <p style="padding-left: 2em;">Observe state \mathbf{s}_t, take action \mathbf{a}_t, call lower-level UE to calculate C_t, and calculate the value of $Q(\mathbf{s}_t, \mathbf{a}_t)$ following Eqn. (4.17) Store $\mathbf{s}_t, \mathbf{a}_t, C_t, Q(\mathbf{s}_t, \mathbf{a}_t)$ for training purposes Compute cost $C(\mathbf{s}_t, \mathbf{a}_t)$</p> <p>For $t = T, T-1, \dots, 1$:</p> <p style="padding-left: 2em;">Calculate Δ_t according to Eqn. (4.18) Update weights $\mathbf{w} = \mathbf{w} + lr \cdot \Delta_t \cdot \nabla f(\mathbf{s}_t, \mathbf{a}_t, t)$, for future $Q(\mathbf{s}_t, \mathbf{a}_t)$ computation</p>

The DCMAC method adapted from (Andriotis & Papakonstantinou, 2019) is a DRL technique. It evolved from actor-critic methods that sometimes use two neural networks, splitting evaluation from action (for example, (Konda & Tsitsiklis, 2003)). The multi-agent reformulation assumes that actions on system components are conditionally independent of one another as a means of reducing the size of the action space. With this assumption, the policy set that guides the actions can be given by $\pi = \prod_1^{|\mathbf{K}|} \pi_1^k \times \prod_1^{|\mathbf{B}|} \pi_2^b$, where $\pi_1^k: \mathbf{S} \rightarrow A_k$ denotes the policy for pavement $k \in \mathbf{K}$ and $\pi_2^b: \mathbf{S} \rightarrow A_b$ denotes the policy for bridge $b \in \mathbf{B}$, greatly reducing the action space and making it possible to solve larger problem instances. For example, for a study location with 5 components for which 3 actions each are considered, $3^5=243$ different Q-functions would be required to approximate the values of the actions in the action space for the SARSA, and traditional DRL methods. The same problem with the multi-agent formulation of DCMAC can be formulated based on $5 \times 3=15$ different actions, 3 for each component, without any loss of generality and/or accuracy.

In DCMAC, deep neural networks are applied to generate the improvement actions and approximate the critic value using actor and critic network parameter vectors θ^π and θ^V , respectively. To optimize the parameters θ^π , an efficient method is used to compute the off-policy gradient estimator \mathbf{g}_{θ^π} (Eqn. (4.20)) with samples generated by a behavior policy $\mu \neq \pi$ using importance sampling.

$$\mathbf{g}_{\theta^\pi} = E_{\mathbf{s}_t \sim \omega, \mathbf{a}_t \sim \mu} [w_t \sum_{i=1}^n \nabla_{\theta^\pi} \log \pi_i(a_t^{(i)} | \mathbf{s}_t, \theta^\pi) A^\pi(\mathbf{s}_t, \mathbf{a}_t)] \quad (4.23)$$

with $w_t = \pi(\mathbf{a}_t | \mathbf{s}_t) / \mu(\mathbf{a}_t | \mathbf{s}_t)$, where θ^π is a n -dimensional vector of agent behavior policies and n is equal to the number of control units; ω is the $|\mathbf{K}|$ -dimensional vector of limiting state distributions under these policies.

The advantage function $A^\pi(\mathbf{s}_t, \mathbf{a}_t)$ in Eqn. (4.21) can be seen as a zero-mean measure expressing how advantageous an action at each state is. It is defined as:

$$A^\pi(\mathbf{s}_t, \mathbf{a}_t) = Q^\pi(\mathbf{s}_t, \mathbf{a}_t) - V^\pi \quad (4.24)$$

DCMAC approximates the advantage function following the temporal difference:

$$A^\pi(\mathbf{s}_t, \mathbf{a}_t | \boldsymbol{\theta}^V) = c(\mathbf{s}_t, \mathbf{a}_t) + \gamma V^\pi(\mathbf{s}_{t+1} | \boldsymbol{\theta}^V) - V^\pi(\mathbf{s}_t | \boldsymbol{\theta}^V) \quad (4.25)$$

The critic network is accordingly updated through the mean squared error:

$$L_V(\boldsymbol{\theta}^V) = E_{\mathbf{s}_t \sim \omega, \mathbf{a}_t \sim \mu} [w_t (c(\mathbf{s}_t, \mathbf{a}_t) + \gamma V^\pi(\mathbf{s}_{t+1} | \boldsymbol{\theta}^V) - V^\pi(\mathbf{s}_t | \boldsymbol{\theta}^V))^2] \quad (4.26)$$

and its respective gradient, which is computed by backpropagating the weighted advantage function through the critic network:

$$\mathbf{g}_{\boldsymbol{\theta}^V} = E_{\mathbf{s}_t \sim \omega, \mathbf{a}_t \sim \mu} [w_t \nabla_{\boldsymbol{\theta}^V} V^\pi(\mathbf{s}_t | \boldsymbol{\theta}^V) A^\pi(\mathbf{s}_t, \mathbf{a}_t | \boldsymbol{\theta}^V)] \quad (4.27)$$

DCMAC extends the hidden layers of the actor network, as shown in Figure 4-1, into distinct output nodes, each utilizing centralized system-state information to decide which action to take in each studied sub-system (here, each roadway segment). In this application, $|K|$ output nodes are defined, one output layer for each segment. Each output node associated with a bridge-free pavement segment generates a probability distribution over the action options for its segment, as portrayed with the bar plots in the bottom right of Figure 4-1. Each output layer for segments with both pavements and a bridge generates the joint distribution over combinations of action options for both the pavement and bridge portions. These distributions are shown as the bar plots in the bottom right of Figure 4-1.

A critic neural network (upper part in Figure 4-1) is constructed to approximate the total cost of the improvement action plan over the planning horizon, including implementation impacts, over the planning horizon. This requires evaluation of the recursive cost functions (Eqn. (4.14)). To train the actor and critic neural networks, the DCMAC method is run over repeated episodes. A realization of the condition states is simulated under each episode and the improvement actions to take over the entire planning horizon under this realization are identified. During this training process, realized pavement and bridge deck states, actions selected, and associated total costs are stored in a replay buffer. The replay buffer is used for training the actor and critic networks simultaneously through a process of backpropagation commonly used for training neural networks (Werbos, 1988). Table 4-4 shows the details of the DCMAC algorithm as applied to this roadway improvement problem class.

Table 4-31. Pseudo code for DCMAC.

Construct the actor and critic neural networks; initialize the networks' parameters θ^π and θ^V .

For training, set a replay buffer to store experiences in terms of actions under different states and their costs, batch size, and exploration noise ϵ used in avoiding local optima;

Loop for each episode (iteration or replication):

Initialize states s_1 of the roadway segments at the start of the planning horizon;

Loop for $t = 1, 2, \dots, T$ (e.g. years 1, 2, \dots in a multi-year planning horizon of length T):

Generate behavior policy μ_t at random with exploration noise, otherwise

$$\mu_t \sim \pi(\cdot | s_t, \theta^\pi)$$

Take actions a_t according to μ_t

Call lower-level UE and calculate associated cost c_t ;

Store $s_t, s_t + 1, a_t, \mu_t, c_t$ within replay buffer;

Update states for a given simulated realization;

Sample batch $(s_\tau, s_\tau + 1, a_\tau, \mu_\tau, c_\tau)$ from the replay buffer and approximate the advantage function with Eqn. (4.22):

$$A^\pi(s_\tau, a_\tau | \theta^V) = c_i + \gamma V^\pi(s_{\tau+1} | \theta^V) - V^\pi(s_\tau | \theta^V)$$

Calculate the truncated sample weights:

$$w_t = \min \left\{ \mathcal{C}, \frac{\pi(a_t | s_t)}{\mu_t(a_t | s_t)} \right\}, \text{ where } \mathcal{C} \text{ represents the value at which the sample weights are truncated.}$$

Update the actor and critic parameters according to the gradients:

$$g_{\theta^\pi} = \sum_{\tau} [w_{\tau} \left(\sum_{i=1}^n \nabla_{\theta^\pi} \log \pi_i(a_\tau^{(i)} | s_\tau, \theta^\pi) \right) A^\pi(s_\tau, a_\tau | \theta^V)]$$

$$g_{\theta^V} = \sum_{\tau} [w_{\tau} V^\pi(s_\tau | \theta^V) A^\pi(s_\tau, a_\tau | \theta^V)]$$

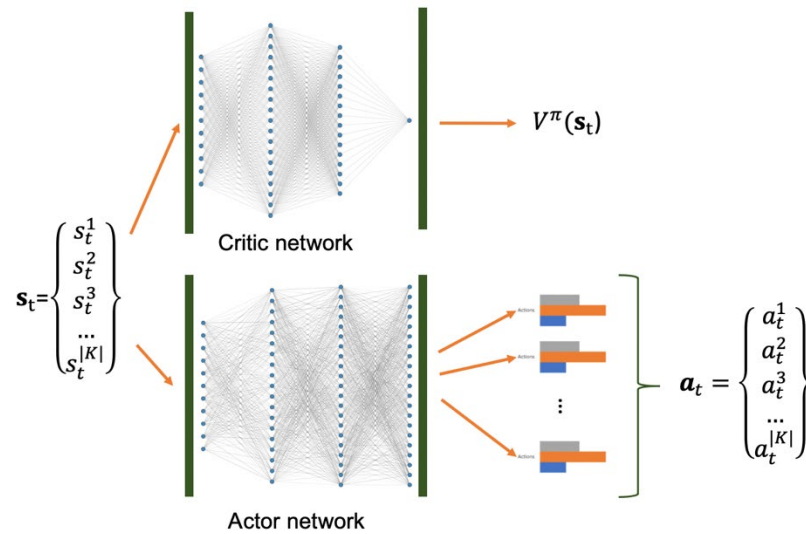


Figure 4-7. Deep centralized multi-agent actor critic neural network (generated with NN-SVG (LeNail, 2019))

EVALUATING THE PROPOSED MULTI-ASSET ROADWAY IMPROVEMENT SCHEDULING MODEL AND SOLUTION METHOD ON AN ILLUSTRATIVE NETWORK

Roadway Network Description

The proposed methodology is applied on a hypothetical traffic network presented in (Medury & Madanat, 2013) expanded to include two bridges. Deterioration dynamics and post-improvement action benefits for pavement segments were adapted from relevant literature (Madanat & Ben-Akiva, 1994; Faddoul, Raphael, Soubra, & Chateauneuf, 2013) and for bridge decks in (PennDOT, 2009; Manafpour, Guler, Radlinska, Rajabipour, & Warn, 2018). The aim of this application is to illustrate the importance of considering uncertainty in deterioration processes, traffic delays at a network level while also incorporating downtime impacts from roadway improvement actions, and post-improvement action conditions. Figure 4-2 and Table 4-5 provide the topology of the network representation and its attributes. As in Medury and Madanat's network, the roadway links are directed with O as the origin node and D as the destination node. Two bridge decks are added to pavement segments No. 7 and No. 9. Each bridge deck has six discrete states. Deterioration transition matrices of the pavements and bridge decks, along with improvement action benefits, are detailed in Appendix E, Table E-1 through Table E-6. The costs and durations of the improvement actions and the user costs are detailed in Appendix F, Table F-1 through Table F-6.

Table 4-5 introduces values used in characterizing the roadway segments (links), including lengths and free flow speeds. Medury and Madanat (2013) provided only capacities that were not within a range that matches realistic roadway characteristics. In this work, segment capacities were computed assuming 2,250 vehicles per hour per lane and a free flow speed of 55 mph (United States Department of Transportation (USDOT), 2021). Minor and major repair actions are assumed to cause the closure of half of the lanes, while any improvement actions taken on the

bridges require full closure. The value of travel time (\$18.70/person-hour) was taken from the USDOT (USDOT, 2016) to calculate travel delay costs. Average vehicle occupancy was set to 1.67 persons per vehicle according to the USDOT (USDOT, 2017). Thus, travel delay costs were set to \$31.22/vehicle-hour. Total OD demand was set to 8,700 vehicles per hour. The test network can be characterized as congested (level of service E) with little redundancy, making even small events disruptive.

Experimental Results

Numerical experiments were conducted to investigate the importance of accounting for traffic impacts and uncertainty in pavement and bridge deck deterioration when developing optimal improvement action schedules. These experiments were run on the roadway network of Figure 4-2, and improvement actions were sampled and implemented according to the computed stochastic policy, $\pi(\cdot | s_t, \theta^\pi)$. Results are given in following subsections.

Table 4-32. Roadway information.

Segment#	Number of lanes	Free flow speed (mile/hour)	Length (mile)
1	4	55	5
2	4	55	5
3	4	55	5
4	2	55	5
5	1	55	5
6	1	55	5
7	1	55	5
8	1	55	5
9	2	55	5
10	2	55	5
11	2	55	5

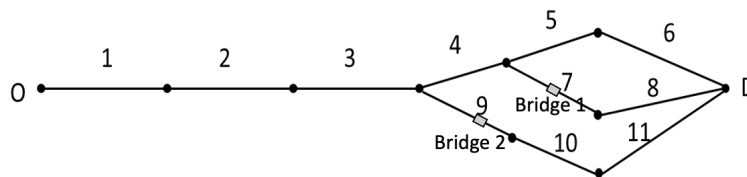


Figure 4-8. Roadway network.

Accounting for traffic impacts

To evaluate the importance of incorporating more realistic traffic delays at the network level in improvement action scheduling, decisions obtained from the proposed bilevel model are compared against those from a single-level version that excludes traffic impacts. This model seeks to minimize total improvement action cost over a planning horizon of 20 years with discount factor of 0.95. For the sake of comparing results to the single-level version that

excludes traffic impacts to the proposed bilevel model solutions, the cost of travel delays incurred during the execution of improvement actions is included in the cost objective in runs of both models. As exact solution is not obtainable due to the high dimensionality of the problem instance, best threshold policies for both single and bilevel models were obtained as a basis for comparison.

Table 4-6 shows the lifecycle costs incurred for solutions with and without traffic disruption for each of the three solution approaches over a planning horizon of 20 years for 5,000 replications, each with a randomly chosen initial state. Road improvement and user costs of the solution obtained for the bilevel model (considering traffic impacts) are significantly higher than the costs associated with the single-level model solution that does not account for traffic impacts. However, the overall cost of the solution of the bilevel model is lower.

The total costs for the solutions of both single- and bilevel threshold models are also provided (Table 4-6). For the single-level model, the total costs excluding/including costs of traffic delay under all methods are \$9.58/\$41.60 (threshold), \$10.06/\$43.68 (SARSA) and \$9.51/\$40.07 (DCMAC) million. When reassessed in a bilevel conceptualization, where traffic effects are included, these values, including the cost of traffic delay, are \$37.15 (threshold), \$39.28 (SARSA) and \$36.02 (DCMAC) million. Savings in total costs of approximately 10% was attained by accounting for traffic impacts in the execution of improvement actions. The difference in total cost savings between the threshold and optimal scheduling approaches may widen for larger problem instances, where complete enumeration over the threshold values, and therefore identification of the optimal threshold, may not be possible. Similarity in total costs for the solutions is likely due to the homogeneity of the network elements.

DCMAC outperforms SARSA for both single and bilevel models (i.e., with and without inclusion of traffic impacts). Figure 4-3 and Figure 4-4 show how the total costs evolve during the training process of the SARSA and DCMAC methods applied to the bilevel formulation, respectively. The figures indicate that the SARSA method converges faster than the DCMAC method; however, the final policy generated by the DCMAC method outperforms that produced by the SARSA method. The parameters used for SARSA and DCMAC methods are included in Appendix G. It is noteworthy that the threshold solutions also consistently outperformed the activity schedules obtained through the SARSA method.

An example of pavement states and transitions for pavement segment 3 over the planning horizon found using optimal prioritization via DCMAC and accounting for traffic disruption is shown in Figure 4-5. Minor repairs are applied in years 8 and 10 while the pavement is in mediocre, fair, or good condition. Major repairs are implemented in years 1 and 18 when the pavement has deteriorated to a poor condition. State transitions for all pavement segments and bridges are given in Figure 4-6.

Table 4-33. Road improvement cost and traffic delay cost (with $\rho = 0.05$).

		Road Improvement Costs, $c_1(\cdot)$, + User Costs $c_2(\cdot)$ (\$M)	Weighted Traffic Delay Costs, $\rho c_{vot} g(a_t)$ (\$M)	Total Costs (\$M)
Excluding traffic (single-level)	Optimal threshold (complete enumeration)	9.58	32.02	41.60
Excluding traffic (single-level)	~Optimal prioritization via SARSA	10.06	33.62	43.68
Excluding traffic (single-level)	~Optimal prioritization via DCMAC	9.51	30.56	40.07
Including traffic (bilevel)	Optimal threshold (complete enumeration)	12.23	24.92	37.15
Including traffic (bilevel)	~Optimal prioritization via SARSA	12.86	26.42	39.28
Including traffic (bilevel)	~Optimal prioritization via DCMAC	13.45	22.57	36.02

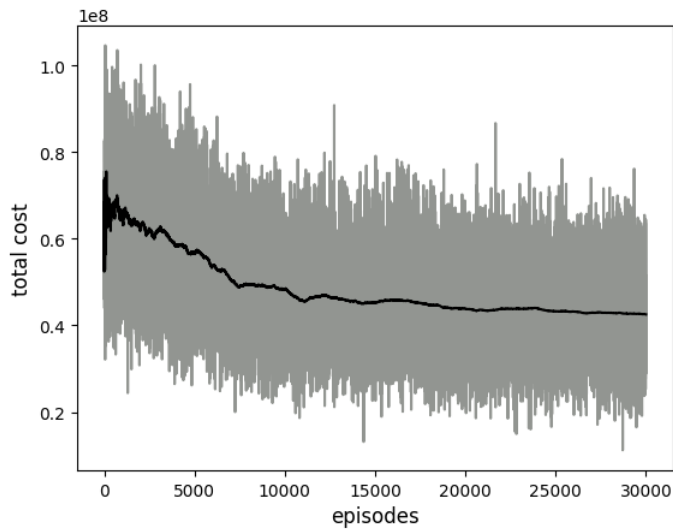


Figure 4-9. Expected total cost during SARSA learning for bilevel model (with traffic).

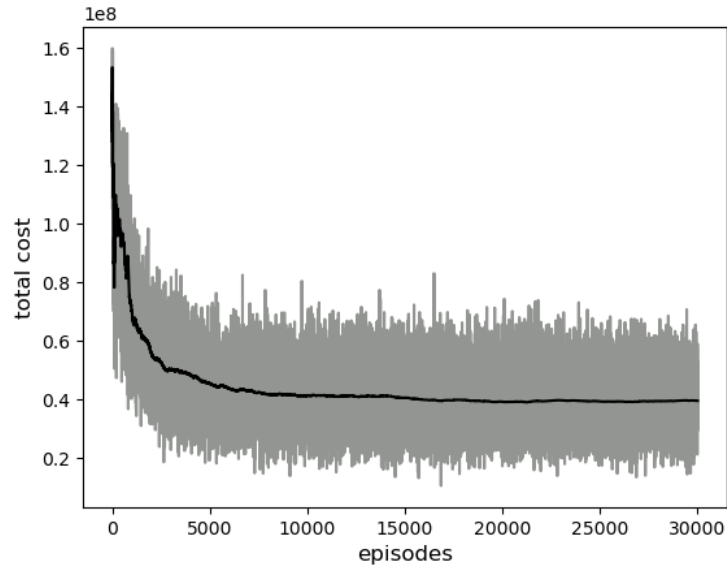


Figure 4-10. Expected total cost evolution during learning by the DCMAC method applied on the bilevel model (with traffic).

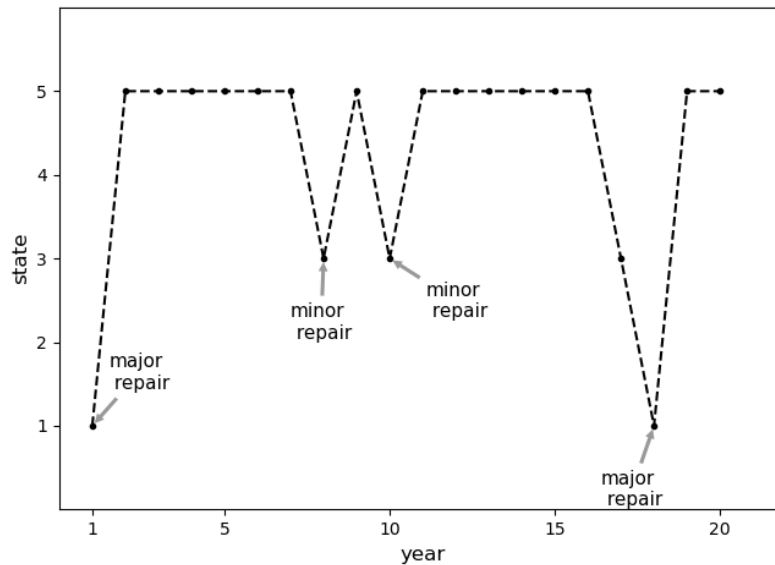


Figure 4-11. Pavement states and decisions for pavement segment 3.

The choice to execute minor or major repairs for pavements and bridges is influenced by improvement action costs, user costs, and traffic delays. Most pavement segments are maintained to a level of at least state 4. Due to their costs, major repairs are seldom implemented on pavement segments before they are in poor condition (state 1). Bridges are maintained to their highest level (state 6) through minor repairs to avoid high user costs that exceed the costs of minor repairs. Improvement actions may be postponed to the following year to avoid the potential traffic delay impacts of taking an action in the current year.

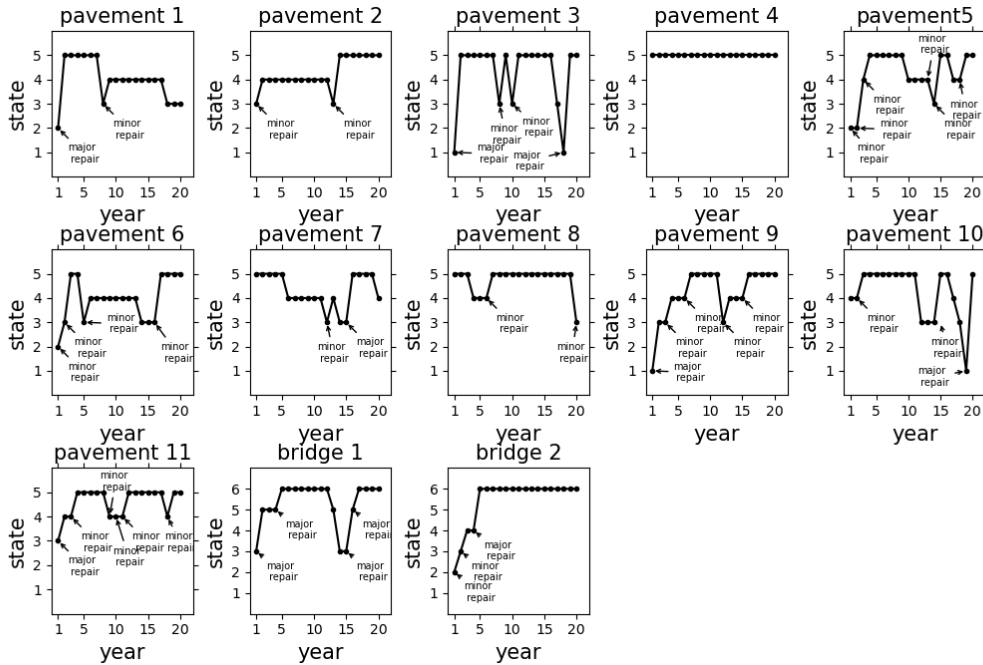


Figure 4-12. States and decisions for all pavements and bridges.

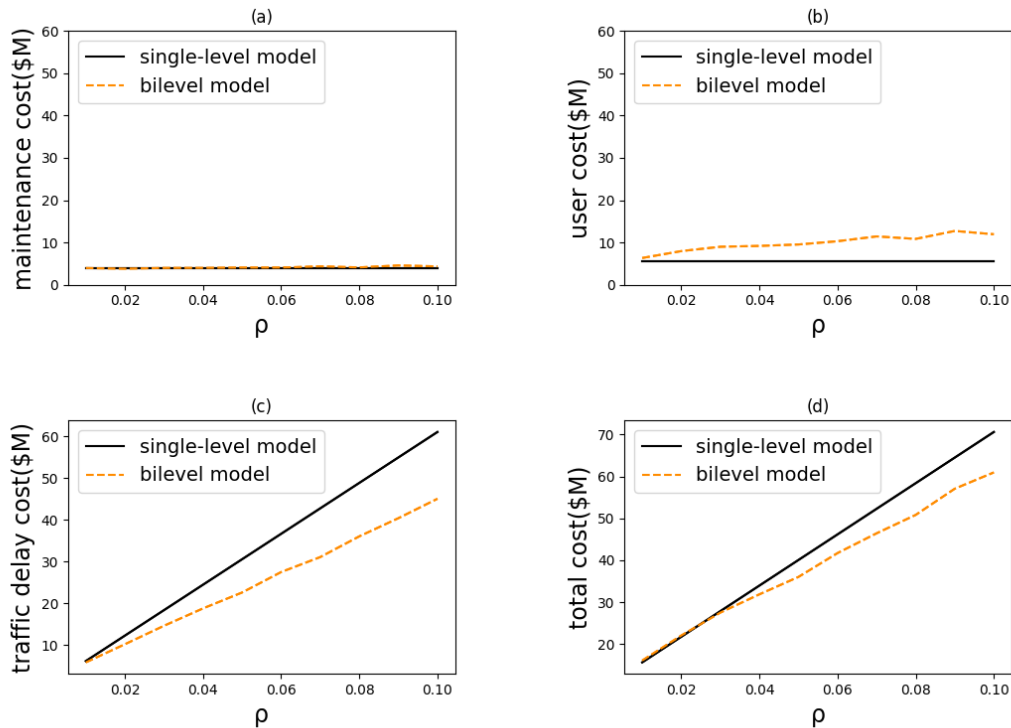


Figure 4-13. Costs under different values of ρ .

To test the traffic flow impacts on prioritization, parameter ρ is assigned a value between 0.01 and 0.10. The higher the value of ρ , the greater the weight given to traffic delay in the total cost function of Eqn. (4.1). Results are plotted in Figure 4-7 and show that accounting for traffic

delay in determining activity priorities and schedules (i.e., solution of the bilevel program) leads to lower total cost solutions. When the traffic delays are included in the total cost for the single-level model (that does not account for traffic delays in solution determination), the resulting schedules are substantially more costly. Moreover, as ρ increases, improvement actions are more likely to be deferred. This leads to increased user costs.

By accounting for traffic delays in developing an improvement plan, the range in savings spans between 18.99% and 38.36% in traffic delay and 1.39% to 17.90% in total cost for ρ set to 0.01 and 0.1, respectively. Even giving some influence to traffic effects in prioritization and scheduling results in scheduling substantially fewer improvement activities, as the cost to users in terms of delay of even a few actions is substantial. That is, it was found that accounting for traffic delay in prioritization and scheduling led to less traffic delay and decreased total cost over the planning horizon.

It was also noted that when ρ is set to 0.13 or higher, even fewer activities are scheduled. It is surmised that added delays are avoided by limiting improvement activities; that is, their benefits do not outweigh their costs in terms of traffic delays. This avoidance would be eliminated by incorporating delays due to poor roadway condition due to inaction. The literature, however, frequently indicates that within the range of highway pavement roughness and vehicle types in more developed countries, the application of pavement treatments has minimal effect on vehicle speeds (Wang, Harvey, Lea, & Kim, 2014). Therefore, the effect of pavement condition on travel time was not evaluated as a primary impact on vehicle operating costs in a related NCHRP study (Chatti & Zaabar, 2012).

Importance of stochasticity

To assess the value of the stochastic solution, the expected cost of the optimal stochastic solution, obtained over 5,000 realizations of pavement and bridge conditions drawn from the transition matrices, is compared with the cost of the optimal deterministic solution obtained by presuming deterioration measures for pavements and bridge decks that transition deterministically according to expected state conditions obtained from the transition matrices. For example, while a pavement is in state 3 and given that minor repair is implemented, a stochastic transition could imply that this improvement action changes the pavement's state to state 5 with probability of 0.45, state 4 with probability of 0.4, 3 with probability of 0.12 and 2 with probability of 0.03. Under the deterministic transition assumption, the pavement's state will then become 4 ($5 * 0.45 + 4 * 0.4 + 3 * 0.12 + 2 * 0.03 = [4.27] = 4$). Thus, the deterministic policy is generated assuming deterministic transitions, but its outcomes are evaluated under the stochastic deterioration transition matrices. The cost of the resulting actions, i.e. policy, was re-evaluated under the stochastic deterioration transition matrices. This cost was then compared to that of the optimal solution obtained given the original stochastic deterioration transition matrices. These costs are compared in Figure 4-8.

Figure 4-8 shows that failure to recognize uncertainty in deterioration rates leads to increasing expected roadway improvement and traffic delay costs. Roadway improvement costs, summation of improvement and user costs, cost of traffic delays and, thus, the total cost of the deterministic model are each higher than the same costs of the solution obtained from running the stochastic model. The roadway improvement cost of the solution obtained from the stochastic model is 32% lower than that of the deterministic model. The stochastic model also produced schedules with 27% lower cost in terms of traffic delays than the deterministic model. This

implies that taking stochasticity into consideration can generate significantly improved policies and the complexity of modeling uncertainty is worth the effort.

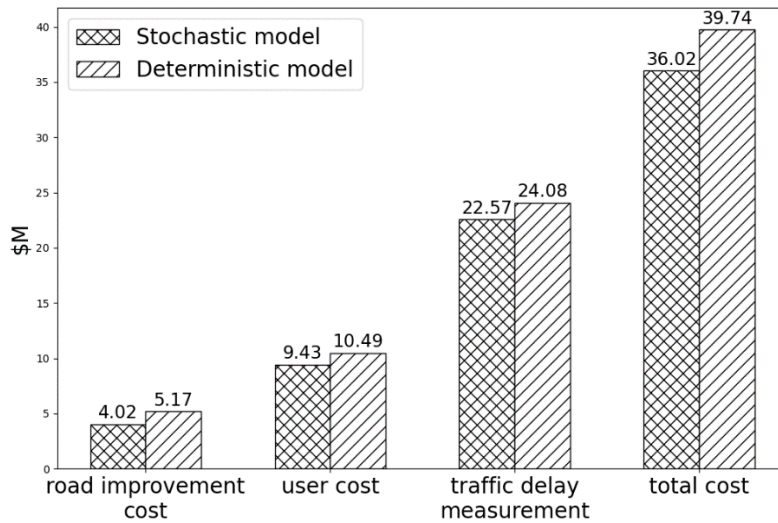


Figure 4-14. Influence of including stochasticity in deterioration on realized cost of the optimal improvement action schedule (with $\rho = 0.05$).

Taking a multi-asset class approach

Experiments were run to compare the difference between single and multi-asset roadway improvement strategies.

To reflect how well the assets are maintained during the planning horizon, a metric of asset state is used as introduced in Eqn. (4.25).

$$\mathbb{E}(s^i) = \mathbb{E} \left(\frac{1}{N_i} \sum_{k=1}^{N_i} \sum_{t=1}^T \frac{s_t^i}{\max(S^i)} \right) \quad (4.28)$$

Equation (4.25) computes the expected value of the mean condition over the perfect condition of all the assets belonging to the same class (pavements or bridges). A higher value of $\mathbb{E}(s^i)$ implies better condition.

Two approaches were implemented for assessing the value of taking a multi-asset class approach. The problem was first solved to produce a policy on only the pavements of the test network while presuming that both bridges are in ideal condition. Given the state of the pavements and the impact of planned improvements to the pavements assuming the determined policy is implemented, the problem is re-solved from the bridge perspective. In a second approach, the optimal policies for the pavements and bridges were generated separately presuming the other asset to be in ideal condition. The total costs of the outcomes from these two approaches were compared to the total cost obtained from solution of the multi-asset class formulation as proposed herein.

Results of these comparisons are given in Table 4-7. The costs for the single-asset approach when trained separately or sequentially were \$37.28M and \$37.85M, respectively. Both costs are greater than the total cost at \$36.02M of the solution obtained from the multi-asset class approach. That is, taking a multi-asset approach created a substantial savings at 5%. Greater

savings can be expected for roadway networks with increased heterogeneity in the network attributes.

Table 4-34. Multi-asset class versus single-asset class management (with $\rho = 0.05$).

	Single-asset Mgmt (trained separately by asset class) Pavements	Single-asset Mgmt (trained separately by asset class) Bridges	Single-asset Mgmt (trained sequentially) Pavements	Single-asset Mgmt (trained sequentially) Bridges	Multi-asset Mgmt Pavements	Multi-asset Mgmt Bridges
Improvement cost (\$M)	3.53	0.31	3.59	0.44	3.55	0.47
Expected condition, $E(s^i)$ (Eqn. (4.19))	0.84	0.92	0.84	0.89	0.85	0.88
User costs (\$M)	9.37	0.34	9.46	0.42	8.92	0.51
Cost of traffic delay(\$M)	23.73 ^a	23.73 ^a	23.94 ^a	23.94 ^a	22.57 ^a	22.57 ^a
Total cost (\$M)	37.28 ^a	37.28 ^a	37.85 ^a	37.85 ^a	36.02 ^a	36.02 ^a

^a Denotes pavements + bridges.

The results indicate that the total cost of the multi-asset class strategy (\$36.02 million) is significantly reduced from the sum of the two single-asset management strategies. While both single asset approaches spent similarly on improvements, the multi-asset class approach invested more in pavements. With only two small bridges, the pavements constitute the vast majority of the network by length. Thus, they contribute more to total user costs. Improvements to pavements, thus, can significantly reduce user costs, and therefore, total costs.

CONCLUSIONS

Maintaining roadway pavements and bridge decks is key to providing high levels of service for road users. Yet activities associated with maintenance, rehabilitation, and improvement of the roadway surfaces entail downtime with negative impacts for roadway network users. The focus, traditionally, of prioritizing and scheduling roadway improvement activities is on the outcome, and thus, often does not account for this downtime; however, such activities are frequent and users regularly live with some level of ongoing roadway improvement activity and its effects. Many agencies have included these downtime effects in project-level lifecycle analysis (Walls & Smith, 1998), but the recognition of these negative impacts during such activities should also be included in network-level asset maintenance and improvement planning.

This work presents the Multi-asset Class Roadway Improvement Scheduling Problem that considers capacity loss during improvement actions (i.e., downtimes), traffic impacts of improved serviceability after the actions are complete, and uncertain deterioration mechanisms jointly across multiple asset classes. Solution is obtained through cutting-edge, deep reinforcement learning methods. This formulation and solution framework can support the agencies responsible for roadway improvement and the users these roadways serve. They can provide the core needed for a decision support tool that can aid them in making cost-effective investment decisions over integrated roadway asset classes (specifically pavements and bridge decks), explicitly recognizing traffic impacts to the public and scheduling with them in mind.

The authors are extending this work to address additional complexities, including the impact of traffic congestion on deterioration and incorporation of updated deterioration data through continuous roadway condition monitoring to support condition-based prioritization and scheduling. For the latter, the role of new data sources to provide frequently updated bridge and pavement conditions is under investigation to ensure that decisions reflect current conditions. The proposed DRL methodology can support this dynamic application. DRL approaches can directly use continuous state-spaces in MDP problems. Thus, they can be used to model deterioration in a continuous framework as well, providing the relevant continuous state vector at the input layer.

The approach here balances user experience (i.e., user costs and travel delays) against spending on improvements. It implicitly presumes an agency will spend funds to maintain a certain level of service. This work can be also extended to include constraints on annual and/or multi-year maintenance budgets, as the suggested framework can support such formulations as well.

CHAPTER 5

Value of Information in Infrastructure Asset Management Policies

INTRODUCTION & OVERVIEW

Efficient management of structures and infrastructure is an ever-timely issue of paramount importance, aiming at proper inspection and maintenance policies, handling various stochastic deteriorating effects, and suggesting optimal actions that serve multi-purpose lifecycle objectives. In overall lifecycle management, inspection plays a key role, especially for critical infrastructure and rapidly deteriorating systems. The development of new and innovative sensing technologies, data acquisition techniques, and information processing methodologies further encourage the use of Structural Health Monitoring (SHM) in essential facilities (Farrar & Worden, 2012; Frangopol, Strauss, & Kim, 2008). However, these new possibilities come with relevant questions related to the actual value and necessity of increased quality measurements or continuous structural health information in facilitating optimal actions. SHM is defined as the development of online and automated condition assessment and damage detection capabilities for all types of infrastructure (Worden, Dervilis, & Farrar, 2019). Further, SHM frameworks seek to determine appropriate mappings from raw response measurements to condition and performance indicators, which can subsequently support decision-making toward cost-effective intervention and maintenance actions that increase safety and mitigate risks (Chatzi, Papakonstantinou, Hajdin, & Straub, 2017). Quantification of gains using SHM is a multi-stage process ranging from instrumentation to data processing and inference using state-of-the-art techniques like relevant machine learning algorithms. Nonetheless, the primary focus in this chapter is the final decision stage, which uses extracted and post-processed values of condition indicators resulted from the manifested system dynamics. More specifically, the decision stage pertains to the type and sequence of actions that are selected in order to optimize a predefined lifecycle objective. When the objective is to maximize long-term safety and resilience and to effectuate preventive maintenance actions, SHM typically constitutes a natural choice, as it can be used to diagnose faults and even determine the root cause of performance and condition deterioration processes, e.g., (Abdallah, et al., 2018). However, to what measurable extent is the acquired information able to support improved policy-planning in an engineering environment, and how can we objectively quantify the resulting gains?

An important discussion in this direction, originating beyond infrastructure decision-making (Raiffa, 1968; Lindley, 1971; Howard, 1966), is whether the benefits of the various observational strategies (e.g., SHM-aided plans or in situ visual and specialized non-destructive evaluation inspections) can be quantified in terms of lifecycle value-based metrics. The question that summarizes this discussion is how much is information worth or, similarly, how much is an SHM system worth investing in? (Pozzi & Der Kiureghian, 2011; Thöns & Faber, 2011; Straub, et al., 2017). In response, recent research efforts have systematically focused on

describing an overarching risk- and reliability-based framework for quantifying the Value of Information (VoI) and, similarly, the Value of Structural Health Monitoring (VoSHM), which can universally accommodate different lifecycle phases and types of stressors and hazards (Thöns, 2019; Diamantidis, Sykora, & Sousa, 2019).

This chapter casts the pertinent formulations within the context of stochastic optimal control, particularly Markov decision processes and partially observable Markov decision processes. Regardless of the employed decision rule, the concept of VoI can be utilized to (i) evaluate the amount the decision-maker is willing to pay for information prior to a single decision step of the decision process, either considering the long- or short-term benefits, e.g., (Straub & Faber, 2005) or (Fauriat & Zio, 2018), respectively; or (ii) to quantify the overall gain that information may yield as per a fixed inspection/monitoring policy, applied over the entire service life of a system, e.g. (Straub, 2014). The latter measure of VoI may be used to assess whether it is worth adopting a certain observational strategy over others from the beginning or the remainder of the system's life. Similarly, within the context of SHM, VoI may be quantified as the difference between the expected cost of maintaining the system in absence of SHM information, and the cost given availability of monitoring information (Thöns & Faber, 2011; Thöns, Schneider, & Faber, 2015; Pozzi & Der Kiureghian, 2011; Zonta, Glisic, & Adriaenssens, 2014). Along the same lines, POMDP-based VoI analysis and quantification approaches have been developed in (Papakonstantinou, Andriotis, & Shinozuka, 2016; Memarzadeh & Pozzi, 2016; Li & Pozzi, 2019). VoSHM is herein examined as a more specialized definition of VoI, describing relative costs between intermittent/optional observational schemes (e.g., periodic, or non-periodic inspection visits) and SHM-aided plans, where the flow of observations/data is typically continuous (Papakonstantinou, Andriotis, Gao, & Chatzi, 2019).

In this chapter, within the context of MDPs/POMDPs, an analysis of these value-based information metrics is presented and the underlying steps for their computation are demonstrated in a numerical experiment of a three-component deteriorating engineering system operating in a stochastic environment under different information scenarios, including no information, optional inspection visits, and continuous availability of observations, also resembling SHM systems. Quantification is based on point-based POMDP value iteration solutions of the respective service life inspection and maintenance optimization problems. Overall, the presented methodology can answer the practical question of how much inspection or monitoring data information is eventually worth in each case.

MARKOV DECISION PROCESS

MDPs provide solutions for optimal sequential decision-making in stochastic environments with uncertain action outcomes and exact observations. The environment, E , is defined by a finite set of states, S , a stochastic interstate transition model, a reward function, r , and a finite set of actions, A . At each decision step t , the decision-maker (called agent) observes the current state $s_t \in S$, takes an action $a_t \in A$, receives a reward as a result of this state and action, $r(s_t, a_t)$, and goes to the next state $s_{t+1} \in S$, according to the underlying Markovian transition probabilities, $p(s_{t+1}|s_t, a_t)$. It is, therefore, assumed that the current state and selected action are sufficient statistics for the next state, regardless of the entire prior history of state and action sequences. It is also important to note here that the Markovian property is not restrictive in any sense, since environments that do not directly possess it can be easily transformed to Markovian ones through state augmentation techniques, e.g., (Papakonstantinou & Shinozuka, 2014).

The state-dependent sequence of actions defines the agent's policy, π . Agent's policy can be either deterministic, $\pi(s_t): S \rightarrow A$, mapping states to actions, or stochastic, $\pi(a_t|s_t): S \rightarrow P(A)$, mapping states to action probabilities. For a deterministic policy, π is a single value, given s_t . In the case of discrete actions, a stochastic policy π , given s_t , is a vector defining a probability mass function over all possible actions, whereas for continuous actions, the policy is a probability density function. To keep notation succinct and general, all policies are shown in non-vector notation in the remainder of this work. Policy, π , is associated with a corresponding total return, R_t^π , which is the total reward collected under this policy, from any time step t to the end of the planning horizon T :

$$R_t^\pi = r(s_t, a_t) + \dots + \gamma^{T-t} r(s_T, a_T) = \sum_{i=t}^T \gamma^{i-t} r(s_i, a_i) \quad (5.29)$$

where γ is the discount factor, a positive scalar less than 1, indicating the increased importance of current against future decisions. The total return in Eqn. (5.1) is a random variable, as state transitions and, potentially, policies are stochastic. Conditioning the total return on the current state-action pair, s_t, a_t , the action-value function, Q^π , is defined as the expected return over all possible future states and actions:

$$Q^\pi(s_t, a_t) = \mathbb{E}_{s_{i>t} \sim E, a_{i>t} \sim \pi} [R_t^\pi | s_t, a_t] \quad (5.30)$$

Using Eqns. (5.1) and (5.2), the action-value function can be defined through the following convenient recursive form for any given policy, π :

$$Q^\pi(s_t, a_t) = r(s_t, a_t) + \gamma \mathbb{E}_{s_{t+1} \sim E, a_{t+1} \sim \pi} [Q^\pi(s_{t+1}, a_{t+1})] \quad (5.31)$$

The value function, or total expected return from state s_t , for policy π , is defined as the expectation of the action-value function over all possible actions at the current step:

$$V^\pi(s_t) = \mathbb{E}_{a_t \sim \pi} [Q^\pi(s_t, a_t)] \quad (5.32)$$

Under standard conditions for discounted MDPs, out of all possible policies there exists at least one deterministic policy that is optimal, maximizing $V^\pi(s_t)$ (Puterman, 1994). For a deterministic policy, with a given model of transitions $p(s_{t+1}|s_t, a_t)$ and the aid of Eqns. (5.3) and (5.4), the optimal action-value and value functions, $Q(s_t, a_t)$ and $V(s_t)$, respectively, follow the Bellman equation:

$$\begin{aligned}
V(s_t) &= \max_{a_t \in A} \{Q(s_t, a_t)\} \\
&= \max_{a_t \in A} \left\{ r(s_t, a_t) + \gamma \mathbb{E}_{s_{t+1} \sim E} \left[\max_{a_{t+1} \in A} Q(s_{t+1}, a_{t+1}) \right] \right\} \\
&= \max_{a_t \in A} \left\{ r(s_t, a_t) + \gamma \mathbb{E}_{s_{t+1} \sim E} [V(s_{t+1})] \right\} \\
&= \max_{a_t \in A} \left\{ r(s_t, a_t) + \gamma \sum_{s_{t+1} \in S} p(s_{t+1} | s_t, a_t) V(s_{t+1}) \right\}
\end{aligned} \tag{5.33}$$

Eqn. (5.5) describes the standard MDP objective, which is typically solved using value iteration, policy iteration, or linear programming formulations. A concise MDP presentation can also be seen in (Papakonstantinou & Shinozuka, 2014).

PARTIALLY OBSERVABLE MARKOV DECISION PROCESS

POMDPs generalize Markov decision processes to partially observable environments, i.e., to cases where observations are unable to reveal the actual state of the system with certainty. Similar to MDPs, in the POMDP framework the decision-maker/agent starts at a state, s_t at every decision step, t , takes an action, a_t , receives a reward, r_t , transitions to the next state, s_{t+1} , and receives an observation, $o_{t+1} \in \Omega$, based on its state and action, according to the probability defined by an observation model, $p(o_{t+1} | s_{t+1}, a_t)$. This process is schematically depicted in Figure 5-1. More formally, a POMDP is a 7-tuple $\mathcal{L} = \langle S, A, \mathbf{P}, \Omega, \mathbf{O}, \mathbf{R}, \gamma \rangle$ where S , A and Ω are finite sets of states, actions, and possible observations, respectively, and \mathbf{P} , \mathbf{O} , and \mathbf{R} are the transition, observation, and reward models, respectively.

As a result of partial observability, at every decision step t , the agent cannot be fully aware of its state, s_t (shaded nodes in Figure 5-1), which may only be perceived through an observation o_t that is a noisy indicator of that state. Therefore, the agent can now only form a belief \mathbf{b}_t about its state, where \mathbf{b}_t is a probability distribution over the set S of all possible discrete states. The new belief \mathbf{b}_{t+1} , i.e., the posterior state distribution for a given action and observation, can be readily computed through a Bayesian update (Papakonstantinou & Shinozuka, 2014):

$$\begin{aligned}
b(s_{t+1}) &= p(s_{t+1} | o_{t+1}, a_t, \mathbf{b}_t) \\
&= \frac{p(o_{t+1} | s_{t+1}, a_t)}{p(o_{t+1} | \mathbf{b}_t, a_t)} \sum_{s_t \in S} p(s_{t+1} | s_t, a_t) b(s_t)
\end{aligned} \tag{5.34}$$

where probabilities $b(s_t)$, for all $s_t \in S$, form the belief vector \mathbf{b}_t of length $|S|$, and the denominator of Eqn. (5.6), $p(o_{t+1} | \mathbf{b}_t, a_t)$, is the standard normalizing constant. As such, beliefs can be seen as alternative states of this environment, and POMDPs can be accordingly regarded as belief-MDPs, as the schematic in Figure 5-2 shows. Further, the total expected return takes an expression similar to Eqn. (5.5):

$$V(\mathbf{b}_t) = \max_{a_t \in A} \left\{ \sum_{s_t \in S} b(s_t) r(s_t, a_t) + \gamma \sum_{o_{t+1} \in \Omega} p(o_{t+1} | \mathbf{b}_t, a_t) V(\mathbf{b}_{t+1}) \right\} \tag{5.35}$$

Despite this convenient conceptual consistency with MDPs, POMDPs are not as easy to solve. Note that the new belief-state space is not discrete but continuous now, forming a $(|S| - 1)$ -dimensional simplex. However, it has been proven that the optimal value function is piece-wise linear and convex and can thus be described by a finite number of affine hyperplanes, (Sondik, 1971). This important result reduces the decision problem to determining a finite set of vectors, also known as α -vectors:

$$V(\mathbf{b}_t) = \max_{\alpha \in \Gamma} \left\{ \sum_{s_t \in S} b(s_t) \alpha(s_t) \right\} \quad (5.36)$$

A suitable set Γ and its corresponding α vectors, properly supporting the belief space, is what point-based algorithms seek to determine in order to solve the problem. Further details and insights about point-based methods can be found in (Shani, Pineau, & Kaplow, 2013). Eqn. (5.8) is eventually solved using value iteration. However, performing exact value iteration on the α -vector space is generally impractical, except for very small POMDP problems, since the new set of α -vectors generated at every iteration step scales exponentially with the cardinality of the observation set, $|\Omega|$ (Pineau, Gordon, & Thrun, 2003).

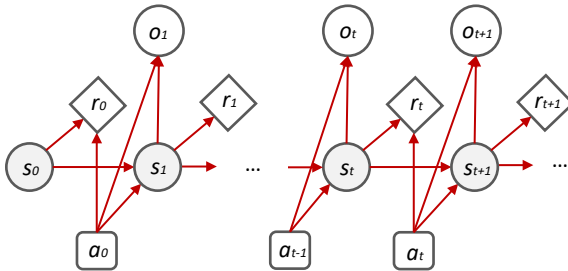


Figure 5-15. Probabilistic graphical model of a POMDP in time (shaded nodes denote hidden states).

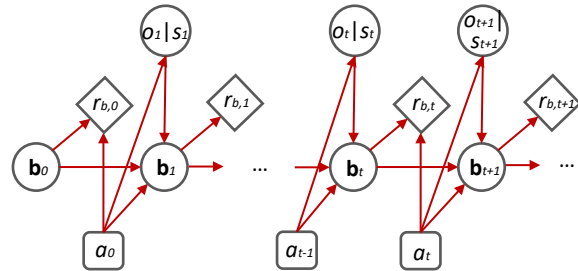


Figure 5-16. Probabilistic graphical model of a POMDP as a belief-MDP in time (observations depend on states which are hidden).

VALUE-BASED INFORMATION GAINS

Stepwise Value of Information in POMDPs

As described above, a POMDP can be defined through a tuple $\mathcal{L} = \langle S, A, \mathbf{P}, \Omega, \mathbf{O}, \mathbf{R}, \gamma \rangle$. Based on the decomposable nature of the reward and the effects of different observational and intervention actions, the tuple can be rewritten as $\mathcal{L} = \langle S, A_M \times A_O, [\mathbf{P}_{a_M}]_{a_M \in A_M}, \Omega_e \times \Omega_O, [\mathbf{O}_{a_O}]_{a_O \in A_O}, \mathbf{R}_M + \mathbf{R}_O + \mathbf{R}_D, \gamma \rangle$, where A_M is a set of maintenance actions a_M ; A_O is a set of observation actions a_O ; \mathbf{P}_{a_M} is the transition model for different maintenance actions a_M ; Ω_e is a set of default observations (which the decision-maker always receives from the environment, regardless of the selected action); Ω_O is a set of observations, and is a union of observation sets Ω_{a_O} of the different observation actions a_O ; \mathbf{O}_{a_O} is the observation model for different observation actions a_O ; \mathbf{R}_M , \mathbf{R}_O , and \mathbf{R}_D are the reward matrices for maintenance, observations, and damage state costs, respectively. Although, for notational efficiency, we assume the reward matrices to

have the same dimensions $|S| \times |A|$, the maintenance costs are independent of a_o , and the observation action costs are independent of a_M , whereas the damage costs are independent of both.

If the decision-maker chooses a trivial observation action (which is uninformative and has a zero-cost associated), it will receive the default observation from Ω_e plus an uninformative observation from Ω_o . Thus, the decision-maker will overall receive the default observation, i.e., $\Omega \equiv \Omega_e$. Default observations are not necessarily uninformative; hence the respective POMDPs do not necessarily imply that the trivial actions yield no information. In deteriorating systems, failure, or near-failure states, for example, are often self-announcing, meaning that they are “observable” regardless of the selected observation action.

Similarly, the trivial maintenance action is an action with no cost, i.e., $r_M = 0$, and yields a natural (uncontrolled) environment transition. As denoted by the respective subscripts, state transitions \mathbf{P}_{a_M} merely depend on maintenance actions, meaning that only maintenance actions a_M can change the state of the system, whereas observation actions a_o can only change the agent’s perception about the state of the system, thus perfectly sufficing to define the observation model \mathbf{O}_{a_o} . Based on the above, we can define the stepwise VoI associated with a certain policy π as:

$$\text{VoI}_{step}^{\pi}(a_o) = \mathbb{E}_{o_e, o_o} [V^{\pi}(\mathbf{b}^{a_M, a_o, o_e, o_o})] - \mathbb{E}_{o_e} [V^{\pi}(\mathbf{b}^{a_M, o_e})] \quad (5.37)$$

Eqn. (5.9) describes the gain the decision-maker expects when taking an observation action at a certain time step t , following a policy π in the future. Subtracting the actual cost of the observation action $r_{b,o} \in \mathbb{R}_o$ from this gain, we obtain the net step VoI under a policy π as:

$$\text{netVoI}_{step}^{\pi}(a_o) = \text{VoI}_{step}^{\pi} - |r_{b,o}| \quad (5.38)$$

Net step VoI expresses the net gain at step t as a result of additional information, also considering the cost to acquire this information (e.g., inspection cost). If nontrivial observation actions reveal the actual state of the system with certainty, i.e., $\mathbf{O}_{\text{nontrivial}} = \mathbf{I}$ (identity matrix), we can similarly define the stepwise Value of Perfect Information (stepwise VoPI), VoPI_{step}^{π} , and net stepwise VoPI, $\text{netVoPI}_{step}^{\pi}$, similarly to Eqns. (5.9) and (5.10). In such a case, in the term $\mathbb{E}_{o_e, o_o} [V^{\pi}(\mathbf{b}^{a_M, a_o, o_e, o_o})]$ of Eqn. (5.9), uncertainty is only attributed to the state transition, which is controlled by the chosen maintenance, $\text{VoPI}_{step}^{\pi}(a_o) = \mathbb{E}_{s' \sim \mathbf{b}^{a_M}} [V^{\pi}(s')] - \mathbb{E}_{o_e} [V^{\pi}(\mathbf{b}^{a_M, o_e})]$. It has been derived in (Andriotis, Papakonstantinou, & Chatzi, 2021) that for policy π : $\text{VoPI}_{step}^{\pi} \geq \text{VoI}_{step}^{\pi} \geq 0$ and equality $\text{VoPI}_{step}^{\pi} = 0$ hold if Ω_{a_o} is a unit set, i.e., nontrivial observation actions also yield uninformative observations. Equality $\text{VoPI}_{step}^{\pi} = \text{VoI}_{step}^{\pi}$ holds if $\mathbf{O}_{\text{nontrivial}} = \mathbf{I}$; that is, nontrivial observation actions reveal the actual system state with certainty. This also holds for optimal policy $\pi = \pi^*$, thus $\text{VoPI}_{step}^{\pi^*} \geq \text{VoI}_{step}^{\pi^*} \geq 0$.

Lifecycle Gain from Changing Control Settings

The expected lifecycle gain of one control setting versus another can be expressed as the value difference between the two settings, when different action sets are available for each setting, but

these apply to the same system, i.e., the two settings have the same state space and the same deterioration dynamics (transition model for the uncontrolled case) as well as the same discounted horizon. Further, to assess the expected lifecycle gain of one observational scheme versus another (e.g., SHM, inspection visits, etc.), the tuple elements related to maintenance actions have to be the same, thus we considered the following two tuples as the POMDP settings:

$$\mathcal{L}_1 = \left\langle S, A_M \times A_O^1, [\mathbf{P}_{a_M}]_{a_M \in A_M}, \Omega_e \times \Omega_O^1, [\mathbf{O}_{a_O}^1]_{a_O \in A_O^1}, \mathbf{R}_M + \mathbf{R}_O^1 + \mathbf{R}_D, \gamma \right\rangle \quad (5.39)$$

$$\mathcal{L}_2 = \left\langle S, A_M \times A_O^2, [\mathbf{P}_{a_M}]_{a_M \in A_M}, \Omega_e \times \Omega_O^2, [\mathbf{O}_{a_O}^2]_{a_O \in A_O^2}, \mathbf{R}_M + \mathbf{R}_O^2 + \mathbf{R}_D, \gamma \right\rangle$$

Then, the expected life-cycle gain, $G_{\mathcal{L}_1, \mathcal{L}_2}$, from following the optimal policy in \mathcal{L}_2 versus \mathcal{L}_1 , starting at any belief $\mathbf{b} \in B$, is computed as:

$$G_{\mathcal{L}_1, \mathcal{L}_2}(\mathbf{b}) = V_2^*(\mathbf{b}) - V_1^*(\mathbf{b}) \quad (5.40)$$

where V_1^*, V_2^* are the optimal value functions of each tuple, $\mathcal{L}_1, \mathcal{L}_2$, respectively. Equivalently, Eqn. (5.12) describes the potential benefits as a result of different sources and/or accuracy of information from scheme \mathcal{L}_1 to \mathcal{L}_2 at belief \mathbf{b} . Thus, Eqns. (5.11) and (5.12) will be used to derive and elaborate the gains related to different observational schemes and their relation to VoI and VoSHM.

Value of Information

Considering Eqn. (5.11) suppose A_O^1 is a unit set, containing only a trivial observation action. Then, $\mathbf{R}_O^1 = \mathbf{0}$. This technically means that Ω_O^1 is defined by a unit set as well. As such, overall, from all states, only one observation is possible, which is the default observation, i.e., $\Omega^1 \equiv \Omega_e$. In this case, tuple \mathcal{L}_1 defines the default control problem (also often called prior in the literature) of \mathcal{L}_2 , i.e., $\mathcal{L}_1 \doteq \mathcal{L}_{def}$ and $\mathcal{L}_2 \doteq \mathcal{L}$, thus Eqn. (5.12) gives the VoI of the observational scheme adopted in \mathcal{L}_2 (Straub, 2014):

$$G_{\mathcal{L}_{def}, \mathcal{L}}(\mathbf{b}) = VoI_{\mathcal{L}}(\mathbf{b}) = V^*(\mathbf{b}) - V_{def}^*(\mathbf{b}) \quad (5.41)$$

In addition to the previous assumption, let us now assume that A_O^2 is a unit set with only a nontrivial action available at no cost, and $|\Omega_O^2| = |S|$ with $\mathbf{O}_{nontrivial}^2 = \mathbf{I}$ (identity matrix). In this case, the agent operates under perfect information at every decision step of \mathcal{L} . This reduces the POMDP defined by \mathcal{L} to an MDP problem, i.e., $\mathcal{L} \doteq \mathcal{L}_{MDP}$. Under these assumptions, using Eqn. (5.12) we obtain the Value of Perfect Information (VoPI):

$$G_{\mathcal{L}_{def}, \mathcal{L}_{MDP}}(\mathbf{b}) = VoPI_{\mathcal{L}}(\mathbf{b}) = V_{MDP}^*(\mathbf{b}) - V_{def}^*(\mathbf{b}) \quad (5.42)$$

If the value functions in Eqns. (5.13) and (5.14) include the cost related to observational actions, then, according to (Straub, et al., 2017), they can also be associated with the net VoI, as explained in the previous section. As intuitively understood and formally proven in (Andriotis, Papakonstantinou, & Chatzi, 2021), VoPI is an upper bound of VoI, and both information gains

should be non-negative, in the sense that information should not be expected to hurt decisions. Notwithstanding its intuitive nature, it is also showcased in (Andriotis, Papakonstantinou, & Chatzi, 2021) that this remark is not necessarily true if the decision-maker is following an inspection and maintenance policy other than the optimal policy prescribed by the solution of Eqn. (5.8).

Value of Structural Health Monitoring

The VoSHM refers to the possible gains from investing in lifelong SHM devices and continuous data practices, instead of, or in addition to, planning inspection visits at distinct times during the structural service life. As such, the VoSHM relates to the critical decision, either at the design stage or later, of whether a monitoring scheme is worth being adopted, and if so, of which type. VoSHM quantifies essentially the benefits of continuous data collection and information inflow in the decision-support system.

In this work, to quantify the VoSHM, we examine another special case of Eqn. (5.11). We assume that A_0^1 contains at least one nontrivial available action. Conversely, A_0^2 contains only one available observation action, which is, however, not the trivial one and is costless, i.e., $R_0^2 = \mathbf{0}$. For the two POMDP settings, the nontrivial observation actions may follow different observation models. Thereby, $\mathcal{L}_1 \doteq \mathcal{L}_{1,opt}$ corresponds to the scenario of optional inspection visits, whereas $\mathcal{L}_2 \doteq \mathcal{L}_{2,perm}$ corresponds to an alternative observational scheme with permanent characteristics, as is provided by an SHM system. Along these lines, the VoSHM is defined as:

$$G_{\mathcal{L}_{1,opt}, \mathcal{L}_{2,perm}}(\mathbf{b}) = VoSHM_{\mathcal{L}_{1,opt}, \mathcal{L}_{2,perm}}(\mathbf{b}) = V_{2,perm}^*(\mathbf{b}) - V_{1,opt}^*(\mathbf{b}) \quad (5.43)$$

It should be noted that the expected VoSHM lifecycle gain defined in Eqn. (5.15) cannot be strictly seen as Vol, as it can also take negative values. This may happen, for example, if the state information provided by an optional inspection visit is more accurate than the outcome of the permanent monitoring system, for any possible reason. A VoSHM value lower than the cost of a SHM system (including acquirement, installation, maintenance, and operation costs, etc.) simply suggests that there is no benefit for the decision-maker to invest in SHM but, instead, optimal planning with selected inspection visits should be preferred.

Using Eqn. (5.15) we can compute the VoSHM at every possible belief point that the system can visit throughout the planning horizon. Typically, the belief of foremost interest is the root belief, \mathbf{b}_0 , which reflects the probability distribution over all possible states at the initial conditions, i.e., for the defined time step $t = 0$. In this case, the VoSHM quantifies the lifecycle value of the monitoring system. For $t > 0$, which usually corresponds to $\mathbf{b}_t \neq \mathbf{b}_0$, Eqn. (5.15) describes the remaining VoSHM from that time onward. The notion of remaining VoSHM can be of particular practical importance in cases where the optimal salvage time of the SHM system needs to be determined.

If the nontrivial observation actions in $\mathcal{L}_{1,opt}, \mathcal{L}_{2,perm}$ share the same observation probability model, i.e., with the respective settings denoted as $\mathcal{L}_{1,opt} \doteq \mathcal{L}$, $\mathcal{L}_{2,perm} \doteq \mathcal{L}_{perm}$, we obtain a non-negative value in Eqn. (5.15). This could practically refer to a case where both inspections and SHM are based on the same sensing units. Thus, the VoSHM can be seen in this case as the Relative Value of Continuous Information (RVoCI), since it quantifies the possible gain if the nontrivial observation is continuously and freely available:

$$\begin{aligned}
VoSHM_{\mathcal{L},\mathcal{L}_{perm}}(\mathbf{b}) &= RVoCI_{\mathcal{L}}(\mathbf{b}) \\
&= VoI_{\mathcal{L}_{perm}}(\mathbf{b}) - VoI_{\mathcal{L}}(\mathbf{b}) \\
&= V_{perm}^*(\mathbf{b}) - V^*(\mathbf{b})
\end{aligned} \tag{5.44}$$

The obtained $RVoCI_{\mathcal{L}}$ value from Eqn. (5.16) will be a non-negative gain in the above inspection settings, as shown in (Andriotis, Papakonstantinou, & Chatzi, 2021).

NUMERICAL APPLICATION WITH THREE-COMPONENT SYSTEM

Here, we have considered a three-component inspection and maintenance problem with stationary deterioration to assess VoI, VoSHM, and their specialized cases, as discussed in previous sections. For the reported results, the point-based algorithms of Focused Real-Time Dynamic Programming (FRTDP) (Smith & Simmons, 2005; Smith & Simmons, 2006; Kurniawati, Hsu, & Lee, 2008), and Perseus (Spaan & Vlassis, 2005) have been implemented to solve the POMDP problems and to determine the optimal service life strategies.

Environment and Description of Control Settings

For the purposes of a parametric numerical investigation in the presence of various observability accuracy levels, we consider a small three-component system. An infinite horizon case with $\gamma=0.95$ is analyzed. The discount factor, γ , reflects the current value of future costs, thus largely depending on economic features, such as interest rate and inflation. Stochastic deterioration of the components, for all $i \in \{1,2,3\}$, is defined by independent transition matrices, $P_{(i),0}$, whereas whenever a repair action is taken the components share the same transition matrix $P_{(i=1,2,3),rep}$:

$$\begin{aligned}
\mathbf{P}_{(1),0} &= \begin{bmatrix} 0.82 & 0.13 & 0.05 \\ & 0.87 & 0.13 \\ & & 1.00 \end{bmatrix}, \mathbf{P}_{(2),0} = \begin{bmatrix} 0.72 & 0.19 & 0.09 \\ & 0.78 & 0.22 \\ & & 1.00 \end{bmatrix}, \\
\mathbf{P}_{(3),0} &= \begin{bmatrix} 0.79 & 0.17 & 0.04 \\ & 0.85 & 0.15 \\ & & 1.00 \end{bmatrix}, \mathbf{P}_{(i=1,2,3),rep} = \begin{bmatrix} 0.90 & 0.10 & \\ 0.80 & 0.20 & \\ & 0.70 & 0.30 \end{bmatrix}
\end{aligned} \tag{5.45}$$

As indicated by Eqn. (5.17), each component is described by three condition levels with stationary transition dynamics, i.e., transition from condition level k to j is independent of time, component age or deterioration rate. For example, for component 3, the transition probability from state 1 to state 3 is 0.04. Overall, the examined system can be fully specified by 27 states. Markovian transition probabilities of structural systems can be constructed based on simulated or real data of longitudinal responses, system conditions, rankings, etc., e.g., in (Papakonstantinou & Shinozuka, 2014; Andriotis & Papakonstantinou, 2018; Manafpour, Guler, Radlinska, Rajabipour, & Warn, 2018), either through maximum likelihood estimation or expectation-maximization schemes in the presence of latent state variables. In order to quantify the VoSHM for this three-component system, two POMDP control settings are evaluated. For Setting 1, four observation and maintenance control actions are available for each component, including the possibility of inspection visits at belief points suggested by the POMDP solution. These actions are ‘no observation and no repair,’ ‘observation and no repair,’ ‘no observation and repair,’ and ‘observation and repair.’ The ‘no observation’ observation action is the trivial observation action,

and the default observation is considered uninformative. As such, the default control problem is here called blind, $\mathcal{L}_{def} \doteq \mathcal{L}_{blind}$. The total number of system actions is 64. For Setting 2, observations of nontrivial actions are available at no cost at every decision step, corresponding to a permanent monitoring observation scheme. Accordingly, only 2 maintenance control actions need to be considered, i.e., ‘no-repair’ and ‘repair.’ Based on the possible action combinations, 8 system actions are available for Setting 2. Observation matrices, for all components, are given as:

$$\mathbf{o}^{(i=1,2,3)} = \begin{bmatrix} p & \frac{(1-p)}{2} & \frac{(1-p)}{2} \\ \frac{(1-p)}{2} & p & \frac{(1-p)}{2} \\ \frac{(1-p)}{2} & \frac{(1-p)}{2} & p \end{bmatrix} \quad (5.46)$$

Eqn. (5.18) assigns an observation accuracy of $0 \leq p \leq 1$ every time an ‘observation’ is taken, meaning that the correct state is observed with probability p , whereas either one of the other states is observed uniformly at random with probability $1-p$. Negative rewards (or costs) for individual components are given in Table 5-1 for different states and actions. Observation actions are considered 1/12, 1/18, and 1/30 of the repair cost for condition levels 1, 2, and 3, respectively. Observation actions have constant costs with respect to states, whereas repair costs are considered to increase with damage severity. These values establish representative proportions between inspection and repair costs (Jiang, Corotis, & Ellis, 2000; Luque & Straub, 2019) and can vary as per the specific nature of the studied engineering system. System-level interdependence among components is established through the reward function, with certain penalties added to the cumulative component costs at different system state configurations. That is, for system states $\{(2,2,1)\}$, $\{(2,2,2),(1,2,3),(2,2,3)\}$, $\{(3,3,1),(3,3,2)\}$, and $\{(3,3,3)\}$, penalties are -5.0, -10.0, -14.0, and -18.0, respectively, where vector (i,j,k) denotes component condition level combinations, i.e., $(3,3,1)$ indicates that there are 2 components in condition level 3 and one component in condition level 1. These system-level state rewards are combined with the rewards of the individual components, shown in Table 5-1.

Obtained Optimal Policies

For both POMDP settings, FRTDP, SARSOP, and Perseus point-based algorithms are implemented. As shown in the analysis results presented in Figure 5-3 and Figure 5-4, for $p=0.90$, Setting 1 practically converges after 1,000 s, whereas Setting 2 converges after 110 s for all algorithms. It can be seen that the precision of the solution of Setting 1 is somewhat lower than the precision of Setting 2, for FRTDP and SARSOP. This can be attributed to the fact that the system in Setting 1 operates in a much more challenging POMDP environment with more actions and, consequently, larger reachable belief space. A realization of the converged policy is shown in Figure 5-5 and Figure 5-6. For Settings 1 and 2, each component needs to perform different policies in order for their combined behavior to collectively minimize the total expected cost of the system. In Figure 5-5, depicting a policy realization for the case of optional inspections, component 1 requires an inspection visit roughly every two years, whereas its ‘repair’ actions are mostly taken at the inspection times. Component 2 requires inspections at almost every decision step (all time steps except $t=10$ in the realization of Figure 5-5). Component 3 policy combines features of the other two policies, choosing frequent inspections,

with a few ‘no observation and no repair’ actions. These policy patterns are intuitively anticipated, as the transition dynamics of component 3 are between the other two cases defined by components 1, 2. Figure 5-6 illustrates a service life policy realization for the case of permanent monitoring (Setting 2). In this POMDP setting, observations are always available at no cost due to the permanent monitoring system and continuous data assumption, as explained in earlier sections.

Table 5-35. Individual component costs (negative rewards) of maintenance and observation actions for three-component deteriorating system.

Condition Levels		1	2	3
Maintenance rewards (r_M)	1: Do Nothing	0	0	0
Maintenance rewards (r_M)	2: Repair	-12	-18	-30
Observation rewards (r_O)	1: No observation	0	0	0
Observation rewards (r_O)	2: Observation	-1	-1	-1
Damage rewards (r_D)		0	-5	-12

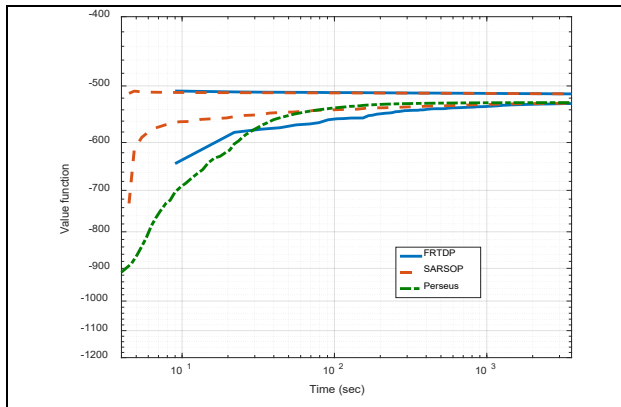


Figure 5-17. Performance of different point-based POMDP algorithms in the three-component system problem, with $p=0.90$, for Setting 1 (optional monitoring setting).

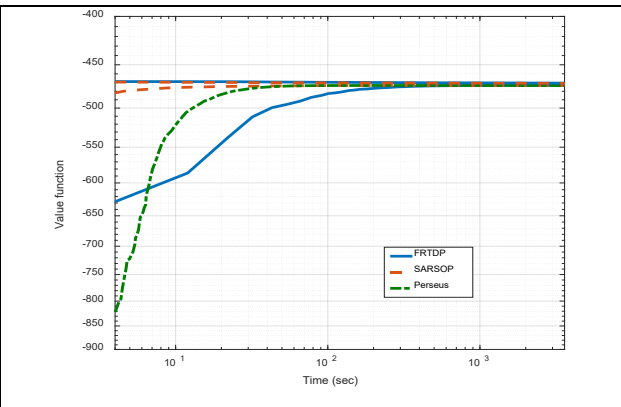


Figure 5-18. Performance of different point-based POMDP algorithms in the three-component system problem, with $p=0.90$, for Setting 2 (permanent monitoring setting).

The converged value functions and VoI for each setting as well as the VoSHM are shown as functions of the observability accuracy level, p , in Figure 5-7. VoSHM equals the RVoCI, as Settings 1 and 2 share the same observation matrices for their observation actions. It can be observed that as the observation accuracy increases, the VoSHM increases and is concave down, reaching a plateau at higher levels of accuracy. The VoSHM of the system ranges from ~3% to ~11% of the value of Setting 1, for $p=0.50$ to $p=1.00$, respectively. This means that any permanent monitoring system with continuous data and lifetime cost lower than these amounts should be preferred, in place of any inspection plan, including the optimal one. The VoI also increases with increased observability, for both settings; however, it is concave up. This pattern is more prominent for the value function of Setting 1, where a plateau is practically reached for $p < 0.60$. This indicates that the observation quality is quite poor at this region, so the decision-

maker does not choose to pay for inspection and, consequently, the value of Setting 1 becomes equal to the value of the optimal blind policy. The VoPI is ~25% of the optimal blind policy cost and, by definition, is reached by the VoI of Setting 2, for $p=1.00$.

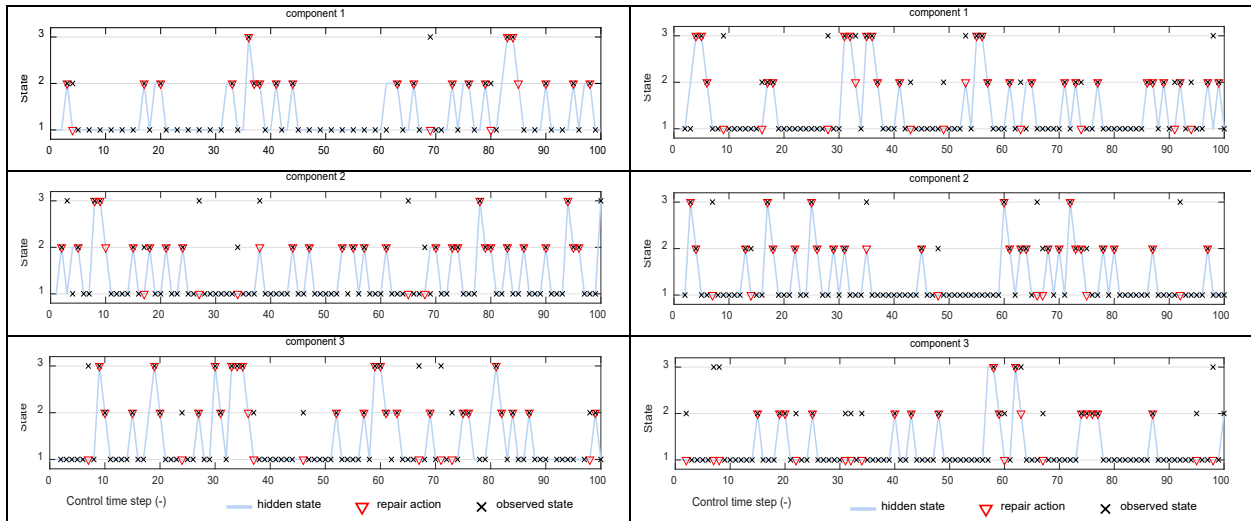


Figure 5-19. Policy realization of three-component system Setting 1 (optional inspection setting), with $p=0.90$, for all components.

Figure 5-20. Policy realization of three-component system Setting 2 (permanent monitoring setting), with $p=0.90$, for all components.

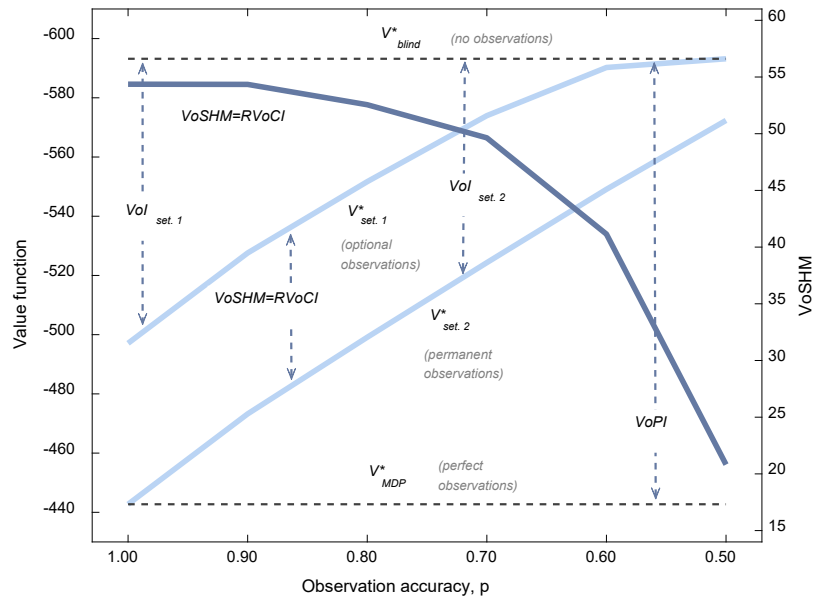


Figure 5-21. Optimal value functions of three-component system for Settings 1 and 2 and respective VoSHM and VoI, for different observability levels.

CONCLUSIONS

In this chapter, a methodology to compute the Value of Information (VoI) and the Value of Structural Health Monitoring (VoSHM) within the context of MDP/POMDPs is presented. Respective stepwise and long-term value-based information metrics are analyzed, and their relations to the POMDP optimality equations are provided. The key findings are summarized below:

- For the quantification of VoI, the first POMDP setting evaluated involves optimization of maintenance actions for the default decision problem (no observation actions available), whereas the second setting optimizes both maintenance and observation actions. This process complies with standard VoI definitions. For the quantification of VoSHM, the first setting corresponds to an observational scheme with optimal optional inspections, whereas the second setting operates under the assumption of continuously available data and observations.
- The two metrics are defined over the operational life of the system, quantifying the expected long-term cumulative gains upon availability of inspection- or monitoring-based structural health information. A stepwise definition of VoI is also introduced, which is a non-negative convex function, over the space of all possible posterior state probability distributions.
- Details for formulating the underlying MDP/POMDP problem settings and the quantification of possible gains related to structural health information (either obtained by inspections or SHM) are presented using point-based value iteration algorithmic approaches.
- Results are presented for a three-component deteriorating system, which verifies the theoretical discussion and results. The overall outcome of this analysis is a quantitative answer to the practical question of how much is structural health information and data from inspections and/or monitoring worth, as well as how information of increased precision can affect decisions.

Potential extensions of the present work include, among others, consideration of different types of inspection and continuous monitoring observation models directly calibrated based on real data, and integration of advanced learning techniques with the decision-making process for online extraction of efficient damage and condition indicators from high-dimensional and heterogeneous monitoring data.

CHAPTER 6

Pavement Distress Recognition via Wavelet-based Clustering of Smartphone Sensor Data

INTRODUCTION

Road condition maintenance is a persistent challenge due to the scale of transportation systems and the logistical complexities of roadway inspections (Wang K. C., 2000; Flintsch & McGhee, 2009; Wu, et al., 2020). Timely response to road pavement distress not only is crucial to keep vehicle passengers safe, but also extends ride quality and comfort. It is also highly desirable to distinguish pavement degradations at early stages before they transform to severe abnormalities, which may cause safety incidents and increase the cost of restorative maintenance.

Manual visual inspections were formerly the conventional way to monitor road quality; however, human factors, safety, personal biases, and the time-consuming nature of the process have led researchers to explore alternative approaches. The current state-of-the-practice on most U.S. highways is the highway-speed collection of images and laser scans with subsequent human-augmented analysis of both distresses and ride quality. A growing number of studies have pursued the use of on-vehicle sensing combined with machine learning (ML) to enhance the visual inspection process (Tsai & Chatterjee, 2017; Basavaraju, Du, Zhou, & Ji, 2019). In particular, a recent focus has been on using smart phone accelerometer data, given the ubiquity of the sensors and the direct connection between vehicle dynamics and roadway quality. These efforts have predominantly employed supervised ML and so rely on the availability of labeled sensor data. This severely limits the generalizability of the results.

This chapter explores an unsupervised learning approach that does not require exhaustively labeled data sets and generalizes across variations in vehicle dynamics and roadway characteristics. The main idea is to automatically identify and characterize deviations in vehicle response for a particular combination of smartphone and vehicle. While the detector itself cannot generalize over different vehicles, the detection of anomalies along a specific roadway segment can do so. In an envisioned deployment setting, unsupervised defect detection would be repeatedly reported for a specific road segment for many different types of vehicles, and the aggregate of these reports could be used to derive a deeper understanding into roadway quality.

As a first step toward realizing this concept, here we present an unsupervised learning framework for road quality assessment. The framework brings wavelet signal processing and clustering techniques together in an analytical process that eliminates the need for empirical hyperparameter tuning. It takes advantage of multi-objective Pareto optimization to organize the hyperparameter space and automatically select optimal configurations over features and clustering techniques. Evaluation over real-world data shows the capability of the framework in detecting road pavement distress, but also shows that low-cost crowdsourced data may not be

adequate to distinguish nuanced variations in pavement distress. The presented framework is generalizable, allowing it to be used in future studies on the aggregation of unsupervised learning analyses from multiple vehicles.

Prior Work

In general, pavement assessment can be categorized as manual visual, image processing, laser profiles/scans, or vibration-based (Chang, Chang, & Chen, 2006; Ho, Snyder, & Zhang, 2020; Lee & Yoon, 2018). Here we focus on vibration-based methods, in particular those that utilize ML for data analysis. Due to the need for data sets in ML, data acquisition has attracted the majority of attention in prior studies (Marcelino, de Lurdes Antunes, & Fortunato, 2018). This is often achieved with purpose-built sensor arrays onboard a vehicle, for instance to identify the impact of temperature change on pavement distress (Ho, Snyder, & Zhang, 2020). In particular, in (Ho, Snyder, & Zhang, 2020) four sensors on each wheel's control arm and one sensor inside the vehicle were mounted for this purpose.

As an alternative to custom-designed sensor arrays, other research efforts have explored using smartphone accelerometer data to crowdsource pavement condition assessment (Basavaraju, Du, Zhou, & Ji, 2019; Allouch, Koubâa, A., Abbes, & Ammar, 2017). These studies utilized a supervised ML approach to fit a statistical model to labeled sensor data. Applications of these methods have varied from simple binary classification to more complex multi-class surface condition classification. For example, work in (Basavaraju, Du, Zhou, & Ji, 2019) developed Support Vector Machine (SVM)-, Decision Tree (DT)-, and Neural Network (NN)-based models to classify smartphone-based data as smooth condition, potholes, and transverse cracks. Work in (Allouch, Koubâa, A., Abbes, & Ammar, 2017) created a real-time android application named RoadSense to predict the condition of pavement according to all three smartphone accelerometer axes (x, y, and z) and gyroscope by using the C4.5 DT classifier (Quinlan, 1992). Two additional classification tasks were investigated in (Souza, Souza, Cherman, Rossi, & Souza, 2017). The first was a binary classification task to recognize regular versus irregular road segments. The second was a multi-class classification task to distinguish between speed hump, vertical patch, raised pavement markers, and raised crosswalk irregularities. Four classifiers (SVM, Random Forest (RF), Naive Bayes (NB), and 1-Nearest Neighbor) were trained on various designed features for these tasks.

Unsupervised learning comprises less of the existing literature (Wang, Wang, Xiao, Qiu, & Zhang, 2018; Eriksson, Girod, Hull, & Newt, 2008). Many of the works that utilize unsupervised learning make specific assumptions on accessibility to road performance indicators as their input for roadway clustering and asset management. For instance, work in (Taleqani, Bridgelall, Hough, & Nygard, 2019) used the DBSCAN clustering algorithm to classify the quality of road segments, using the accelerometer and gyroscope sensors of a smartphone (Ester, Kriegel, Sander, & Xu, 1996). The roughness of clusters was investigated using the road impact factor (RIF) index that is defined as average g-force magnitude per unit of distance. The RIF-index was calculated on raw sensor data based on different window sizes (25 cm to 150 cm) to estimate the effect of window size. The silhouette coefficient (SC) metric was used to evaluate the quality of identified clusters (Rousseeuw, 1987). The use of agglomerative clustering for data pre-processing was investigated in (Titus-Glover, 2019).

Both supervised and unsupervised ML models are highly impacted by the quality of the features extracted from raw data (Souza, Souza, Cherman, Rossi, & Souza, 2017). Using NNs to automatically learn features from sensor data has been evaluated in image-based assessment

studies (Roberts, Giancontieri, Inzerillo, & Di Mino, 2020; Eisenbach, et al., 2017). Feature learning via deep NNs is ideal, but deep models are also data-hungry; they need a large training dataset, which currently remains impractical. More conventionally, statistical features are extracted from acceleration data represented in the time or spectral domains, or via wavelet transforms. There is no clear preference on any of these domains for pavement condition assessment. Time and spectral domain features were extracted from accelerometer and gyroscope sensors in (Allouch, Koubâa, A., Abbes, & Ammar, 2017). The authors of (Souza, Souza, Cherman, Rossi, & Souza, 2017) extended their work in (Souza, Giusti, & Batista, 2018) and provided a real-time mobile-based system, named Asfault, for road pavement condition evaluation by using built-in smartphone sensors and ML techniques; 62 features, including 23 temporal and 39 spectral statistics, were extracted from the magnitude acceleration time series. The ReliefF algorithm was utilized in this work to rank these features based on their importance on the target task (Robnik-Šikonja & Kononenko, 2003). Spectral irregularity, average magnitude, fundamental frequency, spectral flux, and root-mean-square (RMS) were reported as the top five features in this study. In (Basavaraju, Du, Zhou, & Ji, 2019), 23 temporal, 39 spectral, 20 linear spectral frequencies (LFS), and 36 continuous wavelet transform (CWT) statistics (using the Haar function) from different acceleration axes (x-, y-, z-, and magnitude-acceleration) were considered. The performance of four classifiers on different combinations of these features (varied from 20 to 472 features) was reported.

Compared to featurization over the time and spectral domains, wavelet-based featurization presents two clear advantages. Its resolution in both time and spectral domains allows it to resolve complex non-stationary signals (Javed, Gouriveau, & Zerhou, 2014). Additionally, a variety of available mother wavelet types have proven useful for capturing the different frequency characteristics of road distress (Wu, et al., 2020). However, determining a wavelet's optimal set of hyperparameters, such as the number of scales/orders, has typically required extensive empirical calibration and model fitting (Seraj, van der Zwaag, Dilo, Luarasi, & Havinga, 2015).

Contributions of this Work

In this work, we pursue the combination of wavelet featurization and unsupervised clustering. The core contribution of this work is the integration of these processes in a manner that enables automated optimization of both featurization and clustering, without the need for exhaustive empirical hyperparameter fitting. In particular, the framework we propose leverages multi-objective Pareto optimization to identify the ideal wavelet representation and clustering hyperparameters that optimize the quality of the resulting data clusters. This contribution expands the generalizability of unsupervised ML for pavement assessment, as each individual vehicle's dynamics and instrumentation can be featurized and clustered separately and then considered in aggregate for network-level asset management. As such, the work presented here opens up avenues for establishing a low-cost crowdsourcing framework capable of working in a variety of realistic settings.

METHODOLOGY

The schematic overview of the proposed framework is shown in Figure 6-1. In summary, the raw sensor data are vibration responses of a vehicle in the z-direction. The *Featurization* component extracts features from the raw data. The *Unsupervised Distress Recognition* carries out

unsupervised learning in the constructed features space via clustering. The *Clustering Evaluation* evaluates the identified clusters along several metrics. Finally, the *Automated Design Selection* searches over the hyperparameter space to identify optimal settings that correspond to optimal organizations of the sensor data into various pavement conditions. The rest of this section describes each of these components in greater detail.

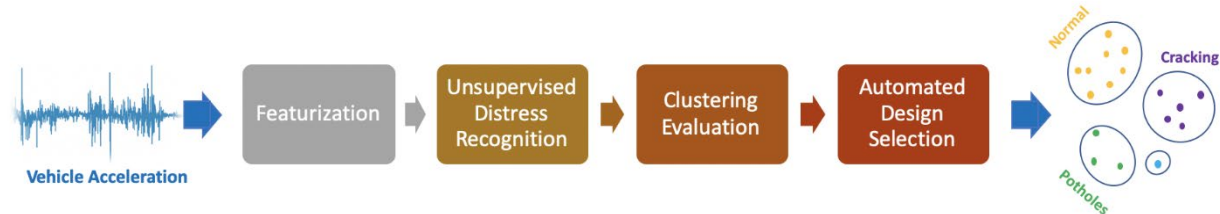


Figure 6-22. Schematic overview of the proposed framework.

Featurization

As summarized in the introduction, there is currently no well-established process for featurizing accelerometer response data for pavement assessment. However, recent research has indicated that wavelets are more effective than other approaches, due to their ability to overcome the complexity of non-stationary signals. It is worth noting that time and frequency domain representations can be combined with wavelet descriptors; however, this subsequently expands the dimensionality of the feature space (the number of features), which then poses further demands on the amount of data needed to fit ML models. Therefore, in this study we focus on wavelet featurization.

The wavelet transform utilizes wavelike finite duration oscillations/functions known as wavelets. Shifting and scaling are two main concepts in wavelet transformation. A wavelet can be stretched or shrunk in time to match the shape of a signal and shifted over the entire signal to capture various locations. The scale factor is a key hyperparameter in wavelet featurization which determines the degree of compression and expansion of the mother wavelet and is inversely proportional to frequency. In other words, larger-scale values stretch the wavelet and correspond to gradual changes of signal; small-scale values compress the wavelet and relate to rapid changes of signal. Scale value determination is a non-trivial task in wavelet domain analysis which is usually performed at various scales to decompose the signal into various frequencies (Wei, Fwa, & Zhe, 2005). The correlation between the signal and the wavelet function is indicated through a coefficient. The higher the value of the coefficient, the better the correlation between the signal and wavelet function (Griffiths, 2012).

The Discrete Wavelet Transform (DWT) and Continuous Wavelet Transform (CWT) are the two established classes of wavelet transformation. DWT coefficient computation is more efficient than CWT, because DWT coefficients are calculated on selected scales and time intervals. In contrast, CWT coefficients are computed by decomposition of continuous time-series signal into wavelets over the real axis and provide a more fine-grained representation of a signal. In DWT, the level of decomposition is a key hyperparameter that needs to be determined. At each level of decomposition, the signal is separated into two parts using a low-pass and a high-pass filter. The result from the high-pass filter is kept, and the result from the low-pass is filtered again until the desired number of levels is reached (Griffiths, 2012). The result is an array of ordered coefficients, including approximation and detail coefficients.

The comparison of these two different transforms and discussion on how they differ from each other is outside the scope of this work. Interested readers can find more details in (Altunkaynak & Ozger, 2016). Prior work has shown the continuous Morlet and discrete Daubechies 6 (DB6) wavelets to be the most effective for pavement condition assessment due to their ability to identify essential features of the signal (Basavaraju, Du, Zhou, & Ji, 2019; Altunkaynak & Ozger, 2016). Per the extensive study conducted in (Griffiths, 2012), Morlet and DB6 mother wavelets are capable of capturing frequency variations of vehicle vibration signal. As a result, they are the focus of this work, and they provide a reasonable comparison of continuous and discrete wavelet featurizations. These two mother wavelet functions are shown in Figure 6-2. The statistical features obtained here, as well as their number, are shown in the experimental evaluation.

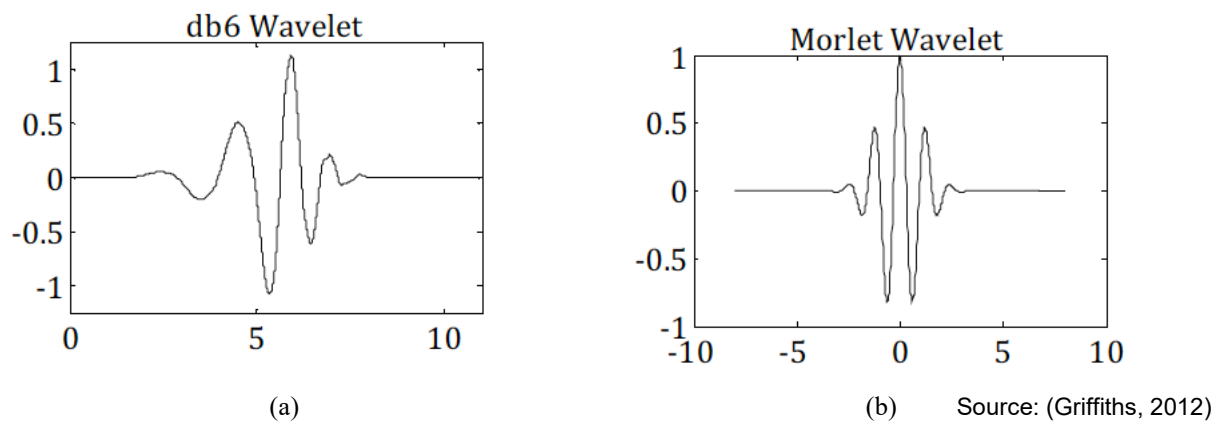


Figure 6-23. Common mother wavelet functions suitable for vibration signal (a) DB6 (b) Morlet.

Unsupervised Distress Recognition

Following featurization to obtain features from raw sensor data, unsupervised clustering is performed to separate the accelerometer responses corresponding to different types of roadway defects from responses that indicate sound roadway surfaces in good condition. The premise is that different types of pavement defects will each cause different deviations in vehicle response, causing them to fall into separate clusters. From a condition assessment point of view, the largest cluster is expected to correspond to “sound” pavement. While there are many clustering algorithms, we consider two popular distance-based clustering algorithms: k-means and agglomerative hierarchical clustering.

K-means, a commonly employed clustering algorithm, works by finding cluster centroids and then associates each data point (in feature space) with a cluster based on Euclidean distance. The algorithm proceeds in iterations. The k centroids are initially selected at random over the data, and the rest of the data are assigned to the various clusters represented by the centroids in a way that optimizes a designed objective function. The objective function measures the sum of squared errors, which effectively means that at each iteration, data points are assigned to the centroid to which they are closest. The centroids are then recomputed to reflect the distribution of data points in a cluster. This process of assigning data points based on current centroids and updating centroids based on the current data assignment continues until a convergence criterion has been met; centroids do not change anymore (Xiong, Wu, & Chen, 2008). The number of clusters, k, must be determined a priori, making it a critical hyperparameter.

In contrast to k-means, the number of clusters does not need to be specified ahead of time for agglomerative clustering. This algorithm belongs to a family of clustering algorithms that construct nested clusters by successive merging/agglomeration or splitting (Zaman, Kamranfar, Domeniconi, & Shehu, 2019). The agglomerative algorithm is a merging approach that starts with the assumption that each point is a cluster, and it continues by merging such clusters until the dendrogram root is reached. Different numbers of clusters are achieved by cutting the dendrogram at different places. Linkage distance is the criterion used in the agglomerative algorithm as the merging strategy to quantify how close two clusters are, and the algorithm combines pairs of clusters, which minimizes this criterion (Pedregosa, et al., 2011). The Ward function is used as the linkage criterion in this study (Ward, 1963). It measures the sum of squares growth that is experienced by merging two clusters and picks the pairs that minimizes this amount. Although agglomerative clustering does not require the number of clusters as a hyperparameter, in order to provide the same experimental setting as k-means and to have a better understanding of where the best dendrogram cut is according to clustering validation metrics, we consider the same number of clusters, k , as specified in k-means for the agglomerative algorithm.

Clustering Evaluation

Unsupervised learning is challenging to evaluate. The absence of ground-truth labels makes the data acquisition phase easy and inexpensive, but it makes the evaluation phase harder. Internal metrics are designed to describe the quality of found cluster based on how well the clusters capture the structure of the data in the absence of any ground truth (Rendón, Abundez, & Arizmen, 2011). While such an evaluative approach is considered here, we also consider the potential of using a small subset of labeled data to augment Pareto optimization, referred to here as external metrics. There is a clear trade-off; having a small set of labeled data is labor-intensive but, as will be shown, it aids in evaluating the quality of clusters and in turn improves the optimization of the automated design selection. As it is realistic to assume that there are some labeled data but not sufficient for generalizable supervised learning, this component of our framework considers both external and internal metrics to evaluate the quality of identified clusters along several "performance indices." These performance indices are utilized as the input objectives for optimization in the following component of our framework, as we describe later. We first list the internal and external metrics we employ to obtain performance indices.

Internal Metrics

Internal metrics are designed in unsupervised learning literature to quantify the relationship of points within each cluster and the relationship of the clusters to each other. The main intuition is that if the data points within a cluster are closer to one another than to data points in other clusters, this indicates that the clustering quality is good and should be reflected in the performance indices. Specifically, we use the Calinski-Harabasz Index (CH) (Caliński & Harabasz, 1974) and the Davies-Bouldin Index (DB) (Davies & Bouldin, 1979).

Calinski-Harabasz Index (CH): Introduced as one of the best validation clustering indices, it is also known as the variance ratio criterion. CH-index is defined as the ratio of the within-cluster variance SS_W and between-cluster variance SS_B (Arbelaitz, Gurrutxaga, Muguerza, Pérez, & Perona, 2013; Pedregosa, et al., 2011). It is desired to obtain a large value for SS_B indicating large distances between clusters' centroids and the centroid of the whole dataset compared to

small SS_W value indicating small distances of data points to their assigned cluster's centroids. In essence, a higher CH-index value suggests the clusters are dense and well-separated.

$$CH - Index = \frac{SS_B}{SS_W} * \frac{N_c - k}{k - 1} \quad (6.47)$$

where N_c is the number of data points that are clustered into k clusters. The CH-Index equation can be expanded in terms of SS_B and SS_W definitions as follows:

$$CH - Index = \frac{\sum_{i=1}^k d(C_i, M)}{\sum_{i=1}^k \sum_{X_j \in CL_i} d(X_j, C_i)} * \frac{N_c - 1}{k - 1} \quad (6.48)$$

where C_i is the centroid of cluster i , M is the centroid of the entire dataset, and CL_i is cluster i (Łukasik, Kowalski, Charyanowicz, & Kulczycki, 2016).

Davies-Bouldin Index (DB): Distances of data points inside clusters are calculated according to their corresponding cluster representative, and they are compared with cluster representatives' distances.

$$DB - Index = 1/k \sum_{i=1}^k \text{Max}_{i \neq j} \frac{\delta(CL_i) + \delta(CL_j)}{D(CL_i, CL_j)} \quad (6.49)$$

where k is the number of clusters, CL_i is cluster i , and δ denotes the intra-cluster, while D indicates the inter-cluster distances; δ and D can be calculated as follows:

$$\delta(CL_i) = \sum_{X_j \in CL_i} \frac{d(X_j, C_i)}{|CL_i|} \quad (6.50)$$

$$D(CL_i, CL_j) = d(C_i, C_j)$$

where C_i is the centroid of cluster I (Petrovic, 2006). In contrast to the CH-index, smaller values of the DB-index indicate better clustering results.

External Metrics

We consider three external metrics that allow us to exploit a small set of labeled data to provide insight into the quality of the clusters identified over the larger (mostly unlabeled) dataset: Cluster Entropy, Label Distribution Entropy, and F-measure. The first two metrics are adaptations of our own.

Cluster Entropy (CE): Cluster entropy estimates the purity of the clusters by means of the class labels assigned to its participating data points. By considering all labeled data points within a cluster $i \in \{1, \dots, k\}$, CE_i summarizes the distribution of the class labels inside a cluster i (Rendón, Abundez, & Arizmen, 2011). Specifically,

$$CE_i = - \sum_c p(c|i) \log p(c|i) \quad (6.51)$$

where i is the cluster being considered, c varies over the available class labels, and $p(c|i)$ measures the probability that a class label c falls in cluster i . The ideal value for CE_i is zero, which occurs when all data points inside a cluster carry the same class label. In our adaptation, we use a weighted version of CE to provide a summary metric over all clusters and additionally differentiate between large and small clusters. Specifically,

$$CE_{weighted} = \sum_{i=1}^k \frac{N_i}{N} * CE_i \quad (6.52)$$

where k is the number of clusters, N_i is the number of data points inside cluster i , N is the size of the entire dataset, and CE_i is the CE value of cluster i measured as above. Per the adaption, the contribution of larger clusters is more.

Label Distribution Entropy (LDE): LDE was introduced in (Kamranfar, Bynum, Lattanzi, & Shehu, 2020) to track the distributions of labels over clusters. LDE modifies CE to consider the fraction of each class label that is captured in each cluster instead of the frequency of class labels within a cluster. Like CE , a smaller value of LDE indicates better clustering quality.

F-score: This metric uses a combination of two important concepts that are widely used in supervised learning, precision, and recall (Rendón, Abundez, & Arizmen, 2011). F-score allows us to consider both the purity and label distribution of clusters. Specifically,

$$F - score = \frac{2 * P_{a,b} * R_{a,b}}{P_{a,b} + R_{a,b}} \quad (6.53)$$

where P and R stand for precision and recall, respectively. $R_{a,b} = \frac{N_{a,b}}{N_a}$, $R_{a,b} = \frac{N_{a,b}}{N_a}$ and $P_{a,b} = \frac{N_{a,b}}{N_b}$; $P_{a,b} = \frac{N_{a,b}}{N_b}$ where $N_{a,b}$ is the number of samples from class a placed in cluster b , N_b is the size of cluster b , and N_a is the number of samples with label a . Larger values of F-score indicate better clusters.

Automated Design Selection

The process of featurizing data and then clustering them requires significant hyperparameter selection, regardless of the particular features or clustering algorithm chosen. Such hyperparameters include the level/scale of wavelet resolution that results in viable features, as well as clustering hyperparameters such as the number of clusters for k-means and agglomerative clustering in this study. Conventionally, finding the optimal or near-optimal set of hyperparameters is challenging and is routinely addressed empirically by researchers. However, this poses significant difficulties for practical implementations in a crowdsourced setting, as each individual vehicle-sensor combination will result in a different set of optimal parameters, directly impacting the generalizability of the end result. In addition, choosing among the various types of wavelet or clustering algorithms among all available ones is a problem. Therefore, this work goes beyond conventional hyperparameter selection and effectively considers decisions with regard to types of wavelet and types of clustering algorithms as hyperparameters themselves. In other words, we are not only interested in tuning the featurization and learning algorithms' hyperparameters, but we are also interested in determining in an automated manner which featurization and learning algorithms yield best results.

The question of what constitutes best results is an important one. When the target/objective is optimizing a single performance index, such as the CH-index, optimization is straightforward. However, various indices capture different performance indices, as described above. So, instead we consider here a multi-objective setting, where the various indices listed above are each optimization objectives. Rather than aggregating them into one single objective function, which would necessitate an ad-hoc process of weighting them based on some arbitrary decision on what is more important, we employ multi-objective Pareto optimization (Santiago, et al., 2014). In principle, multi-objective optimization can identify superior configurations over the hyperparameter space compared to single-objective optimization; however, various objectives can be conflicting. That is, changes to one or more hyperparameters may improve on one objective but worsen another. For instance, a clustering result with lower cluster entropy does not necessarily also have a higher CH-index.

Multi-objective Pareto optimization addresses specifically the above setting via the concept of dominance. When a configuration a is better than configuration b in terms of all indices of interest, configuration a is said to dominate configuration b . This definition is also known as strong dominance. Occasionally, in the literature, equality is permitted, diluting *better* to *no worse*, and the result is known as weak dominance. We employ strong dominance in our framework. The concept of dominance allows two concepts to be associated with each configuration, a *Pareto Rank* (PR) and a *Pareto Count* (PC). The PR of a configuration a is the number of other configurations that dominate a . The PC of a configuration a is the number of other configurations that a dominates. It follows that desirable configurations are those with smaller PR values (ideally zero). When two configurations have the same PR value, the desired configuration is the one with larger PC values. PR is a powerful concept that is very popular in optimization literature, particularly under the umbrella of evolutionary computation. In particular, configurations with PR values of 0 are known as the *Pareto Front*.

The Automated Design Selection component of our framework carries Pareto-based multi-objective optimization, computing the PR and PC of each configuration in the hyperparameter space. Configurations are first ordered from low to high PR. Configurations with the same PR value are further ordered from high to low PC.

EXPERIMENTAL EVALUATION

Dataset

In order to prototype and illustrate the capabilities of the proposed framework, an experimental study was performed. First, a series of representative residential roadways in the northern Virginia region were identified based on observed defects and roadway conditions. Five different road conditions were identified: normal, cracking, patching, bridge joints, and potholes.

A 2018 Honda Accord vehicle and iPhone XS smartphone were used to collect response data along these road segments. The built-in accelerometer sensor of an iPhone XS model was utilized, with data capture in the z-direction of the accelerometer, representing vertical motion of the vehicle. To maximize the accuracy of measurement, we mounted the phone horizontally on the floor mat of the passenger side footwell in order to eliminate complications from accelerometer axis reorientation. Acceleration was sampled at 1,000 Hz, with subsampling to 200 Hz in order to account for inconsistencies in the sample rate. Prior work in pavement suggested that this was a reasonable choice for sample rate (Chatterjee & Tsai, 2020; Yi,

Chuang, & Nian, 2015; Basavaraju, Du, Zhou, & Ji, 2019; Eriksson, Girod, Hull, & Newt, 2008). Stratified sampling was used for subsampling, with the data split into equal intervals and a sample drawn randomly from each interval to generate 200 samples per second. This process minimized the probability of information loss (Neyman, 1992). In order to generate labels for some data, videos were collected during driving. The dataset contains about 30 minutes of response recordings, with about 3% (less than a minute) labeled. The data were windowed into one-second segments. This resulted in 1,706 individual observations of 200 samples each. Only 54 out of 1,706 data points were labeled by a pavement expert according to the videos. The distribution of the labels is as follows: normal: 16, cracking: 20, patching: 5, bridge joints: 5, and pothole: 8.

Analytical Configuration

Each data point was featurized using a wavelet transformation approach, as described in the methodology. Both discrete and continuous wavelets were considered, in particular, the DB6 and Morlet wavelets described previously. Other than wavelet type, the scale and level of wavelets are hyperparameters that must be tuned. For the DB6 wavelet, the level range from 3 to 6 was chosen as the common interval, while the common scale values of factor 2 such as 1, 2, 4, 8, 16, and 32 were considered for the Morlet wavelet. This effectively set the range for the hyperparameter optimization. Larger ranges could be selected, with a cost to the computational efficiency of the optimization.

Both approximation and detail coefficients of DB6 were computed, and the skewness, kurtosis, standard deviation, mean, and root mean square (rms) statistics were extracted out of all coefficients as features. This resulted in 20, 25, 30, and 35 features for levels of 3, 4, 5, and 6, respectively. Standard deviation, rms, median, skewness, kurtosis, mean, and maximum values were extracted from each scale of the Morlet wavelet as well and appended to the previously extracted features from lower scales to create the comparable number of features from both types of wavelets. As an example, we extracted 7 features from both scales 1 and 2, but for scale 1 the first 7 features were utilized while for scale 2 the first 14 features were considered. Therefore, in the continuous domain we dealt with 7, 14, 21, 28, 35, and 42 features per wavelet scale. For the number of clusters in both k-means and agglomerative, a range of 2 to 11 clusters was identified. Overall, hyperparameter choices included 10 possible numbers of clusters, 2 choices of clustering algorithms, and 4 potential levels of wavelets for discrete wavelet (DB6). Another option was to use continuous wavelets (Morlet) with six possible scales. Given all of the potential hyperparameter choices, 200 design/hyperparameter configurations were deemed feasible. As described in the methodology, since there is no limitation for using internal metrics, we first considered them as the only optimization objectives over the 200 hyperparameter configurations. Then the results of all five evaluation metrics (combination of internal and external) for evaluating the clustering results were investigated.

Dataset Evaluation

To illustrate the behavior of the presented framework in greater detail, this chapter presents an analysis from two roads in the dataset. A normal driver's perspective on quality of one road was good, while the other one was labeled as poor. Such information was expected to be reflected in the spectrogram and scalogram diagrams of vibration signals. Figure 6-3 indicates (a) the vibration signal (b) spectrogram, and (c) scalogram obtained from the Morlet wavelet. All three

diagrams agree on detecting two different behaviors in the signal. The vibration pattern of the first 30 seconds (first 6000 samples) is different from the rest, and such separation was also reflected in the spectrogram and scalogram. The first part of the shown signal was considered as typical “normal” roadway condition, with lower response amplitudes and frequencies. The second part was from a poor-quality roadway. Note the existence of a short normal behavior (good road condition) within the second part of the signal, also visible in all three diagrams.

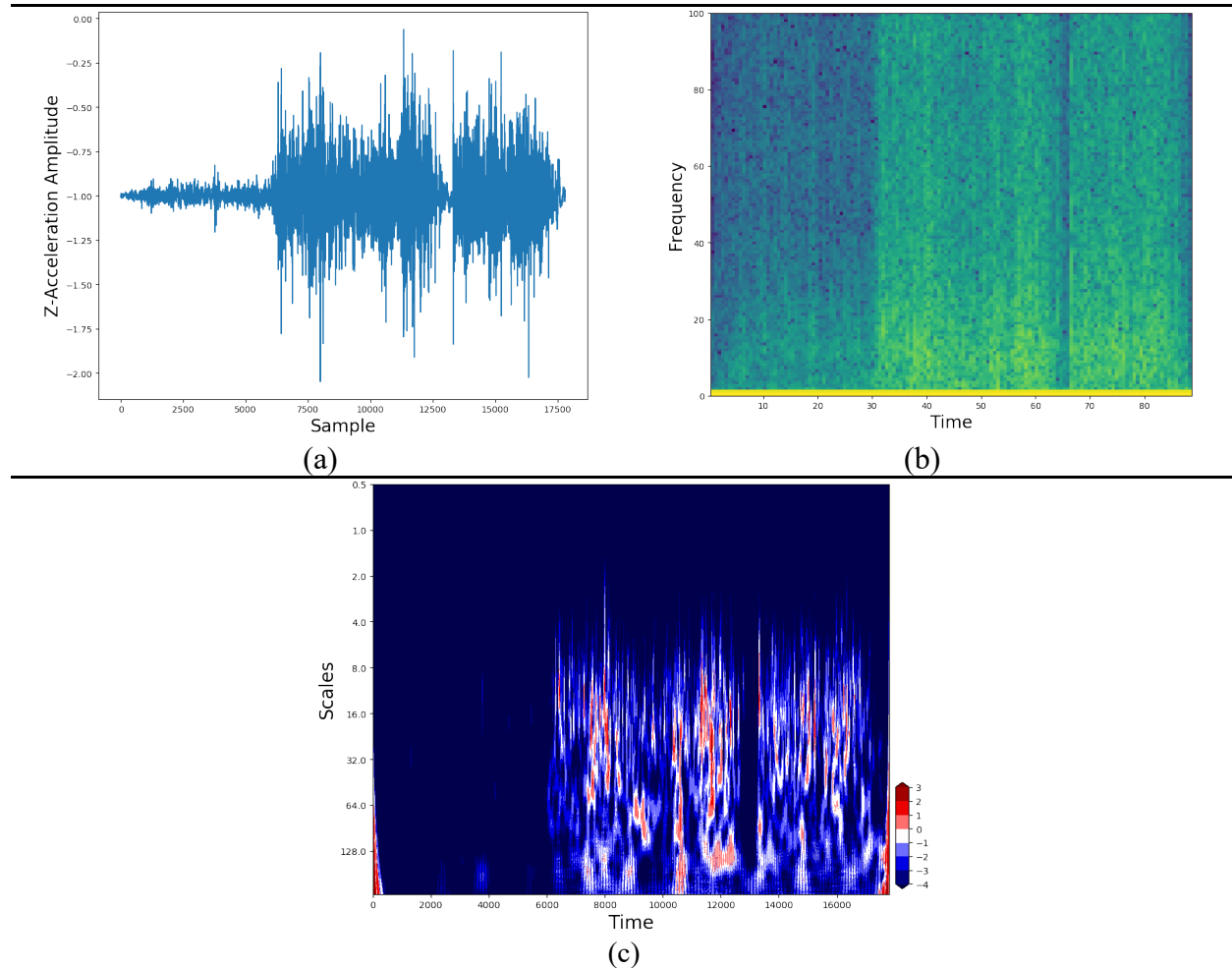


Figure 6-24. Good- versus poor-quality road condition from a user’s perspective: (a) z-acceleration signal, (b) spectrogram, and (c) scalogram from Morlet wavelet. All three diagrams detect two different behaviors in the signal, with the second starting after the first 30 seconds (first 6,000 samples).

To provide a deeper insight into the results, we execute two settings. First, we only consider the internal metrics as the objectives for optimization by the framework and relate the configurations in the Pareto Front with the highest Pareto Count in Table 6-1. For comparison, Table 6-2 shows the top Pareto Count configurations in the Pareto Front when all the internal and external metrics are considered as optimization objectives by the framework. This comparison

(c)

helps us understand if the optimal configuration is changed by additionally considering the external metrics as optimization objectives.

A comparison of the Pareto-optimal configurations selected across the above-described settings shows that the continuous wavelet is more suitable for this dataset (regardless of internal or external indices). By considering both wavelet types, the Morlet was always found to be the best configuration among all generated ones.

A comparison of Table 6-1 to Table 6-2 shows that, when both wavelet types are considered, adding external metrics does not dramatically change the optimal configuration. There are slight differences between winners of “both wavelet types” reported in Table 6-1 and Table 6-2, particularly in terms of clustering and number of clusters, but wavelet type and number of features remained constant (Morlet with 7 features). While the presence of labeled data can always assist in finding the best configuration, the above comparison shows that external metrics do not play a significant role in the optimization; even with no label information, similar results can be obtained by merely using internal indices.

Table 6-36. Pareto-optimal winners selected by internal evaluation metrics.

Wavelet Type	Mother Wavelet, No. Features, Clustering, No. Clusters	CH-Index	DB-Index
Discrete Wavelet	DB6, 20, k-means, 2	872.86	1.1
	DB6, 20, hierarchical, 2	812.18	1.095
Continuous Wavelet	Morlet, 7, k-means, 9	17,135.8	0.51
	Morlet, 7, hierarchical, 11	17,078.54	0.51
Both Types	Morlet, 7, k-means, 9	17,135.8	0.51
	Morlet, 7, hierarchical, 11	17,078.54	0.51

Table 6-37. Pareto-optimal winners selected by internal and external evaluation metrics.

Wavelet Type	Mother Wavelet, No. Features, Clustering, No. Clusters	CH-Index	DB-Index	Cluster Entropy	Label Distribution Entropy	F-measure
Discrete Wavelet	DB6, 20, k-means, 7	4558	1.33	1.12	0.90	2.36
Continuous Wavelet	Morlet, 7, hierarchical, 9	1383	0.52	0.8	0.83	2.45
Both Types	Morlet, 7, hierarchical, 9	1383	0.52	0.8	0.83	2.45

The best design configuration for the experimental dataset was selected as the Morlet wavelet in scale 1 (7 features) for featurization, with nine clusters found by agglomerative hierarchical clustering. Distribution of known conditions over the nine detected clusters is shown in Figure 6-4 and Table 6-1. Figure 6-4 visualizes the proportion of class labels within each cluster as pie charts. Table 6-3 discloses more details about the distribution of samples in each cluster. It can be inferred from Figure 6-4 and Table 6-3 that the majority of *good/normal* road segments are clustered together (in Cluster 1) and they are distinguishable from other segments, a promising result that suggests that underlying structure exists among the *good*-quality roads. Therefore, Cluster 1 can be labeled as *good*, and data points that are assigned to this cluster can be classified as good-quality roads.

Among the four pavement defects considered here, *cracking* can be considered as the starting point in the pavement damage process, except for bridge joints. The *cracking* label has the most overlap among the clusters due to the fact that cracking can manifest in various ways; however, this more nuanced representation is not captured in the dataset labels. Alligator cracks may cause a different vehicle response than transverse cracks, and sometimes they are even so fine as to be clustered with normal condition roadways. This behavior is shown in Clusters 1 and 9 in Figure 6-4, with *good* and *cracking* segments placed together, while in Clusters 5 and 6 cracked roadways segments are grouped with other forms of distress. Additionally, Clusters 3 and 8 contain only cracked segments, suggesting an underlying structure among vehicle responses on roadways with *cracking* labels.

Cluster 7 contains 4 out of the 5 road segments with the *patching* label. Only one segment of patched roadway is placed in Cluster 5, where the majority of observations correspond to *cracks*. An image of a representative patched road segment in Cluster 7 and the one in Cluster 5 are shown in Figure 6-5. The left panel in Figure 6-5 shows a utility patch, categorized as Cluster 5. The right panel shows another, more generalized *patch*. Vehicle response would be expected to vary significantly across these two patches and result in two different cluster labels. As Figure 6-4 shows, potholes and bridge joints are clustered together (Clusters 4, 6, and 7). Like previous roughness types, shallow and severe potholes are not individually categorized, nor are the various types of bridge joints. A pothole and a bridge joint could potentially cause similar vehicle responses, generally as high-amplitude, short-duration impulses. Less severe potholes were categorized as Clusters 2 and 5, dominated by cracked pavement. More severe potholes were placed in Clusters 4, 6, and 7, along with bridge joints. In practical applications, the clustering of potholes with bridge joints is not a major concern, as bridge joint locations are known to roadway management agencies, and these responses can be filtered out prior to any asset management application.

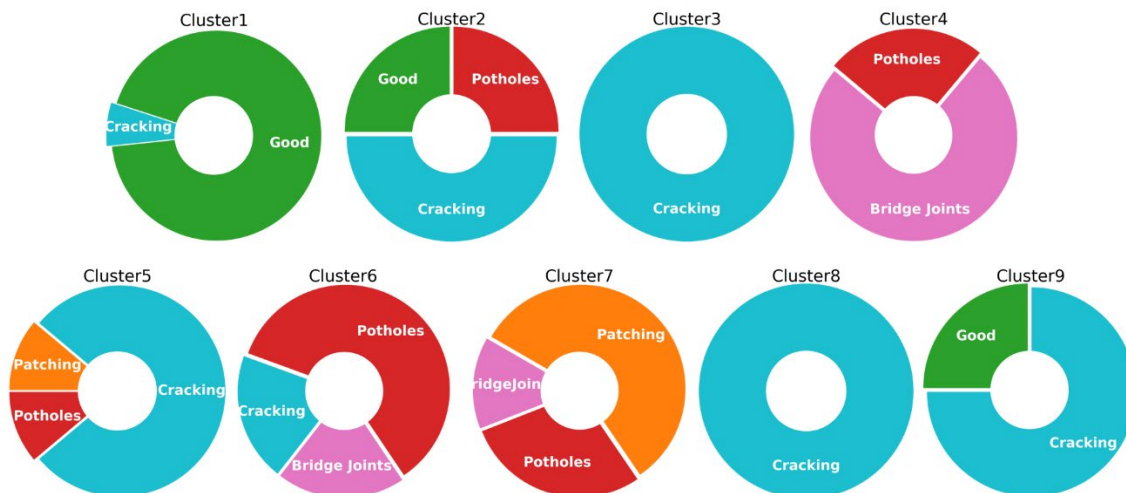


Figure 6-25. Distribution of known conditions over nine clusters recognized by hierarchical clustering.

Table 6-38. Distribution of samples with known conditions over nine clusters detected by Pareto-optimal winner.

Cluster	Good	Cracking	Patching	Bridge Joints	Potholes
Cluster 1	14	1	0	0	0
Cluster 2	1	2	0	0	1
Cluster 3	0	2	0	0	0
Cluster 4	0	0	0	3	1
Cluster 5	0	7	1	0	1
Cluster 6	0	1	0	1	3
Cluster 7	0	0	4	1	2
Cluster 8	0	4	0	0	0
Cluster 9	1	3	0	0	0
Total known labels	16	20	5	5	8



Figure 6-26. Two roads with patching labels.

Additionally, the similarities among CWT-extracted feature distributions were computed for all road qualities in 54 labeled data points. Since the Pareto optimization process identified 7 features for 5 distress types, a distance matrix of 35 by 35 was created and the Earth Mover Distance (EMD) was computed to measure the distance/similarity of any two distributions. The EMD can be defined as the minimum required work/cost for the best match between two sets of data points (Andoni, Indyk, & Krauthgamer, 2008). Figure 6-6(a) illustrates the EMD matrix for CWT features per class label, with darker shading indicating shorter distances. Therefore, it can be seen that distances of feature distributions among patching, bridge joints, and potholes labels are small, which confirms that they are difficult to separate via statistical categorization. Normal road segments are distinguishable from other road abnormalities, although some overlap with cracking is apparent. Figure 6-6(b) illustrates the EMD matrix for the clusters rather than class labels for the Pareto-optimal configuration. Cluster 1 is the most distinctive cluster. This cluster was labeled as good/normal pavement condition and has strong separability from other pavement conditions. The similarity of feature distributions in Clusters 4 through 9 also confirms the label overlaps detected in Figure 6-4.

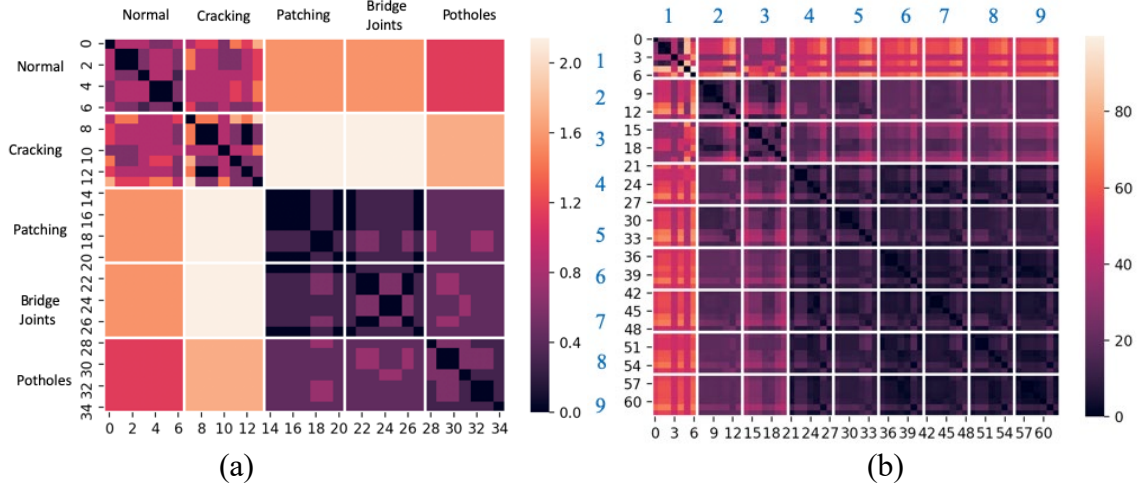


Figure 6-27. (a) Earth Mover Distance matrix per class label among CWT feature distributions for 54 labeled data, (b) Earth Mover Distance matrix among CWT feature distributions of Pareto-optimal configuration.

CONCLUSIONS

In this chapter, we present an unsupervised learning framework that combines Pareto-optimized wavelet featurization with clustering for pavement condition assessment. Wavelet features are ideal, as they address the non-stationary behavior of vehicle vibration dynamics. However, significant empirical tuning is required to find the optimal setting and configuration for any given wavelet representation. We take advantage of the concept of Pareto optimality to go beyond conventional hyperparameter selection and automate the process of selecting the wavelet type as well as the choice of clustering algorithm. The study is motivated by the appeal of crowdsourcing any particular vehicle’s response data, using only the z-acceleration data gathered from a smartphone as a low-cost data collection device in a multi-condition road environment. The experimental results show that the presented framework is capable of detecting various pavement distress classes, even at early stages, but that low-cost smartphone data may not be adequate to distinguish fine-grained pavement defects. Our proposed low-cost framework is general and scalable with no dependence on human-intensive data labeling.

The framework suggested in this chapter can be readily applied in real-world roadways and scaled to a variety of applications. Other vibration axes like X-, Y-, or other wavelet types or clustering algorithms can be substituted in data acquisition, featurization and learning phases of the framework, respectively. It should be noted that the framework is generalizable in terms of other ranges of wavelet levels/scales. Moreover, we tested the framework on a single vehicle to investigate what can be obtained from the baseline setting where there is limited access to data resources, but the final goal is to evaluate it with the presence of multiple vehicle dynamics. To expand the current work, we intend to fuse various vibration signals from multiple vehicle sensor configurations for monitoring the condition of the roadways in terms of multiple clusters of pavement defects. This can also bring the focus on tracking these clusters over time to see if gradual pavement degradations can be captured in an agnostic manner.

CHAPTER 7

Summary, Conclusions and Future Work

SUMMARY

In summary, the outcomes of the first phase of this research are:

- A deeper understanding of the nature of crowdsourced vehicle response data and its utility, specific to the perception of asset (roadway and bridge) condition, with its impact on free-flow speeds and capacities, and the ability to detect deteriorated conditions through latent space modeling of the data and developed machine learning algorithms;
- Development of probabilistic predictive models for multi-asset (pavement and bridge) roadway system serviceability levels, with and without maintenance or other improvements, while considering inspection accuracy needs, activity impacts and other associated costs;
- Conceptualization of the multi-asset, strategic planning of maintenance, repair, and rehabilitation options (improvement actions) and their prioritization for implementation as a bilevel, stochastic mathematical program that:
 - explicitly accounts for system-wide traffic impacts from reduced capacity from deterioration and construction work zones, and post-improvement increased capacity and speed (a user equilibrium is sought in a lower-level traffic assignment problem);
 - takes into account uncertainty in asset state over time due to stochastic evolution of deterioration processes (a Markov decision process problem formulation of the upper-level decision process involving probabilistic state transitions due to deterioration);
- Solution algorithms based on concepts of machine learning:
 - Comparison to existing mathematical modeling approaches missing one or more of the key study elements through analysis of a test network from the literature;
 - Comparison of optimally derived prioritized schedules using the developed normative approach to schedules derived from a relevant descriptive, state-based (threshold) maintenance strategy implementation;
- Comparison with other current practices, including decision-tree approaches; and
- Development of a value of information framework and strategies for assessing the value of information.

CONCLUSIONS

Asset management is a data-driven process aimed at delivering the best levels of service for roadway assets given the available resources. Current practices vary in sophistication.

Consequently, there are many opportunities to improve the data collection process, the models used to support decisions that select actions, and the process used to determine the most appropriate action at any point in time for an asset. However, there are also significant barriers to implementation, including the role played by proprietary data and software in the asset management process, the desire of agencies to understand the decision-making process, and the organizational structures that silo decision making by asset type.

This project demonstrated the applicability of new types of data, including processing, models for asset deterioration and activity cost and duration that reflect current practices, strategies for assessing the value of information, and an optimization model for scheduling activities that captures uncertainty in deterioration, disruption to users, and cross-asset tradeoffs.

Use of crowdsourced vehicle response data shows promise as a low-cost way to perform asset collection at high frequency (potentially near-continuously on high-volume systems). An unsupervised learning framework that combines Pareto-optimized wavelet featurization with clustering is developed to provide low-cost pavement condition data using methods that are general and scalable. While there may be some limitation regarding fine-grained pavement defects, the framework can be extended to capture data from multiple vehicles over time. It can also be extended to other sources of data, for instance on-board vehicle imaging or LIDAR.

A detailed, realistic deterioration modeling framework, following principles of Markov decision processes and partially observable MDPs, is developed for both pavements and bridges. The framework uses common condition measures (IRI and CCI for pavements, and deck condition for bridges) and four maintenance categories (Do Nothing, Minor Repair, Major Repair, and Reconstruction) to determine state transition probabilities and costs. Condition data are also dependent on the inspection type: no inspection, low-fidelity, and high-fidelity inspections. The accuracy of the information and the cost of inspection are associated with each inspection type.

A methodology to compute the Value of Information and the Value of Structural Health Monitoring within the context of MDP/POMDPs is presented. Respective stepwise and long-term value-based information metrics are analyzed, and their relations to the POMDP decision making are provided. These results provide quantitative answers to the practical question of how much condition information is worth and how that information affects decisions.

A multi-asset class roadway improvement scheduling problem that considers capacity loss during improvement actions (i.e., downtimes), traffic impacts of improved serviceability after the actions are complete, and uncertain deterioration mechanisms jointly across multiple asset classes is formulated and solved. The solution found using cutting-edge, deep reinforcement learning methods for an illustrative example shows the value of decisions integrated over asset classes (in this case, pavements and bridge decks) and the importance of user disruption.

FUTURE WORK

Phase 2 of this research will extend the work of Phase 1. The objectives of this proposed effort are to:

- Extend developed condition monitoring and forecasting capabilities to exploit continuously sensed, multi-sourced data technologies for persistent condition updates on multiple assets from varying vehicle types;
- Extend methods from Phase 1 for capturing roadway characteristics from sensed data for continuous, multi-vehicle sensing implementations;

- Extend the MDP upper-level conceptualization of the prioritization problem to a partially observable MDP model to incorporate data uncertainty and continuously sensed and updated-predicted asset condition states;
- Create methods that explicitly account for uncertainty in state predictions with data updates;
- Develop a solution algorithm for adapting decisions that exploit updated information as captured in the stochastic, bilevel program with POMDP at the upper-level and user equilibrium (UE) at the lower-level;
- Employ developed methods to evaluate and demonstrate the potential benefits of continuous monitoring for updated prioritization and policy options; and
- Create simpler, intuitive tools, prescriptive guidelines, and/or implementable policies based on knowledge gained from earlier tasks that can be deployed in practice for large, complex roadway networks.

The objectives of the proposed effort will be realized through completion of tasks focused on predictive analytics, estimating and controlling serviceability, enhanced prioritization, adding context to decision tools, and evaluation and demonstration.

The outcomes of this effort will include condition monitoring and prediction techniques that use the latest sensing technologies, machine learning techniques and decision support tools for prioritizing and scheduling maintenance, repair, and rehabilitation actions across assets in a dynamically changing and uncertain environment with high-frequency asset condition data and updated forecasts.

References

- 112th Congress. (2012). Moving Ahead for Progress in the 21st Century Act. Retrieved July 15, 2019, from <https://www.govinfo.gov/content/pkg/PLAW-114publ94/pdf/PLAW-114publ94.pdf>
- 114th Congress. (2015). Fixing America's Surface Transportation Act. Retrieved July 14, 2019, from <https://www.govinfo.gov/content/pkg/PLAW-114publ94/pdf/PLAW-114publ94.pdf>
- Abdallah, I., Dertimanis, V., Mylonas, H., Tatsis, K., Chatzi, E. N., Dervilis, N., . . . Maguire, E. (2018). Fault diagnosis of wind turbine structures using decision tree learning algorithms with big data. Trondheim, Norway: European Safety and Reliability Conference (ESREL).
- ADOT. (2018). Production Rates Guidelines for Arizona Highway Construction. Arizona Department of Transportation.
- Alaska Department of Transportation & Public Facilities. (2019). *Transportation Asset Management Plan*.
- Allouch, A., Koubâa, A., A., Abbes, T., & Ammar, A. (2017). Roadsense: Smartphone application to estimate road conditions using accelerometer and gyroscope. *IEEE Sensors Journal*, 17(13), 4231-4238.
- Altunkaynak, A., & Ozger, M. (2016). Comparison of discrete and continuous wavelet–multilayer perceptron methods for daily precipitation prediction. *Journal of Hydrologic Engineering*, 21(7). doi:04016014
- Andoni, A., Indyk, P., & Krauthgamer, R. (2008). Earth Mover Distance over high-dimensional spaces. *SODA*, 8, 343-352.
- Andriotis, C. P., Papakonstantinou, K. G., & Chatzi, E. N. (2021). Value of structural health information in partially observable stochastic environments. *Structural Safety*, 93. doi:102072
- Andriotis, C. P., & Papakonstantinou, K. G. (2018). Extended and generalized fragility functions. *Journal of Engineering Mechanics*, 144(9), 04018087.
- Andriotis, C., & Papakonstantinou, K. (2019). Managing engineering systems with large state and action spaces through deep reinforcement learning. *Reliability Engineering and System Safety*, 191, 1-17.
- Andriotis, C., & Papakonstantinou, K. (2021). Deep reinforcement learning driven inspection and maintenance planning under incomplete information and constraints. *Reliability Engineering and System Safety*, 212. doi:107551

- Arbelaitz, O., Gurrutxaga, I., Muguerza, J., Pérez, J. M., & Perona, I. (2013). An extensive comparative study of cluster validity indices. *Pattern Recognition*, 46(1), 243-256.
- ASCE. (2021). Infrastructure Report Card: <https://www.infrastructurereportcard.org/>. American Society of Civil Engineering.
- Basavaraju, A., Du, J., Zhou, F., & Ji, J. (2019). A machine learning approach to road surface anomaly assessment using smartphone sensors. *IEEE Sensors Journal*, 20(5), 2635-2647.
- Beckmann, M., McGuire, C., & Winsten, C. (1956). *Studies in the economics of transportation*. New Haven: Yale University Press.
- Bryce, J., Elkins, G., & Thompson, T. (2020). Sensitivity Analysis of Highway Economic Requirements System Pavement Performance Models. *Journal of Transportation Engineering, Part B: Pavements*, 142(2). doi:04020006
- Caliński, T., & Harabasz, J. (1974). A dendrite method for cluster analysis. *Communications in Statistics-theory and Methods*, 3(1), 1-27.
- Caltrans. (2018). *California Transportation Asset Management Plan*. Retrieved July 13, 2019, from http://www.tamptemplate.org/wp-content/uploads/tamps/033_california.pdf
- Chang, J.-R., Chang, K.-T., & Chen, D.-H. (2006). Application of 3D laser scanning on measuring pavement roughness. *Journal of Testing and Evaluation*, 34(2), 83-91.
- Chatterjee, A., & Tsai, Y.-C. (2020). Training and Testing of Smartphone-Based Pavement Condition Estimation Models Using 3D Pavement Data. *Journal of Computing in Civil Engineering*, 34(6). doi:04020043
- Chatti, K., & Zaabar, I. (2012). *Estimating the Effects of Pavement Condition on Vehicle Operating Costs*. NCHRP Report 720. Retrieved from <https://www.nap.edu/catalog/22808/estimating-the-effects-of-pavement-condition-on-vehicle-operating-costs>
- Chatzi, E. N., Papakonstantinou, K. G., Hajdin, R., & Straub, D. (2017). Observation-based decision-making for infrastructure. Zagreb: Workshop on the Value of Structural Health Monitoring for Reliable Bridge Management.
- Chen, L., & Bai, Q. (2019). Optimization in Decision Making in Infrastructure Asset Management: A Review. *Applied Sciences*, 9(1380).
- Chen, L., Henning, T., Raith, A., & Shamseldin, A. (2015). Multiobjective Optimization for Maintenance Decision Making in Infrastructure Asset Management. *Journal of Management in Engineering*, 31(6).
- Chen, Z., Liang, Y., Wu, Y., & Sun, L. (2019). Research on Comprehensive Multi-Infrastructure Optimization in Transportation Asset Management: The Case of Roads and Bridges. *Sustainability*, 11(4430).

- Chu, J., & Chen, Y. (2012). Optimal threshold-based network-level transportation infrastructure life cycle management with heterogeneous maintenance actions. *Transportation Research Part B: Methodological*, 46(9), 1123-1143.
- Chu, J., & Huang, K. -H. (2018). Mathematical programming framework for modeling and comparing network-level pavement maintenance strategies. *Transportation Research Part B: Methodological*, 109.
- Connecticut Department of Transportation. (2019). *Highway Transportation Asset Management Plan*.
- Davies, D. L., & Bouldin, D. W. (1979). A cluster separation measure. *IEEE transactions on pattern analysis and machine intelligence*, 2, 224-227.
- de León Izeppi, E., Morrison, A., Flintsch, G. W., & McGhee, K. K. (2015). *Best practices and performance assessment for preventive maintenance treatments for Virginia pavements*. Virginia Center for Transportation Innovation and Research.
- Delaware Department of Transportation. (2019). *Transportation Asset Management Plan*.
- Diamantidis, D., Sykora, M., & Sousa, H. (2019). *Quantifying the value of structural health information for decision-support: guide for practicing engineers*. COST Action TU1402 - Quantifying the Value of Structural Health Monitoring.
- District Department of Transportation. (2019). *Transportation Asset Management Plan*.
- Durango-Cohen, P. L. (2004). Maintenance and Repair Decision Making for Infrastructure Facilities without a Deterioration Model. *Journal of Infrastructure Systems*, 10(1), 1-8.
- Durango-Cohen, P., & Sarutipand, P. (2009). Maintenance optimization for transportation systems with demand responsiveness. *Transportation Research Part C: Emerging Technologies*, 17(4), 337-348.
- Eisenbach, M., Stricker, R., Seichter, D., Debes, K., Sesselmann, M., Ebersbach, D., . . . Gross, H.-M. (2017). How to get pavement distress detection ready for deep learning? A systematic approach. *2017 international joint conference on neural networks (IJCNN)* (pp. 2039-2047). IEEE.
- Eriksson, J., Girod, L., Hull, B., & Newt, R. (2008). The pothole patrol: using a mobile sensor network for road surface monitoring. *Proceedings of the 6th international conference on Mobile systems, applications, (pp. 29-39)*.
- Ester, M., Kriegel, H.-P., Sander, J., & Xu, X. (1996). A density-based algorithm for discovering clusters in large spatial databases with noise. *KDD-96*, 34, pp. 226-231.
- Faddoul, R., Raphael, W., Soubra, A.-H., & Chateaufneuf, A. (2013). Incorporating Bayesian Networks in Markov Decision Processes. *Journal of Infrastructure Systems*, 19(4), 415-424.

- Farrar, C. R., & Worden, K. (2012). *Structural health monitoring: A machine learning perspective*. John Wiley & Sons.
- Fauriat, W., & Zio, E. (2018). An importance measure to assess the value of a component inspection policy. *3rd International Conference on System Reliability and Safety (ICSRS), IEEE*, 368-375.
- FDOT. (2020). *Cost Per Mile Models for Long Range Estimating*. Florida Department of Transportation.
- FHWA. (1999). *Status of the Nation's Highways, Bridges and Transit: Conditions and Performance, Report to Congress*. Washington D.C.: Federal Highway Administration.
- FHWA. (2016, October 24). *Asset Management Plans and Periodic Evaluations of Facilities Repeatedly Requiring Repair and Reconstruction Due to Emergency Events*. *Federal Register*, 81(205). Retrieved July 15, 2019, from <https://www.federalregister.gov/documents/2016/10/24/2016-25117/asset-management-plans-and-periodic-evaluations-of-facilities-repeatedly-requiring-repair-and>
- FHWA. (2019). *Bridge Replacement Unit Costs*. Federal Highway Administration.
- FHWA. (2021). *Asset Management Peer Exchanges 2020-2021*. Washington, DC: Federal Highway Administration.
- Flintsch, G. W., & McGhee, K. K. (2009). *Quality management of pavement condition data collection*. Washington DC: Transportation Research Board.
- Frangopol, D. M., Lin, K. Y., & Estes, A. C. (1997). Life-cycle cost design of deteriorating structures. *Journal of Structural Engineering*, 123(10), 1390-401.
- Frangopol, D. M., Strauss, A., & Kim, S. (2008). Bridge reliability assessment based on monitoring. *Journal of Bridge Engineering*, 13(3), 258-270.
- George, K., Rajagopal, A., & Lim, L. (1989). Models for predicting pavement deterioration. *Transportation Research Record*, 1215, 1-7.
- Golabi, K., Kulkarni, R. B., & Way, G. B. (1982). A statewide pavement management system. *Interfaces*, 12(6), 5-21.
- Goodspeed, C., & Brown, J. (2017). *Gilford Rapid Bridge Deck Replacement, A project Summary*. University of New Hampshire.
- Government Accountability Office. (2000). *Highway infrastructure: FHWA's Model for Estimating Highway Needs is Generally Reasonable, Despite Limitations*. Washington DC: United States Government Accountability Office. Retrieved from <https://www.gao.gov/assets/rced-00-133.pdf>

- Griffiths, K. R. (2012). An improved method for simulation of vehicle vibration using a journey database and wavelet analysis for the pre-distribution testing of packaging. PhD Dissertation, University of Bath.
- Haas, R., Hudson, W., & Cowe Falls, L. (2015). *Pavement Asset Management*. John Wiley & Sons, Inc.
- Hawaii Department of Transportation. (2019). Statewide Transportation Asset Management Plan.
- Ho, C.-H., Snyder, M., & Zhang, D. (2020). Application of Vehicle-Based Sensing Technology in Monitoring Vibration Response of Pavement Conditions. *Journal of Transportation Engineering, Part B: Pavements*, 146(3). doi:04020053
- Howard, R. A. (1966). Information value theory. *IEEE Transactions on Systems Science and Cybernetics*, 2(1), 22-26.
- Javed, K., Gouriveau, R., & Zerhou, N. (2014). Enabling health monitoring approach based on vibration data for accurate prognostics. *IEEE Transactions on industrial electronics*, 62(1), 647-656.
- Jiang, M., Corotis, R. B., & Ellis, J. H. (2000). Optimal life-cycle costing with partial observability. *Journal of Infrastructure Systems*, 6(2), 56-66.
- Johnson, J., & Boyle, Z. (2017). Implementation of AASHTOWare Bridge Management 5.2. 3 to meet agency policies and objectives for bridge management and address FHWA requirements. *Proceedings of the Eleventh International Bridge and Structures Management Conference* (pp. 188-212). Transportation Research Board.
- Kamranfar, P., Bynum, J., Lattanzi, D., & Shehu, A. (2020). Meta-Learning for Industrial System Monitoring via Multi-objective Optimization. *Proceedings of the 16th on Data Science (ICDATA)*.
- Katicha, S. W., Ercisli, S., Flintsch, G. W., Bryce, J. M., & Diefenderfer, B. K. (2016). *VDOT: Development of Enhanced Pavement Deterioration Curves*. Virginia Department of Transportation.
- Konda, V., & Tsitsiklis, J. (2003). On actor critic algorithms. *SIAM Journal on Control and Optimization*, 42(4), 1143-1166.
- Kurniawati, H., Hsu, D., & Lee, W. S. (2008). SARSOP: Efficient point-based POMDP planning by approximating optimally reachable belief spaces. *In Robotics: Science and systems*.
- Labi, S., & Sinha, K. (2003). Measures of Short-Term Effectiveness of Highway Pavement Maintenance. *Journal of Transportation Engineering*, 129(6), 673-683.
- Lee, J.-K., & Yoon, K.-J. (2018). Temporally consistent road surface profile estimation using stereo vision. *IEEE Transactions on Intelligent Transportation Systems*, 19(5), 1618-1628.

- LeNail, A. (2019). NN-SVG: Publication-Ready Neural Network Architecture Schematics. *Journal of Open Source Software*, 4(33), 747. Retrieved from <https://doi.org/10.21105/joss.00747>
- Li, S., & Pozzi, M. (2019). What makes long-term monitoring convenient? A parametric analysis of value of information in infrastructure maintenance. *Structural Control and Health Monitoring*, 26(5), e2329.
- Li, Y., & Madanat, S. (2002). A steady-state solution for the optimal pavement resurfacing problem. *Transportation Research Part A: Policy and Practice.*, 36(6), 525–535.
- Lindley, D. V. (1971). *Making decisions*. London: Wiley Interscience.
- Łukasik, S., Kowalski, P. A., Charyanowicz, M., & Kulczycki, P. (2016). Clustering using flower pollination algorithm and Calinski-Harabasz index. *2016 IEEE Congress on Evolutionary Computation (CEC)* (pp. 2724-2728). IEEE.
- Luque, J., & Straub, D. (2019). Risk-based optimal inspection strategies for structural systems using dynamic Bayesian networks. *Structural Safety*, 76, 60-80.
- Madanat, S. (1993). Optimal infrastructure management decisions under uncertainty. *Transportation Research Part C: Emerging Technologies*, 1(1), 77-88.
- Madanat, S., & Ben-Akiva, M. (1994). Optimal Inspection and Repair Policies for Infrastructure. *Transportation Science*, 28(1), 55-62.
- Maggiore, M., & Ford, K. M. (2015). *Guide to Cross-Asset Resource Allocation and the Impact on Transportation System Performance*. Washington DC: National Academies of Sciences, Engineering, and Medicine. doi:10.17226/22177
- Manafpour, A., Guler, I., Radlinska, A., Rajabipour, F., & Warn, G. P. (2018). Stochastic analysis and time-based modeling of concrete bridge deck deterioration. *Journal of Bridge Engineering*, 23(9), 04018066.
- Marcelino, P., de Lurdes Antunes, M., & Fortunato, E. (2018). Comprehensive performance indicators for road pavement condition assessment. *Structure and Infrastructure Engineering*, 14(11), 1433-1445.
- MDOT. (2014). *Monitoring Highway Assets with Remote Technology*. Michigan Department of Transportation.
- Medury, A., & Madanat, S. (2013). Incorporating network considerations into pavement management systems: A case for approximate dynamic programming. *Transportation Research Part C: Emerging Technologies*, 134-150.
- Memarzadeh, M., & Pozzi, M. (2016). Value of information in sequential decision making: Component inspection, permanent monitoring and system-level scheduling. *Reliability Engineering & System Safety*, 154, 137-151.

- Minnesota Department of Transportation. (2018). *Draft Transportation Asset Management Plan*. Retrieved July 13, 2019, from http://www.tamtemplate.org/wp-content/uploads/tamps/045_minnesotadot.pdf
- Mnih, V., Badia, A. P., Mirza, M., Graves, A., Lillicrap, T., Harley, T., . . . Kavukcuoglu, K. (2016). Asynchronous methods for deep reinforcement learning. *International conference on machine learning* (pp. 1928-1937). PMLR.
- Mnih, V., Kavukcuoglu, K., Silver, D., Rusu, A., Veness, J., Bellemare, M., . . . Hassabis, D. (2015). Human-level control through deep reinforcement learning. *Nature*, *518*, 529-533.
- National Academies of Sciences, Engineering, and Medicine. (2019). *Case Studies in Cross-Asset, Multi-Objective Resource Allocation*. Washington DC: The National Academies Press. doi:10.17226/25684
- New Hampshire Department of Transportation. (2019). Asset Management Plan for Pavement & Bridge on the National Highway System.
- Neyman, J. (1992). On the two different aspects of the representative method: the method of stratified sampling and the method of purposive selection. In *Breakthroughs in Statistics* (pp. 123-150). New York: Springer.
- Ng, M., Lin, D., & Waller, S. (2009). Optimal long-term infrastructure maintenance planning accounting for traffic dynamics. *Journal of Computer-aided Civil and Infrastructure Engineering*, *24*(7), 459-469.
- North Carolina Department of Transportation. (2019). North Carolina Department of Transportation Transportation Asset Management Plan.
- Oakgrove. (2013). Accelerated Bridge Construction-Four Bridge Deck Replacements in Region 5. Oakgrove Construction, Inc.
- Ouyang, Y. (2007). Pavement resurfacing planning for highway networks: parametric policy iteration approach. *Journal of Infrastructure Systems*, *13*, 65-71.
- Ouyang, Y., & Madanat, S. (2004). Optimal scheduling of rehabilitation activities for multiple pavement facilities: exact and approximate solutions. *Transportation Research Part A: Policy and Practice*, *38*, 347-365.
- Ouyang, Y., & Madanat, S. (2006). An analytical solution for the finite-horizon pavement resurfacing planning problem. *Transportation Research Part B*, *40*, 767-778.
- Papakonstantinou, K. G., & Shinozuka, M. (2014). Planning structural inspection and maintenance policies via dynamic programming and Markov processes. Part I: Theory. *Reliability Engineering & System Safety*, *130*, 202-213.
- Papakonstantinou, K. G., Andriotis, C. P., & Shinozuka, M. (2016). POMDP solutions for monitored structures. IFIP WG-7.5 Conference on Reliability and Optimization of Structural Systems.

- Papakonstantinou, K. G., Andriotis, C. P., & Shinozuka, M. (2018). POMDP and MOMDP solutions for structural life-cycle cost minimization under partial and mixed observability. *Structure and Infrastructure Engineering*, 14(7), 869-882.
- Papakonstantinou, K. G., Andriotis, C. P., Gao, H., & Chatzi, E. N. (2019). Quantifying the value of structural health monitoring for decision making. Seoul, South Korea: Proceedings of the 13th International Conference on Applications of Statistics and Probability in Civil Engineering (ICASP13).
- Pedregosa, F., Varoquaux, G., Gramf, A., Michel, V., Thirion, B., Grisel, O., & Blondel, M. (2011). Scikit-learn: Machine learning in Python. *The Journal of Machine Learning Research*, 12, 2825-2830.
- PennDOT. (2009). *Bridge management system 2: Coding manual*. Pennsylvania Department of Transportation.
- PennDOT. (2015). Publication 242, Appendix H: Interstate Management Program Pavement Treatment Matrices. Harrisburg: PennDOT.
- PennDOT. (2017). *Road Maintenance and Preservation (MaP)*. Pennsylvania Department of Transportation.
- PennDOT. (2019). Publication 242 Pavement Policy Manual, May 2015 Edition, Change No. 5. Pennsylvania Department of Transportation.
- Pennsylvania Department of Transportation. (2018). *Transportation Asset Management Plan 2018*. Retrieved July 13, 2019, from http://www.tamptemplate.org/wp-content/uploads/tamps/049_penndot.pdf
- Petrovic, S. (2006). A comparison between the silhouette index and the davies-bouldin index in labelling ids clusters. *Proceedings of the 11th Nordic Workshop of Secure IT Systems*, (pp. 53-64).
- Pineau, J., Gordon, G., & Thrun, S. (2003). Point-based value iteration: An anytime algorithm for POMDPs. *International Joint Conference on Artificial Intelligence*, 3, pp. 1025-1032.
- Pozzi, M., & Der Kiureghian, A. (2011). Assessing the value of information for long-term structural health monitoring. Conference on Health Monitoring of Structural and Biological Systems.
- Puterman, M. L. (1994). *Markov Decision Process: Discrete Stochastic Dynamic*. New York: Wiley.
- Quinlan, J. R. (1992). Learning with continuous classes. *5th Australian joint conference on artificial intelligence*, 92, pp. 343-348.
- Raiffa, H. (1968). *Decision analysis: introductory lectures on choices under uncertainty*. Addison-Wesley.

- Rendón, E., Abundez, I., & Arizmen, A. (2011). Internal versus external cluster validation indexes. *International Journal of computers and communications*, 5(1), 27-34.
- Rhode Island Department of Transportation. (2019). *Transportation Asset Management Plan*.
- Robert, W. (2018). Modeling of life-cycle alternatives in the National Bridge Investment Analysis System. *Proceedings of the Eleventh International Bridge and Structures Management Conference* (pp. 100-113). Transportation Research Board.
- Roberts, R., Giancontieri, G., Inzerillo, L., & Di Mino, G. (2020). Towards low-cost pavement condition health monitoring and analysis using deep learning. *Applied Sciences*, 10(1), 319.
- Robnik-Šikonja, M., & Kononenko, I. (2003). Theoretical and empirical analysis of ReliefF and RReliefF. *Machine learning*, 53(1), 23-69.
- Rousseeuw, P. J. (1987). Silhouettes: a graphical aid to the interpretation and validation of cluster analysis. *Journal of computational and applied mathematics*, 20, 53-65.
- Russell, J. (2021). *FAQ: How much does it cost to build a mile of road?* <https://www.artba.org/about/faq/>. The American Road & Transportation Builders Association. Retrieved from <https://highways.dot.gov/public-roads/autumn-2018/self-enforcing-roadways>
- Santiago, A., Fraire Huacuja, H., Dorronsoro, B., Pecero, J. E., Santillan, C. G., Barbosa, J. J., & Monterrubio, J. C. (2014). A survey of decomposition methods for multi-objective optimization. In *Recent Advances on Hybrid Approaches for Designing Intelligent Systems* (pp. 453-465). Springer.
- Saydam, D., & Frangopol, D. (2014). Risk-based maintenance optimization of deteriorating bridges. *Journal of Structural Engineering*, 141(4), 04014120.
- Sayer, M. W., Gillespie, T. D., & Paterson, W. D. (1986). *Guidelines for conducting and calibrating road roughness measurements*. World Bank.
- Seraj, F., van der Zwaag, B. J., Dilo, A., Luarasi, T., & Havinga, P. (2015). RoADS: A road pavement monitoring system for anomaly detection using smart phones. In *Big data analytics in the social and ubiquitous context* (pp. 128-146). Cham: Springer.
- Shani, G., Pineau, J., & Kaplow, R. (2013). A survey of point-based POMDP solvers. *Autonomous Agents and Multi-Agent Systems*, 27(1), 1-51.
- Smith, T., & Simmons, R. (2005). Point-based POMDP algorithms: Improved analysis and implementation. In *Proc. of UAI*.
- Smith, T., & Simmons, R. (2006). Focused real-time dynamic programming for MDPs: Squeezing more out of a heuristic. In *AAAI*, 1227-1232.
- Sondik, E. (1971). *The optimal control of partially observable Markov processes*. Stanford, CA: Stanford University, Stanford Electronics Labs.

- South Carolina Department of Transportation. (2019). *Transportation Asset Management Plan*.
- Souza, V. M., Giusti, R., & Batista, A. J. (2018). Asfalt: A low-cost system to evaluate pavement conditions in real-time using smartphones and machine learning. *Pervasive and Mobile Computing, 51*, 121-137.
- Souza, V. M., Souza, V. M., Cherman, E. A., Rossi, R. G., & Souza, R. A. (2017). Towards Automatic Evaluation of Asphalt Irregularity Using Smartphone's Sensors. *International Symposium on Intelligent Data Analysis* (pp. 322-333). Cham: Springer.
- Spaan, M. T., & Vlassis, N. (2005). Perseus: Randomized point-based value iteration for POMDPs. *Journal of Artificial Intelligence Research, 24*, 195-220.
- Straub, D. (2014). Value of information analysis with structural reliability methods. *Structural Safety, 49*, 75-85.
- Straub, D., & Faber, M. H. (2005). Risk based inspection planning for structural systems. *Structural safety, 27*(4), 335-355.
- Straub, D., Chatzi, E., Bismut, E., Courage, W., Döhler, M., Faber, M., . . . Thöns, S. (2017). Value of information: A roadmap to quantifying the benefit of structural health monitoring. Vienna, Austria: 12th International Conference on Structural Safety & Reliability (ICOSSAR).
- Sutton, R., & Barto, A. (2018). *Reinforcement Learning: An Introduction* (2nd ed.). Cambridge: The MIT Press.
- Sutton, R., Maei, H., Precup, D., Bhatnagar, S., Silver, D., Szepesvari, C., & Wiewiora, E. (2009). Fast gradient-descent methods for temporal-difference learning with linear function approximation. *Proceedings of the 26th International Conference on Machine Learning*. Montreal.
- Taleqani, A. R., Bridgelall, R., Hough, J., & Nygard, K. E. (2019). Data Driven Analytics of Road Quality. *CATA*, (pp. 454-463).
- Thöns, S. (2019). Quantifying the value of structural health information for decision-support: guide for scientists. COST Action TU1402 - Quantifying the Value of Structural Health Monitoring.
- Thöns, S., & Faber, M. H. (2011). Assessing the value of structural health monitoring. New York: 11th International Conference on Structural Safety & Reliability (ICOSSAR).
- Thöns, S., Schneider, R., & Faber, M. H. (2015). Quantification of the value of structural health monitoring information for fatigue deteriorating structural systems. Vancouver, Canada: 12th International Conference on Applications of Statistics and Probability in Civil Engineering (ICASP).
- Titus-Glover, L. (2019). Unsupervised extraction of patterns and trends within highway systems condition attributes data. *Advanced Engineering Informatics, 42*. doi:100990

- Tsai, Y.-C., & Chatterjee, A. (2017). Comprehensive, quantitative crack detection algorithm performance evaluation system. *Journal of Computing in Civil Engineering*, 31(5). doi:04017047
- United States Department of Transportation (USDOT). (2021, September 19). *Simplified Highway Capacity Calculation Method - Chapter 3 - Policy*. Retrieved from Federal Highway Administration: www.fhwa.dot.gov/policyinformation/pubs/pl18003/chap03.cfm
- United States Department of Commerce. (1964). *Traffic Assignment Manual for Application with a Large, High Speed Computer*. Bureau of Public Roads, Office of Planning, Urban Planning Division.
- USDOT. (2016). The Value of Travel Time Savings: Revised Departmental Guidance for Conducting Economic Evaluations.
- USDOT. (2017). National Household Travel Survey.
- Virginia Department of Transportation. (2016). VDOT: Supporting Document for the Development and Enhancement of the Pavement Maintenance Decision Matrices Used in the Needs-Based Analysis. Virginia Department of Transportation.
- Virginia Department of Transportation. (2019). Commonwealth of Virginia Transportation Asset Management Plan.
- Walls, J., & Smith, M. R. (1998). *Life-cycle cost analysis in pavement design-interim technical bulletin*. Federal Highway Administration, USDOT.
- Wang, K. C. (2000). Designs and implementations of automated systems for pavement surface distress survey. *Journal of Infrastructure Systems*, 6(1), 24-32.
- Wang, T., Harvey, J., Lea, J., & Kim, C. (2014). Impact of pavement roughness on vehicle free-flow speed. *Journal of Transportation Engineering*, 140. doi:04014039
- Wang, W., Wang, S., Xiao, D., Qiu, S., & Zhang, J. (2018). An Unsupervised Cluster Method for Pavement Grouping Based on Multidimensional Performance Data. *Journal of Transportation Engineering, Part B: Pavements*, 144(2). doi:04018005
- Wang, Z., & Pyle, T. (2019). Implementing a pavement management system: The Caltrans experience. *International Journal of Transportation Science and Technology*, 8, 251-262.
- Washington State Department of Transportation. (2018). *Transportation Asset Management Plan*. Retrieved July 13, 2019, from http://www.tamptemplate.org/wp-content/uploads/tamps/054_washingtonstatedot.pdf
- Wei, C., & Tighe, S. (2004). Development of preventive maintenance decision trees based on cost-effectiveness analysis: an Ontario case study. *Transportation research record*, 1866, 9-14.

- Wei, L., Fwa, T. F., & Zhe, Z. (2005). Wavelet analysis and interpretation of road roughness. *Journal of transportation engineering*, 131(2), 120-130.
- Wells, D. T. (1995). Technical Assistance Report: Maintenance, Repair, and Rehabilitation Unit Costs for Pontis. Virginia Transportation Research Council.
- Werbos, P. (1988). Generalization of backpropagation with application to a recurrent gas market model. *Neural Networks*, 1(4), 339-356.
- West Virginia Division of Highways. (2019). *Transportation Asset Management Plan*.
- Worden, K., Dervilis, N., & Farrar, C. (2019). Applying the concept of complexity to structural health monitoring. *Structural Health Monitoring* 2019.
- Wu, C., Wang, Z., Hu, S., Lepine, J., Na, X., Ainalis, D., & Stettler, M. (2020). An automated machine-learning approach for road pothole detection using smartphone sensor data. *Sensors*, 20(19), 5564.
- Xiong, H., Wu, J., & Chen, J. (2008). K-means clustering versus validation measures: a data-distribution perspective. *IEEE Transactions on Systems, Man, and Cybernetics, Part B (Cybernetics)*, 39(2), 318-331.
- Yi, C.-W., Chuang, Y.-T., & Nian, C.-S. (2015). Toward crowdsourcing-based road pavement monitoring by mobile sensing technologies. *IEEE Transactions on Intelligent Transportation Systems*, 16(4), 1905-1917.
- Zaman, A. B., Kamranfar, P., Domeniconi, C., & Shehu, A. (2019). Decoy ensemble reduction in template-free protein structure prediction. *Proceedings of the 10th ACM International Conference on Bioinformatics, Computational Biology and Health Informatics*, (pp. 562-567).
- Zhou, W., Miller-Hooks, E., Papakonstantinou, K., Stoffels, S., & McNeil, S. (2021). A Bilevel, Stochastic Method for Multi-asset Roadway Improvement Scheduling Considering Traffic Impacts. *Working Paper*.
- Zonta, D., Glisic, B., & Adriaenssens, S. (2014). Value of information: impact of monitoring on decision-making. *Structural Control and Health Monitoring*, 21(7), 1043-1056.

Appendix A: List of Acronyms

AC – Asphalt concrete
ADT – Annual Daily Traffic
AADTT – Annual Average Daily Truck Traffic
AASHTO – American Association of State Highway and Transportation Officials
ADOT – Arizona Department of Transportation
ARTBA – The American Road Transportation Builders Association
ASCE – American Society of Civil Engineers
BPR – Bureau of Public Roads
BrM - AASHTOWare™ Bridge Management \CCI – Critical Condition Index
CCI – Critical Condition Index
CE – Cluster entropy
CH – Calinski-Harabasz Index
CI – Condition Index
CM – Corrective maintenance
CWT – Continuous Wavelet Transform
DB – Davies-Bouldin Index
DCMAC - Deep Centralized Multi-Agent Actor Critic
DN – Do Nothing
DOT – Department of Transportation
DRIMS – Dynamic Response Intelligent Management System
DRL - Deep Reinforcement Learning
DT – Decision Tree
DWT – Discrete Wavelet Transform
EMD - Earth Mover Distance
FHWA – Federal Highway Administration
FRTDP - Focused Real-Time Dynamic Programming
HERS – Highway Economic Requirements Systems
IRI – International Roughness Index
LCCA – Life cycle cost assessment
LFS – Linear spectral frequencies
LLCC – Lowest life cycle cost
LRDI – Load Related Distress Index
MDP – Markov Decision Process
ML – Machine Learning
MODAT – Multi-Objective Decision Analysis Tool
NB – Naïve Bayes
NBIAS – National Bridge Investment Analysis System
NHS – National Highway System
NN – Neural Network
O-D – origin-destination

OPC – Overall pavement condition
PCI - Pavement Condition Index
PennDOT- Pennsylvania Department of Transportation
PM – Preventive or routine maintenance
PMS – Pavement Management Systems
POMDP - Partially Observable Markov Decision Process
RC- Rehabilitation/Reconstruction
RIF – Road impact factor
RF – Random Forest
RL – Reinforcement Learning
RM – Restorative maintenance
RMS – Root mean square
SARSA - State Action Reward State Action
SARSA_LFA - SARSA with linear function approximation
SARSOP - Successive Approximation of the Reachable Space under Optimal Policies
SC – Silhouette Coefficient
SHM – Structural Health Monitoring
SVM - Support Vector Machine
TAMP – Transportation Asset Management Plan
TD – Temporal Difference
UE – User Equilibrium
VDOT – Virginia Department of Transportation
VoI – Value of Information
VoSHM – Value of Structural Health Monitoring

Appendix B: Tamp Thresholds and Targets for Bridges and Pavements

To analyze how states classify and categorize thresholds and targets, a comparison table was constructed. Information was gathered from each state’s Transportation Asset Management Plan (TAMP)¹. This information included current conditions of National Highway System (NHS) pavements and bridges in all U.S. states, including Puerto Rico and the District of Columbia. The objective was to determine the percent good, percent fair, and percent poor of NHS interstates, non-interstates, and bridges. By using these percentages, states were able to determine the performance repair targets of interstates, non-interstates, and bridges, which consisted of maintenance, preservation, rehabilitation, or reconstruction.

The National Highway System “comprises a network of roadways that are critically important to national security, defense, and the economy” (Delaware Department of Transportation, 2019). The NHS is comprised of major and minor highways throughout a state, as well as arterials and major strategic and intermodal connectors. In addition to the NHS system, there are also two acts: the Moving Ahead for Progress in the 21st Century Act (MAP-21) and Fixing America’s Surface Transportation (FAST) Act that “requires each state department of transportation to develop and implement a risk-based asset management plan in accordance with the National Highway Performance Program” (112th Congress, 2012; 114th Congress, 2015). In summary, each date is required to meet certain pavement and bridge thresholds and targets as mandated by the Federal Highway Administration (FHWA). These thresholds, also known as performance measures, are typically found in each state’s Transportation Asset Management Plan and also outline the necessary precautions to take in order to get pavements and/or bridges to said target.

The Transportation Asset Management Plan (TAMP) Thresholds and Targets table can be found in Table B-1. The data presented in this table were collected directly from each state’s TAMP. Starting with pavement thresholds, each state measures the length of NHS pavements in the number of lane miles (or some states use the number of centerline miles). By definition, a lane mile is the total length and count of a given pavement section (highway, arterial or connector, as mentioned above). To calculate lane miles, you multiple the centerline mileage of a road by the number of lanes it has (lane mile). This calculation becomes especially important for those states that do not measure pavements by lane mile, instead by centerline mile. According to the FHWA Pavement Condition Criteria, which can be found in 23 CFR Part 490.313(b) and 409(b), the following conditions shown in Table B-2 must be met to determine if a pavement or bridge is in good, fair, or poor pavement condition. Similar criteria are provided for bridges as shown in Table B-3.

¹ FHWA’s repository for TAMPs (http://www.tamptemplate.org/existing-tamp/?fwp_sections=11-risk) and the AASHTO TAMP Library (<https://www.tamptemplate.org/existing-tamp/>).

Table B-1. Pavement targets and thresholds from TAMPs.

State	Total # of Lane-Miles	Baseline Year	NHS Interstate Condition							NHS Non-Interstate Condition						
			Interstate Lane Miles	% Good		% Fair		% Poor		Non-Interstate Lane Miles	% Good		% Fair		% Poor	
				Current %	2021 Target	Current %	2021 Target	Current %	2021 Target		Current %	2021 Target	Current %	2021 Target	Current %	2021 Target
Alabama (AL)	11,491	2016	3,221.55	76.98	50.0	-	-	8.33	5.0	8269.75	86.22	40.00	-	-	22.66	5.0
Alaska (AK)	2,085	2018	1159.7	32.8	10.0	65.8	-	1.4	10.0	924.943	22.6	15.0	69.3	-	8.1	15.0
Arizona (AZ)	13,899	2018	5,405.00	53.1	48.00	46.0	-	0.90	2.00	8,494	34.6	31	61.9	-	3.60	6
Arkansas (AR)	-	-	-	-	-	-	-	-	-	-	-	-	-	-	-	-
California (CA)	36,649	2017	14,159.00	44.90	60.0	52.10	39.0	3.10	1.0	22,490.00	43.50	34.2	54.00	60.90	2.50	5.0
Colorado (CO)	-	2018	-	44.00	46.50	-	-	2.50	1.0	-	42.0	50.5	-	-	3.00	1.50
Connecticut (CT)	4,945	2017	1,738	75.10	64.40	24.40	-	0.50	2.60	3,207	37.1	31.90	59.50	-	3.40	7.60
Delaware (DE)	1,695	2019	-	54.7	50.0	-	-	0.8	2.0	-	59.7	55.0	-	-	1.2	2.0
District of Columbia (DC)	-	2018	-	78.80	-	17.40	-	3.80	-	-	68.20	54.00	22.20	-	9.60	14.00
Florida (FL)	36,928	2018	8,495	54.40	60.00	45.00	-	0.60	5.00	28,433.00	39.70	40.00	60.00	-	0.30	5.00
Georgia (GA)	-	2018	-	63.00	50.00	37.00	-	0.00	5.00	-	42.00	40.00	57.00	-	1.00	5.00
Hawaii (HI)	-	2017	-	15.00	7.00	83.00	-	2.00	4.00	-	18.00	15.00	76.00	-	6.00	4.00
Idaho (ID)	-	2018	-	65.60	50.00	-	-	0.20	4.00	-	50.80	50.00	-	-	0.30	8.00
Illinois (IL)	-	2018	-	85.00	65.00	-	-	15.00	4.90	-	37.60	27.00	-	-	19.40	6.00

State	Total # of Lane-Miles	Baseline Year	NHS Interstate Condition							NHS Non-Interstate Condition						
			Interstate Lane Miles	% Good		% Fair		% Poor		Non-Interstate Lane Miles	% Good		% Fair		% Poor	
				Current %	2021 Target	Current %	2021 Target	Current %	2021 Target		Current %	2021 Target	Current %	2021 Target	Current %	2021 Target
Indiana (IN)	12,441	2018	5,079.00	48.00	-	51.00	-	1.00	-	7,362.00	40.00	-	58.00	-	2.00	-
Iowa (IA)	16,805	2018	3,436.00	57.80	49.40	41.70	-	0.50	2.70	13,369.00	37.50	46.90	58.80	-	3.70	14.50
Kansas (KS)	-	2017	-	67.00	65.00	33.00	-	1.00	0.50	-	63.00	55.00	36.00	-	1.00	1.50
Kentucky (KY)	-	2018	-	35.00	37.00	32.00	23.00	33.00	40.00	-	-	-	-	-	-	-
Louisiana (LA)	11,070	2018	4,005.00	16.50	10.00	-	-	1.10	4.00	7,065.00	18.40	14.00	-	-	10.20	12.00
Maine (ME)	3,109	2017	1,017.00	36.30	40.00	62.50	-	1.20	1.50	2,092.00	31.20	34.00	63.30	-	5.50	5.00
Maryland (MD)	-	2019	-	60.40	60.2	39.10	-	0.50	1.1	-	33.70	34.20	59.30	-	7.00	7.40
Massachusetts (MA)	-	2019	-	70.10	70.00	29.70	-	0.30	4.00	-	32.90	30.00	35.70	-	31.40	30.00
Michigan (MI)	22,427	2017	6,078.00	57.40	47.80	37.70	-	4.90	10.00	16,349.00	49.20	43.70	31.90	-	18.90	24.60
Minnesota (MN)	15,795	2017	4,036.00	60.10	55.00	-	-	0.90	2.00	11,759.00	53.40	50.00	-	-	1.30	4.00
Mississippi (MS)	-	2017	-	67.00	55.00	-	-	0.50	5.00	-	35.00	25.00	-	-	4.00	10.00
Missouri (MO)	-	2017	-	78.00	77.50	-	-	0.00	0.00	-	61.00	61.10	-	-	0.00	1.00
Montana (MT)	11,205	2017	4,700.00	56.70	54.00	41.60	-	0.00	3.00	6,505.00	50.90	44.00	48.30	-	0.40	6.00
Nebraska (NE)	-	2016	-	-	50.00	-	-	-	5.00	-	-	40.00	-	-	-	10.00
Nevada (NV)	-	2017	-	78.00	75.00	-	-	1.00	5.00	-	93.00	40.00	-	-	0.00	5.00

State	Total # of Lane-Miles	Baseline Year	NHS Interstate Condition							NHS Non-Interstate Condition						
			Interstate Lane Miles	% Good		% Fair		% Poor		Non-Interstate Lane Miles	% Good		% Fair		% Poor	
				Current %	2021 Target	Current %	2021 Target	Current %	2021 Target		Current %	2021 Target	Current %	2021 Target	Current %	2021 Target
New Hampshire (NH)	1,483	2017	586.00	97.00	95.00	-	-	0.20	0.80	897.00	73.10	65.00	-	-	9.10	12.00
New Jersey (NJ)	12,233	2017	9,251.00	55.02	50.00	-	-	1.36	2.50	2,982.00	30.37	25.00	-	-	1.18	2.50
New Mexico (NM)	-	2016	-	58.50	60.00	-	-	0.80	8.30	-	34.10	33.80	-	-	5.50	17.00
New York (NY)	26,756	2016	8,054.00	42.40	47.30	54.60	48.70	3.00	4.00	18,702.00	19.10	14.70	72.30	71.00	8.60	14.30
North Carolina (NC)	-	2018	-	70.12	37.00	31.86	-	0.26	2.20	-	35.83	21.00	63.57	-	2.76	4.70
North Dakota (ND)	-	2017	-	80.20	75.60	-	-	0.10	3.00	-	78.50	58.30	-	-	3.40	3.00
Ohio (OH)	-	2018	-	60.10	50.00	-	-	0.10	1.00	-	47.10	35.00	-	-	1.10	3.00
Oklahoma (OK)	12,010	2018	3,956.00	64.40	50.00	34.60	-	1.00	3.00	8,054.00	43.20	45.00	54.10	-	2.70	7.00
Oregon (OR)	-	2018	-	57.00	35.00	42.70	-	0.30	0.50	-	37.00	50.00	60.60	-	2.40	10.00
Pennsylvania (PA)	-	2017	-	67.2	60.0	-	-	0.4	2.0	-	36.8	33.0	-	-	2.3	5.0
Puerto Rico (PR)	2,613	2017	1,243.01	10.80	5.00	72.50	-	13.2	14.0	1,370.02	2.20	2.00	67.50	-	9.00	20.0
Rhode Island (RI)	1,826	2018	378.15	55.05	55.00	44.95	41.00	0.00	4.00	1,447.85	18.01	10.00	62.08	70.00	19.91	20.00
South Carolina (SC)	13,200	2016	3,846	65.00	92.00	-	-	11.00	3.00	9,354	28.00	72.00	-	-	45.00	16.00
South Dakota	-	2018	-	73.20	80.50	-	-	0.00	0.00	-	53.20	74.90	-	-	0.80	0.80

State	Total # of Lane-Miles	Baseline Year	NHS Interstate Condition							NHS Non-Interstate Condition						
			Interstate Lane Miles	% Good		% Fair		% Poor		Non-Interstate Lane Miles	% Good		% Fair		% Poor	
				Current %	2021 Target	Current %	2021 Target	Current %	2021 Target		Current %	2021 Target	Current %	2021 Target	Current %	2021 Target
(SD)																
Tennessee (TN)	-	2018	-	70.00	60.00	-	-	0.00	1.00	-	40.00	40.00	-	-	3.20	4.00
Texas (TX)	-	2018	-	67.23	66.40	32.67	-	0.10	0.30	-	42.57	52.30	31.81	-	35.49	14.30
Utah (UT)	-	2018	-	65.00	60.00	35.00	-	0.00	5.00	-	57.00	35.00	37.00	-	6.00	5.00
Vermont (VT)	1,141	2019	699.00	53.70	35.00	45.80	-	0.50	4.90	442.00	44.40	30.00	46.30	-	9.30	9.90
Virginia (VA)	18,755	2018	5,503	57.80	45.00	41.80	-	0.40	3.00	13,252	33.50	25.00	65.60	-	0.90	5.00
Washington (WA)	14,319	2018	3,812	34.16	30.00	63.98	-	1.87	4.00	10,507	23.74	18.00	74.08	-	2.17	5.00
West Virginia (WV)	3,451	2018	1,103	82.57	75.00	17.27	-	0.16	4.00	2,348	60.70	45.00	39.11	-	0.20	5.00
Wisconsin (WI)	16,613	2018	3,931.75	59.10	45.00	39.20	-	1.70	5.00	12,681.61	36.20	20.00	57.90	-	5.90	12.00
Wyoming (WY)	-	2018	-	85.00	-	12.00	-	3.00	-	-	68.00	-	22.00	-	10.00	-

Table B-2. Bridge targets and thresholds from TAMPs

State	Baseline Year	Total Deck Area	NHS Bridge Condition								
			% Good			% Fair			% Poor		
			Current %	2021 Target	Deck Area	Current %	2021 Target	Deck Area	Current %	2021 Target	Deck Area
Alabama (AL)	2016	60,662,258	41.90	27.0	17,202,404	56.7	-	42,268,110	1.4	3.0	1,191,744
Alaska (AK)	2018	-	39.80	40.0	-	54.2	-	-	6.4	10.0	-
Arizona (AZ)	2018	34,467,021.00	47.80	52	34,467,021.00	51.25	-	-	0.95	4	-
Arkansas (AR)	-	-	-	-	-	-	-	-	-	-	-
California (CA)	2017	234,285,883	66.5	83.5	234,285,883	28.7	15.0	-	4.8	1.5	-
Colorado (CO)	2018	29,940,530	47.0	44.5	14,165,330	49.0	-	14,632,998	4.0	4.0	1,142,202
Connecticut (CT)	2017	32,200,666	15.2	14.0	3,977,856	70.8	-	18,558,709	14.0	8.0	9,664,101
Delaware (DE)	2019	5,939,155	17.4	16.7	1,389,613	77.2	-	4,315,344	5.4	3.0	234,198
District of Columbia (DC)	2018	4,882,712	15.0	25.0	4,882,712	80.2	-	-	4.8	4.0	-
Florida (FL)	2018	-	66.2	50.0	-	-	-	-	1.2	10.0	-
Georgia (GA)	2019	-	52.0	60.0	-	47.0	39.0	-	1.0	10.0	-
Hawaii (HI)	2017	11,614,198	23.0	20.0	11,614,198	75.0	-	-	2.0	2.0	-
Idaho (ID)	2018	8,816,021	18.7	19.0	8,816,021	-	-	-	3.2	3.0	-
Illinois (IL)	2018	73,598,000	29.0	27.0	73,598,000	-	-	-	11.6	14.0	-
Indiana (IN)	2018	32,182,300	98.6	48.3	32,182,300	1.4	-	-	0.0	2.6	-
Iowa (IA)	2017	34,277,439	48.9	44.6	34,277,439	48.4	-	-	2.0	3.2	-
Kansas (KS)	2017	31,801,554	75.0	70.0	31,801,554	24.0	-	-	1.0	3.0	-
Kentucky (KY)	2018	15,477,160	35.0	59.0	3,901,675	60.0	39.0	10,501,301	5.0	2.0	1,074,184

State	Baseline Year	Total Deck Area	NHS Bridge Condition								
			% Good			% Fair			% Poor		
			Current %	2021 Target	Deck Area	Current %	2021 Target	Deck Area	Current %	2021 Target	Deck Area
Louisiana (LA)	2018	79,472,254	44.8	30.0	79,472,254	-	-	-	6.7	9.9	-
Maine (ME)	2017	5,984,451	30.0	40.0	5,984,451	66.3	53.0	-	3.8	7.0	-
Maryland (MD)	2018	-	27.4	28.4	-	70.0	-	-	2.6	2.4	-
Massachusetts (MA)	2019	29,659,839	16.1	15.5	29,659,839	-	-	-	12.6	12.5	-
Michigan (MI)	2017	36,980,431	32.7	26.0	36,980,431	57.5	-	-	9.8	7.0	-
Minnesota (MN)	2017	31,444,986	48.0	50.0	31,444,986	-	-	-	1.9	4.0	-
Mississippi (MS)	2017	70,670,552	62.0	60.0	70,670,552	-	-	-	2.0	5.0	-
Missouri (MO)	2017	55,027,309	36.0	30.9	19,794,713	-	-	31,260,698	7.1	7.1	3,971,898
Montana (MT)	2017	11,367,900	17.4	12.0	11,367,900	75.3	-	-	7.3	9.0	-
Nebraska (NE)	2016	-	61.2	55.0	-	35.5	-	-	3.3	10.0	-
Nevada (NV)	2017	11,805,470	41.4	40.9	11,805,470	58.0	54.5	-	0.6	4.6	-
New Hampshire (NH)	2017	7,282,238	57.0	57.0	7,282,238	-	-	-	7.0	7.0	-
New Jersey (NJ)	2017	61,396,535	20.8	18.6	61,396,535	73.3	-	-	6.0	6.5	-
New Mexico (NM)	2017	13,968	37.0	26.3	13,968	59.9	-	-	3.1	5.1	-
New York (NY)	2016	96,732	20.1	24.0	96,732	68.0	64.3	-	11.9	11.7	-

State	Baseline Year	Total Deck Area	NHS Bridge Condition								
			% Good			% Fair			% Poor		
			Current %	2021 Target	Deck Area	Current %	2021 Target	Deck Area	Current %	2021 Target	Deck Area
North Carolina (NC)	2018	48,739,495	38.1	30.0	48,739,495	55.2	-	-	6.7	9.0	-
North Dakota (ND)	2017	-	65.3	60.0	-	30.9	-	-	3.8	4.0	-
Ohio (OH)	2018	87,682,012	64.9	50.0	87,682,012	-	-	-	2.7	5.0	-
Oklahoma (OK)	2018	36,370	47.2	60.0	36,370	49.6	-	-	3.2	7.0	-
Oregon (OR)	2018	30,200,000	12.6	10.0	30,200,000	85.6	-	-	1.8	3.0	-
Pennsylvania (PA)	2017	88,856,979	25.6	26.0	88,856,979	-	-	-	5.5	6.0	-
Puerto Rico (PR)	2017	1,584,328	18.5	10.0	292,632	-	40.0	1,155,332	8.6	10.0	136,364
Rhode Island (RI)	2018	1,778,176	13.1	16.0	1,778,176	63.0	63.0	-	24.0	21.0	-
South Carolina (SC)	2018	39,508,348	48.0	66.0	39,508,348	-	-	-	6.0	0.0	-
South Dakota (SD)	2019	6,992,061	27.6	22.0	6,992,061	-	-	-	2.8	5.0	-
Tennessee (TN)	2018	25,586,902	39.5	36.0	25,586,902	-	-	-	39.5	36.0	-
Texas (TX)	2018	345,900,000	50.63	50.5	345,900,000	-	-	-	0.88	0.8	-
Utah (UT)	2018	14,451,169	53.0	40.0	14,451,169	-	-	-	46.0	10.0	-
Vermont (VT)	2019	-	-	35.0	-	-	-	-	2.0	6.0	-
Virginia (VA)	2018	69,243,663	33.6	33.0	69,243,663	62.9	-	-	3.5	3.0	-

State	Baseline Year	Total Deck Area	NHS Bridge Condition								
			% Good			% Fair			% Poor		
			Current %	2021 Target	Deck Area	Current %	2021 Target	Deck Area	Current %	2021 Target	Deck Area
Washington (WA)	2018	53,000,000	38.4	30.0	53,000,000	73.30	-	-	7.5	10.0	-
West Virginia (WV)	2019	24,504,470	13.1	15.3	24,504,470	71.6	-	-	15.3	10.0	-
Wisconsin (WI)	2018	38,900,000	55.6	50.0	38,900,000	42.7	-	-	1.7	3.0	-
Wyoming (WY)	2018	-	22.1	-	8,198,622	69.9	-	-	8.1	-	-

Table B-3. FHWA Pavement condition rating system (Source: (Pennsylvania Department of Transportation, 2018))

Pavement Condition Measure	Rating Good	Rating Fair	Rating Poor
IRI (inches/mile)	<95	95-170	>170
Cracking	<5	CRCP: 5-10 Jointed: 5-15 Asphalt: 5-20	CRCP: >10 Jointed: >15 Asphalt: >20
Rutting Inches	<0.20	0.20-0.40	>0.4
Faulting (inches)	<0.10	0.10-0.15	>0.15

Table B-4. FHWA Bridge condition rating system (Source: (Pennsylvania Department of Transportation, 2018))

Bridge Component	Rating Good	Rating Fair	Rating Poor
Deck	≥ 7	5 or 6	≤ 4
Superstructure	≥ 7	5 or 6	≤ 4
Substructure	≥ 7	5 or 6	≤ 4
Culvert	≥ 7	5 or 6	≤ 4

A pavement section receives an overall condition rating of Good only if all three condition ratings (IRI, cracking, and rutting or faulting) are in good condition. The pavement system receives an overall condition rating of Poor if two or more of the three condition ratings are in Poor condition. For all other combinations, the pavement system receives an overall condition rating of Fair.

For the Bridge Condition Rating System, a bridge receives an overall condition rating of Good if the lowest rating of the National Bridge Inventory (NBI) items, consisting of deck, superstructure, and substructure, is a 7, 8, or 9. The bridge system receives an overall condition of Fair if the lowest rating of any NBI item is a 5 or 6. The bridge system receives an overall condition rating of Poor, the lowest rating, if any NBI item is a 1, 2, 3, or 4 (Delaware Department of Transportation, 2019).

For instance, the State of Delaware is currently comprised of 1,695 total lane miles for NHS interstate and non-interstate pavements for the year 2019. There is a dash on the table for “Interstate Lane Miles,” as Delaware’s TAMP only identified total NHS lane miles (that is, the DE TAMP did not separate the lane miles for interstate and non-interstate.) For NHS interstate condition, Delaware has 54.7% of interstate pavements in good condition with a 2021 target of greater than or equal to 50% in good condition and 0.8% of pavements in poor condition with a target of less than or equal to 2.0%. For non-NHS pavements, Delaware has 59.7% of non-interstate pavements in good condition with a 2021 target of greater than or equal to 55% and a poor condition of 1.2% with a 2021 target also less than or equal to 2.0%. For bridges, Delaware has measured approximately 6 million square feet of deck area in the baseline year of 2019. There are 17.4% of bridges in good condition with a 16.7% target, 77.2% in fair condition and 5.4% currently in poor condition, with a 2021 target of less than or equal to 3.0% (Delaware Department of Transportation, 2019).

Appendix C: Decision Trees

Taking a further look at the six Mid-Atlantic states, information can be gathered from decision trees to determine the strategies use to achieve the performance repair targets for interstates, non-interstates, and bridges. These strategies include maintenance, preservation, rehabilitation, or reconstruction action. For the six Mid-Atlantic states, Delaware, Maryland, Pennsylvania, Washington D.C., Virginia, and West Virginia, decisions trees are available for Delaware, Maryland, Pennsylvania, and Virginia. For each of these states, an explanation of each state's decision tree is presented. Where feasible, visuals and tables are included. In all cases, links or references to source documents are included.

DELAWARE

Illustrative decision trees are provided for flexible pavements. The trees are based on structural distress, non-structural distress, and other distress. Indices are determined by inspection.

Source:

https://www.penndot.gov/ProjectAndPrograms/Construction/QAW/2018_QAW_Presentations/Maint%20and%20Assett%20Mngt/Current%20Pavement%20Management%20Initiatives%20of%20Delaware%20DOT.pdf

Structural Distress

The structural distress index is a function of the fatigue index and patches/potholes for flexible and composite pavements; and the fatigue index, patches/potholes, and edge index for surface-treated pavements. Flexible pavement structural index decision trees are differentiated for four roadway classes: interstate/freeway/principal arterial, minor arterial/major collector/minor collector, local, and suburban. Treatments are assigned on the basis of the class and structural index. The structural distress treatments include do nothing, reconstruction, structural overlay, functional overlay, and asphalt concrete (AC) patching. The decision trees are shown in Figure C-1.

Non-Structural Distress

The flexible pavement non-structural index decision tree is also broken into four roadway classes: interstate/freeway/principal arterial, minor arterial/major collector/minor collector, local, and suburban. The non-structural index is based on the transverse index, block index, NWP long index, and raveling. Based on the class and the non-structural index, a treatment is assigned. The non-structural distress treatments include doing nothing, structural overlay, functional overlay, microsurfacing, and crack seal. The decision trees are shown in Figure C-2.

Other Distress

Decision trees for flexible pavement are also based on IRI and rutting. The IRI decision tree is used for both flexible and composite pavements, and treatments are either do nothing or mill and overlay. The decision tree is shown in Figure C-3. For rutting treatments including do nothing, AC patching, functional overlay, and structural overlay, the rutting decision tree is shown in Figure C-4.

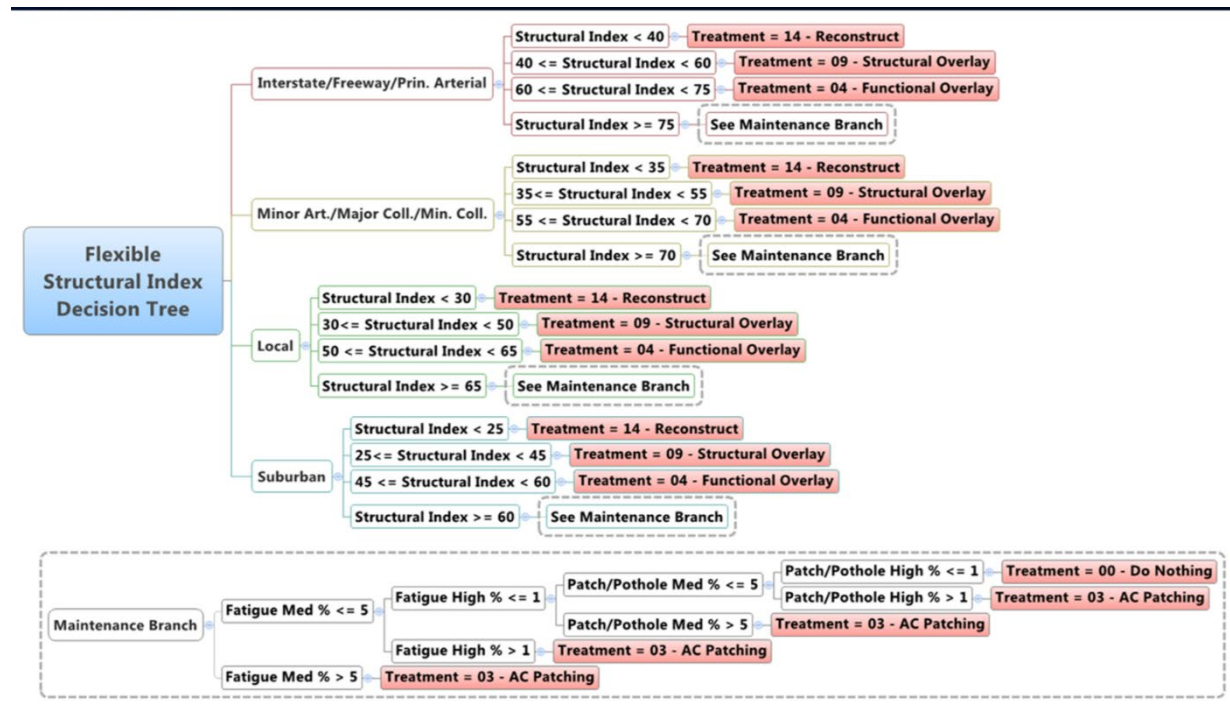


Figure C-1. Delaware flexible pavement decision tree for structural distress.

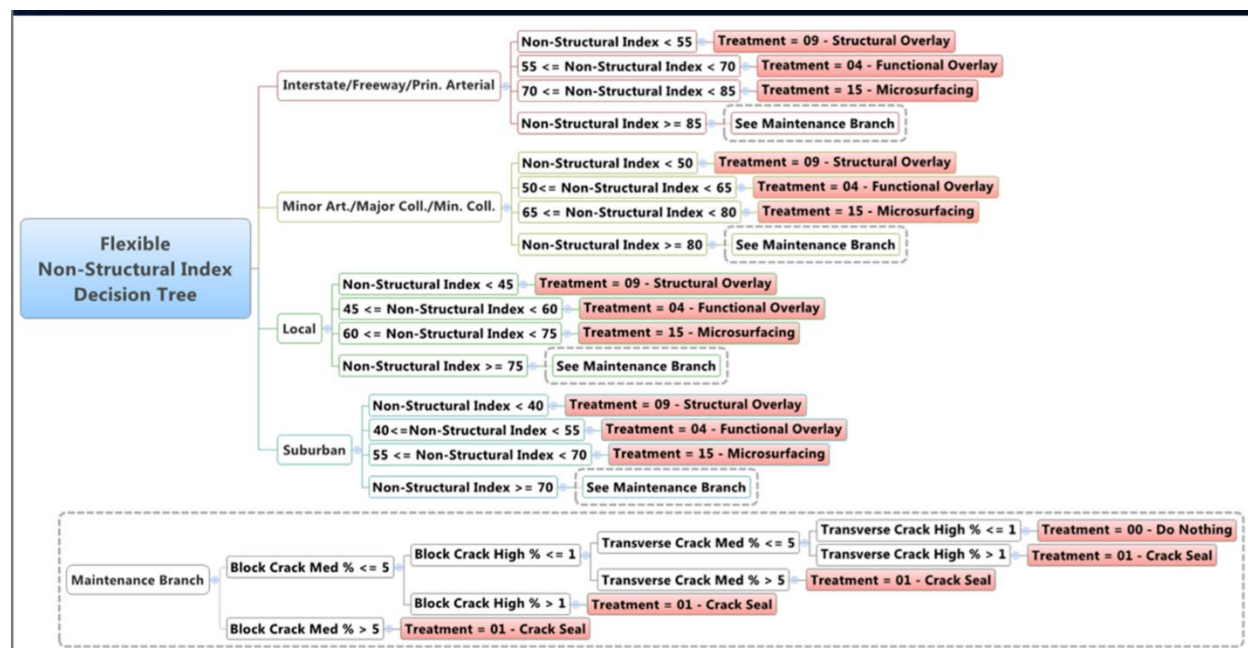


Figure C-2. Delaware flexible pavement decision tree for non-structural distress.

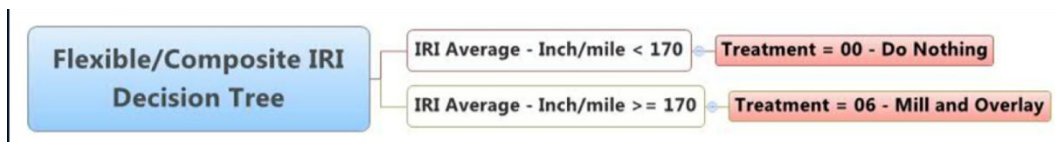


Figure C-3. Delaware flexible and composite pavement decision tree for IRI.

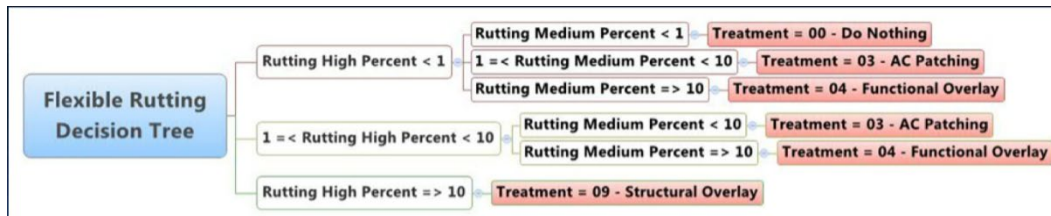


Figure C-4. Delaware flexible pavement decision tree for rutting.

MARYLAND

The Maryland State Highway Authority has comprehensive decision trees for flexible, composite, and rigid pavements. The decision trees are clearly defined and give a variety of options based on the criteria defined in the decision trees.

Source: <https://www.pavementpreservation.org/wp-content/uploads/2011/06/MDSHA-Pavement-Preservation-Guide-March-2011.pdf>

Flexible and Composite Pavement

For flexible and composite pavements, data on IRI, Condition Index (CI), and Friction and Rutting data are maintained in the pavement management system. The initial decision tree is based on the Annual Daily Traffic (ADT) of a particular pavement section. The ADT is split into three categories: 1-4,000 vehicles/day, 4,001-25,000 vehicles/day, and greater than 25,000 vehicles/day. The decision tree then splits each ADT category into three IRI sections: 1-100 inches/mile, 101-170 inches/mile, and greater than 170 inches/mile. Depending on the IRI value, the reader is referred to different decision trees. The decision trees differentiate among:

- CI values of 0-50, 51-75, and 76-100;
- Friction >40 and ≤ 40 ;
- Cracking that is load-related and non-load-related; and
- Low, medium, and high rutting.

A variety of treatments in different classes (for example, overlay, patching or grinding, and grooving) are identified.

Rigid Pavement

For rigid pavement, data on percent patching and the specific types of structural distresses are used. The decision tree for rigid pavements is based on percent patching. If the percent patching is less than 25, then the reader is guided to another table. If the percent patching is greater than or equal to 25, then major (heavy) rehabilitation/reconstruction is the treatment measure.

PENNSYLVANIA

The Pennsylvania Department of Transportation does not have a clear, concise decision tree for their pavements and bridges. Instead, in the 2015 Edition of Publication 242, Appendix H discusses the ‘Interstate Management Program Pavement Treatment Matrices’ (PennDOT, 2015). Unfortunately, these treatment matrices are only for interstates. However, these treatment matrices play the same role as a decision tree. The treatment matrices define the treatment based on pavement distress and their severity. To use the matrix, a user identifies the appropriate treatment matrix based on the pavement type and distress, selects the extent (length, area, or number of slabs/joints) and severity, and the matrix identifies the treatment. Treatment strategies are identified in Table C-1 for bituminous pavements, jointed concrete pavement, and continuously reinforced concrete pavements.

Table C-5. PennDOT treatment strategies.

#	Bituminous Pavement	Jointed Concrete Pavement	Continuously Reinforced Concrete Pavement
0	Do Nothing	Do Nothing	Do Nothing
1	Crack Seal	Joint Seal	Spot Joint Seal
2	Skin patch	Crack Seal	Joint Seal
3	Manual Patch	Spray Patch	Crack Seal
4	Manual Patch, Crack Seal	Mechanized Patch	Spall Repair
5	Manual patch, Skin Patch	Concrete Path (Full Depth)	Longitudinal Joint Repair
6	Mechanized Patch	Slab Stabilization	CRC Patch
7	Base Repair, Manual Patch	Slab Stabilization, Diamond Grind	Concrete Pavement Patch
8	Base Repair, Mechanized Patch	Concrete Patch, Diamond Grind	Replace Terminal Joint
9	Micro Surface/Thin Overlay	Diamond Grind	Rut Filling
10	Resurface	Micro Surface	Major Rehabilitation
11	Level, Resurface	CPR and Overlay	
12	Level, Resurface, Base Repair	Major Rehabilitation/Reconstruction	
13	Mill, Level, Resurface		
14	Mill, Level, Resurface, Base Repair		
15	Major Rehabilitation/Reconstruction		

To illustrate the application of the treatment matrices for bituminous pavements, Table C-2 shows the treatments associated with each Distress Type. Table C-3 is the treatment matrix for fatigue cracking. A pavement with 25% by length medium severity fatigue cracking requires treatment 6 – mechanized patch. That is, treatment matrices connecting distresses to their assigned treatment strategies.

Table C-6. PennDOT treatments for bituminous pavements distress types.

Distress	Treatment
Fatigue Cracking	0, 6, 14, 15
Edge Deterioration	0, 1, 4, 7
Transverse Cracking	0, 1, 13, 14, 15
Raveling/Weathering	0, 6, 9, 13
Miscellaneous Cracking	0, 1, 6, 10, 13, 15
Rut Depth	0, 6, 13
Roughness	0, 11

Table C-7. PennDOT treatment matrix for bituminous pavements for fatigue cracking.

Extent (% length)	Treatment Low Severity	Treatment Medium Severity	Treatment High Severity
0	0	0	0
>0-5%	0	6	14
6-10%	0	6	14
11-15%	0	6	15
16-20%	0	6	15
21-30%	0	14	15
31-40%	0	14	15
41-50%	0	14	15
>50%	0	14	15

VIRGINIA

Virginia DOT uses decision trees to identify preventive maintenance treatment. The decision tree for flexible pavements for interstate highways is based on condition, age, and usage. The condition data serves as a preliminary screening. This data is collected annually. The data includes transverse cracking, longitudinal cracking, alligator cracking, longitudinal joint cracking, patching, potholes, delamination, bleeding, and rutting. The distress is assembled into three indices: Load-Related Distress Rating (LDR), Non-Load Related Distress Rating (NDR), and Critical Condition Index. The CCI is the lower of the LDR and NDR. IRI data is also collected.

Source: https://www.virginiadot.org/vtrc/main/online_reports/pdf/16-r3.pdf

Figure C-5 shows the decision tree. The initial filter is based on the current Distress Decision Matrix and Critical Condition Index filter. Preventive maintenance is considered if the CCI is between 85 and 90. The tree then follows these steps:

- The pavement age since the last resurfacing (trigger value) determines if the pavement is “Old” or “New”
- For “Old” pavements the structural condition, based on the falling weight deflectometer (FWD) data determines if the pavement is “Level 1” or Level 2 (strong)
- “Level 2” pavements receive Preventative Maintenance (PM)
- For “Level 1” pavements, the annual average daily truck traffic (AADTT) is used to determine the actions

- Level 1 Corrective Maintenance (CM), Level 2 Restorative Maintenance (RM), or Level 3 Restorative Maintenance (RM).
- For “New” pavements, if it is a Level 1, the AADTT is used to determine if the pavement needs Level 1 Do Nothing (DN), Level 2 Do Nothing (DN), or Level 3 Restorative Maintenance (RM).

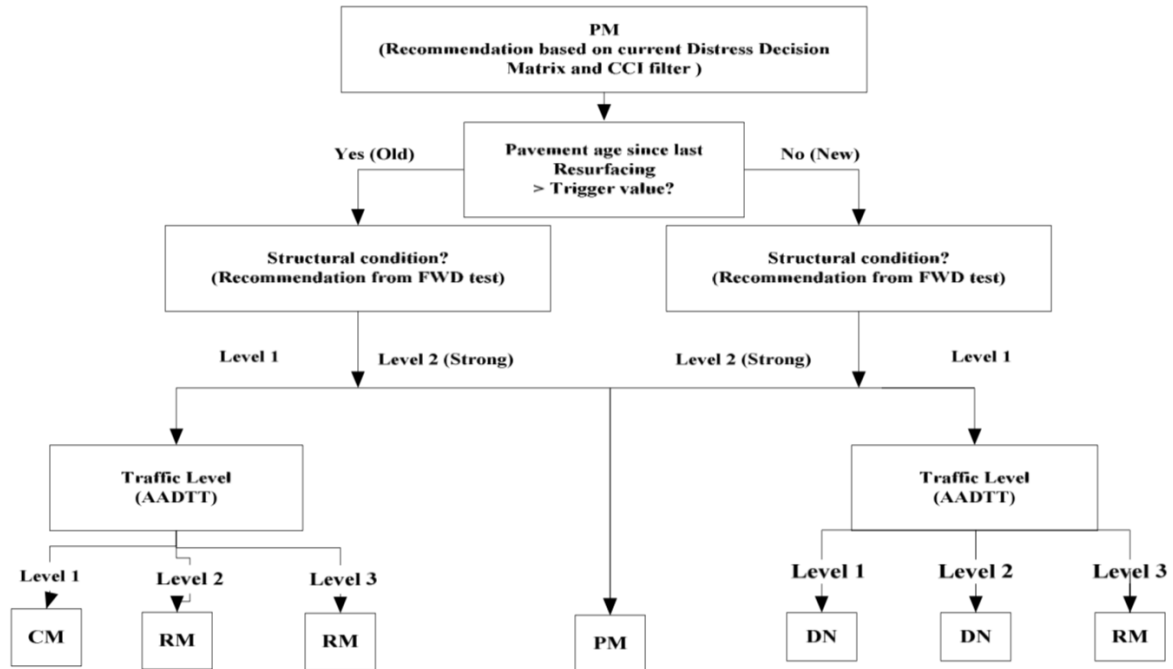


Figure C-5. VDOT decision tree for preventive maintenance on bituminous interstate highways (de León Izeppi, Morrison, Flintsch, & McGhee, 2015).

Appendix D: Maintenance Activities and Gamma Process Parameters

Table D-8. Maintenance activities for interstate and primary pavements under different categories (Virginia Department of Transportation, 2016).

Activity Category	Activities
Do Nothing (DN)	N/A
Routine (Preventive) Maintenance (PM)	1. Minor Patching (<5 of Pavement Area; Surface Patching; Depth 2")
	2. Crack Sealing
	3. Thin Treatments (Chip Seal, Slurry Seal, Latex, Thin Hotmix Asphalt Concrete (THMACO), 'Novachip' etc.)
Corrective Maintenance (CM)	1. Moderate Patching (<10 of pavement area; Partial Depth Patching; Depth 6")
	2. Partial Depth Patching (<10 of Pavement Area; Depth 4"-6") and Surface Treatment
	3. Partial Depth Patching (<10 of Pavement Area; Depth 4"-6") and Thin ($\leq 2''$) AC Overlay
	4. $\leq 2''$ Milling and $\leq 2''$ AC Overlay
Restorative Maintenance (RM)	1. Heavy Patching (<20 of Pavement Area; Full Depth Patching; Depth 12")
	2. $\leq 4''$ Milling and Replace with $\leq 4''$ AC Overlay
	3. Full Depth Patching (<20 of Pavement Area; Full Depth Patching; Depth 9"-12") and 4" AC Overlay
	4. Cold In-Place Recycling
Rehabilitation /Reconstruction (RC)	1. Mill, Break and Seat and 9"-12" AC Overlay
	2. Reconstruction
	3. Full Depth Reclamation

Table D-9. Gamma process scale and shape parameters, $f(t)$ and $g(t)$.

Time (years)	Traffic level (A) $f(t)$	Traffic level (A) $g(t)$	Traffic level (B) $f(t)$	Traffic level (B) $g(t)$	Traffic level (C) $f(t)$	Traffic level (C) $g(t)$	Traffic level (D) $f(t)$	Traffic level (D) $g(t)$	Traffic level (E) $f(t)$	Traffic level (E) $g(t)$
1	0.922	0.178	1.217	0.280	1.394	0.349	1.560	0.420	1.679	0.473
2	0.649	0.101	0.857	0.158	0.981	0.197	1.098	0.237	1.182	0.267
3	0.475	0.061	0.628	0.096	0.718	0.119	0.804	0.143	0.866	0.161
4	0.354	0.038	0.467	0.059	0.535	0.074	0.599	0.089	0.644	0.100
5	12.759	1.135	12.759	1.350	12.759	1.469	12.759	1.577	12.759	1.651
6	12.759	0.952	12.759	1.133	12.759	1.233	12.759	1.323	12.759	1.386
7	12.759	0.801	12.759	0.953	12.759	1.037	12.759	1.113	12.759	1.166
8	12.759	0.675	12.759	0.804	12.759	0.874	12.759	0.938	12.759	0.982
9	12.759	0.570	12.759	0.678	12.759	0.738	12.759	0.792	12.759	0.829
10	12.759	0.481	12.759	0.573	12.759	0.623	12.759	0.669	12.759	0.700
11	12.759	0.407	12.759	0.484	12.759	0.527	12.759	0.566	12.759	0.592
12	12.759	0.344	12.759	0.410	12.759	0.446	12.759	0.479	12.759	0.501
13	12.759	0.292	12.759	0.347	12.759	0.378	12.759	0.405	12.759	0.424
14	12.759	0.247	12.759	0.294	12.759	0.320	12.759	0.343	12.759	0.359
15	12.759	0.209	12.759	0.249	12.759	0.271	12.759	0.291	12.759	0.305
16	12.759	0.177	12.759	0.211	12.759	0.230	12.759	0.247	12.759	0.258
17	12.759	0.151	12.759	0.179	12.759	0.195	12.759	0.209	12.759	0.219
18	12.759	0.128	12.759	0.152	12.759	0.165	12.759	0.177	12.759	0.186
19	12.759	0.108	12.759	0.129	12.759	0.140	12.759	0.151	12.759	0.158
20	12.759	0.092	12.759	0.109	12.759	0.119	12.759	0.128	12.759	0.134

Appendix E: State Transition Probabilities for Illustrative Example

This appendix documents the state transportation probabilities for the illustrative example in Chapter 4. Table E-1 through Table E-3 show the transition probabilities for pavements for the Do Nothing, Minor Repair, and Major Repair options. Table E-4 through Table E-6 show the transition probabilities for bridge decks for the Do Nothing, Minor Repair, and Major Repair.

Table E-10. State transition probabilities for pavements: Do Nothing.

States	5	4	3	2	1
5	0.840	0.121	0.039		
4		0.788	0.142	0.070	
3			0.708	0.192	0.100
2				0.578	0.422
1					1.000

Table E-11. State transition probabilities for pavements: Minor Repair.

States	5	4	3	2	1
5	0.97	0.03			
4	0.85	0.12	0.03		
3	0.45	0.40	0.12	0.03	
2		0.45	0.40	0.12	0.03
1			0.45	0.40	0.15

Table E-12. State transition probabilities for pavements: Major Repair.

States	5	4	3	2	1
5	1.00				
4	0.95	0.05			
3	0.80	0.20			
2	0.70	0.25	0.05		
1	0.45	0.35	0.20		

Table E-13. State transition probabilities for bridge decks: Do Nothing.

States	6	5	4	3	2	1
6	0.85	0.09	0.06			
5		0.77	0.13	0.10		
4			0.78	0.14	0.08	
3				0.92	0.04	0.04
2					0.82	0.18
1						1.00

Table E-14. State transition probabilities for bridge decks: Minor Repair.

States	6	5	4	3	2	1
6	0.97	0.03				
5	0.85	0.12	0.03			
4	0.40	0.45	0.12	0.03		
3		0.40	0.45	0.12	0.03	
2			0.40	0.45	0.12	0.03
1				0.40	0.45	0.15

Table E-15. State transition probabilities for bridge decks: Major Repair.

States	6	5	4	3	2	1
6	1					
5	0.95	0.05				
4	0.80	0.20				
3	0.60	0.30	0.10			
2	0.40	0.40	0.20			
1	0.30	0.40	0.30			

Appendix F: Cost and Duration for Improvement Actions for Illustrative Example

This appendix includes cost and durations of pavement and bridge activities for the illustrative example in Chapter 4. Also included is user cost data.

Table F-1. Cost of pavement improvement actions.

Actions			Cost (\$/m ²)
Do Nothing			0
Minor Repair			16
Major Repair			68
Reconstruction			330

Sources: (Virginia Department of Transportation, 2016; FDOT, 2020; PennDOT, 2017; Russell, 2021)

Table F-16. Duration of pavement improvement actions.

Actions		Days per lane-mile	Additional days per mile for shoulders, etc.
Do Nothing		0	0
Minor Repair		3.5	1
Major Repair		6.5	2
Reconstruction		35	10

Table F-17. Cost of improvement actions for bridges.

Actions	Cost (\$/m ²)
Do Nothing	0
Minor Repair	400
Major Repair	1,200
Reconstruction	2,650

Table F-18. Duration of bridge improvement actions.

Actions	Days per bridge
Do Nothing	0
Minor Repair	12
Major Repair	30
Reconstruction	150

Table F-19. User cost for pavements.

States	Cost (\$/m ²)
5	0
4	8
3	14
2	25
1	200

Table F-20. User cost for bridges.

States	Cost (\$/m ²)
6	0
5	10
4	20
3	50
2	100
1	500

Appendix G: SARSA-LFA and DCMAC Parameters

SARSA-LFA PARAMETERS

The feature functions defined in **Table G-1** were used in Q-value approximation $\tilde{Q}(\mathbf{s}_t, \mathbf{a}_t, t)$ in the experiments.

Table G-1. Feature function

Function class	Description
$I_{\mathfrak{t}}(t)$	= 1 if $t = \mathfrak{t}$; = 0 otherwise
$I_{s_{\mathfrak{t}}^k, a_{\mathfrak{t}}^k, k, \mathfrak{t}}}(s_t^k, a_t^k, k, t)$	= 1 if $s_t^k = s_{\mathfrak{t}}^k$ and $a_t^k = a_{\mathfrak{t}}^k$ for pavement $k = \mathbb{k}$ in year $t = \mathfrak{t}$; = 0 otherwise
$I_{s_{\mathfrak{t}}^b, a_{\mathfrak{t}}^b, b, \mathfrak{t}}}(s_t^b, a_t^b, b, t)$	= 1 if $s_t^b = s_{\mathfrak{t}}^b$ and $a_t^b = a_{\mathfrak{t}}^b$ for bridge $b = \mathbb{b}$ in year $t = \mathfrak{t}$; = 0 otherwise
$I_{s_{\mathfrak{t}}^{G_1}, a_{\mathfrak{t}}^{G_1}, G_1, \mathfrak{t}}}(s_t^{G_1}, a_t^{G_1}, G_1, t)$	= 1 if $s_t^{G_1} = s_{\mathfrak{t}}^{G_1}$ and $a_t^{G_1} = a_{\mathfrak{t}}^{G_1}$ for roadway assets group $G_1 = \mathbb{G}_1$ in year $t = \mathfrak{t}$; = 0 otherwise
$I_{s_{\mathfrak{t}}^{G_2}, a_{\mathfrak{t}}^{G_2}, G_2, \mathfrak{t}}}(s_t^{G_2}, a_t^{G_2}, G_2, t)$	= 1 if $s_t^{G_2} = s_{\mathfrak{t}}^{G_2}$ and $a_t^{G_2} = a_{\mathfrak{t}}^{G_2}$ for roadway assets group $G_2 = \mathbb{G}_2$ in year $t = \mathfrak{t}$; = 0 otherwise
$I_{s_{\mathfrak{t}}^{G_3}, a_{\mathfrak{t}}^{G_3}, G_3, \mathfrak{t}}}(s_t^{G_3}, a_t^{G_3}, G_3, t)$	= 1 if $s_t^{G_3} = s_{\mathfrak{t}}^{G_3}$ and $a_t^{G_3} = a_{\mathfrak{t}}^{G_3}$ for roadway assets group $G_3 = \mathbb{G}_3$ in year $t = \mathfrak{t}$; = 0 otherwise

The first three classes of features were used to approximate $\tilde{Q}(\mathbf{s}_t, \mathbf{a}_t, t)$ via Eqn. (G.1).

$$\begin{aligned}
 \tilde{Q}(\mathbf{s}_t, \mathbf{a}_t, t) = & \sum_{\mathfrak{t} \in \mathbf{T}} \sum_{\mathbb{k} \in K} \sum_{s_{\mathfrak{t}}^k \in S^k} \sum_{a_{\mathfrak{t}}^k \in A_1} I_{s_{\mathfrak{t}}^k, a_{\mathfrak{t}}^k, k, \mathfrak{t}}(s_t^k, a_t^k, k, t) \cdot w_{s_{\mathfrak{t}}^k, a_{\mathfrak{t}}^k}^{\mathbb{k}, \mathfrak{t}} \\
 & + \sum_{\mathfrak{t} \in \mathbf{T}} \sum_{\mathbb{b} \in B} \sum_{s_{\mathfrak{t}}^b \in S^b} \sum_{a_{\mathfrak{t}}^b \in A_2} I_{s_{\mathfrak{t}}^b, a_{\mathfrak{t}}^b, b, \mathfrak{t}}(s_t^b, a_t^b, b, t) \cdot w_{s_{\mathfrak{t}}^b, a_{\mathfrak{t}}^b}^{\mathbb{b}, \mathfrak{t}} \\
 & + \sum_{\mathfrak{t} \in \mathbf{T}} I_{\mathfrak{t}}(t) \cdot w_t, \quad \forall t \in \mathbf{T}
 \end{aligned} \tag{G.54}$$

The weights, w , in Eqn. (G.1) are updated following Eqn. (4.18) and Eqn. (4.19) with learning rate $lr = 0.001$. Learning rates ranging from 0.000001 to 0.1 were tested. A rate of 0.001 led to the best results, and thus, was used in the experiments. To improve the results upon convergence, the last three feature functions were added, as \mathbb{G}_1 : {pavement 1, pavement 2 and pavement 3}; \mathbb{G}_2 : {pavement 7 and bridge 1}; and \mathbb{G}_3 : {pavement 9 and bridge2}.

The Q-value approximation $\tilde{Q}(\mathbf{s}_t, \mathbf{a}_t, t)$ is obtained through Eqn. (G.2).

$$\begin{aligned}
\tilde{Q}(\mathbf{s}_t, \mathbf{a}_t, t) = & \sum_{t \in \mathcal{T}} \sum_{k \in K} \sum_{s_t^k \in S^k} \sum_{a_t^k \in A_1} I_{s_t^k, a_t^k, k, t}(\mathbf{s}_t^k, \mathbf{a}_t^k, k, t) \cdot w_{s_t^k, a_t^k}^{k, t} \\
& + \sum_{t \in \mathcal{T}} \sum_{b \in B} \sum_{s_t^b \in S^b} \sum_{a_t^b \in A_2} I_{s_t^b, a_t^b, b, t}(\mathbf{s}_t^b, \mathbf{a}_t^b, b, t) w_{s_t^b, a_t^b}^{b, t} \\
& + \sum_{t \in \mathcal{T}} \sum_{s_t^{G_1} \in S^k \times S^k \times S^k} \sum_{a_t^{G_1} \in A_1 \times A_1 \times A_1} I_{s_t^{G_1}, a_t^{G_1}, G_1, t}(\mathbf{s}_t^{G_1}, \mathbf{a}_t^{G_1}, G_1, t) \cdot w_{s_t^{G_1}, a_t^{G_1}}^{G_1, t} \\
& + \sum_{t \in \mathcal{T}} \sum_{s_t^{G_2} \in S^k \times S^b} \sum_{a_t^{G_2} \in A_1 \times A_2} I_{s_t^{G_2}, a_t^{G_2}, G_2, t}(\mathbf{s}_t^{G_2}, \mathbf{a}_t^{G_2}, G_2, t) \cdot w_{s_t^{G_2}, a_t^{G_2}}^{G_2, t} \\
& + \sum_{t \in \mathcal{T}} \sum_{s_t^{G_3} \in S^k \times S^b} \sum_{a_t^{G_3} \in A_1 \times A_2} I_{s_t^{G_3}, a_t^{G_3}, G_3, t}(\mathbf{s}_t^{G_3}, \mathbf{a}_t^{G_3}, G_3, t) \cdot w_{s_t^{G_3}, a_t^{G_3}}^{G_3, t} \\
& + \sum_{t \in \mathcal{T}} \mathbf{1}_t(t) w_t, \quad \forall t \in \mathcal{T}
\end{aligned} \tag{G. 2}$$

where $\mathbf{s}_t^{G_1}$ represents the state of pavements 1, 2 and 3 in year t , $\mathbf{s}_t^{G_2}$ represents the state of pavement 7 and bridge 1 in year t , and $\mathbf{s}_t^{G_3}$ represents the state of pavement 9 and bridge 2 in year t . $\mathbf{a}_t^{G_1}$ represents the actions implemented on pavements 1, 2, and 3, $\mathbf{a}_t^{G_2}$ represents the actions implemented on pavement 7 and bridge 1, and $\mathbf{a}_t^{G_3}$ represents the actions implemented on pavement 9 and bridge 2.

DCMAC PARAMETERS

In implementing the DCMAC method, the actor network is constructed with 2 hidden layers, each with 100 neurons per layer and using a ‘Relu’ activation function for each layer. 11 output layers are connected to the last hidden layer. 9 output layers have 3 neurons representing pavements improvement action categories and 2 output layers have 9 neurons representing combinations of actions appropriate for pavements and bridges. All the output layers use a ‘Softmax’ action function. Categorical cross entropy loss function is used for the actor network and the learning rate is set to 0.0001. The critic network has 2 hidden layers, each hidden layers has 300 neurons and uses ‘Relu’ activation function. The output layer has one node and uses a ‘Linear’ activation function. Mean squared error loss function is used for the critic network and the learning rate is set to 0.01.